

A Critical Role of the Transcription Factor Miz-1 in T Cell Activation and Maturation

Dissertation

In Partial Fulfilment of the
Requirements for the Degree of
"doctor rerum naturalium" (Dr. rer. nat.)

Submitted to the Council of the Faculty
of Biological Sciences
of Friedrich Schiller University Jena

by Mägdefrau, Ann-Sophie, M. Sc., B. Sc.
born on 01.03.1991 in Ilmenau

First referee: PD Dr. rer. nat. Christian Kosan, FSU Jena

Second referee: Prof. Dr. rer. nat. Berit Jungnickel, FSU Jena

External referee: Prof. Dr. rer. nat. Dr. habil. med. Dirk Mielenz, FAU Erlangen-Nürnberg

Date of defense: January 20th, 2023

Table of contents

Table of contents	II
List of figures	V
List of tables	VII
List of abbreviations	VIII
Summary	XIV
Zusammenfassung	XV
1. Introduction	1
1.1 Immune system.....	1
1.2 T lymphocytes.....	2
1.2.1 Development of T cells	2
1.2.2 Selection mechanisms of T cells	5
1.2.3 Receptor signaling in T cells.....	6
1.2.4 T cell-mediated immunity.....	8
1.2.5 T cell memory.....	9
1.3 Survival and death of T lymphocytes.....	10
1.3.1 Pathways of T cell apoptosis	10
1.3.2 A role for p53 in survival and death	11
1.3.3 DNA damage response	12
1.4 The transcription factor Miz-1	14
1.4.1 Biochemistry of Miz-1	14
1.4.2 Functions of Miz-1	16
1.4.3 Miz-1 in hematopoiesis.....	18
1.4.4 Miz-1 in stress response pathways.....	19
Aim of the thesis	21
2. Materials	23
2.1 Mice strains.....	23
2.2 Chemicals	23

2.3 Reagents, kits, and enzymes	25
2.4 Antibodies	26
2.5 Primers	27
2.6 Consumables and devices	28
2.7 Software.....	28
3. Methods.....	29
3.1 Cell culture methods	29
3.1.1 Isolation of primary T cells.....	29
3.1.2 Cultivation of primary T cells	29
3.1.3 Irradiation experiments.....	30
3.2 Molecular biology methods.....	30
3.2.1 DNA isolation and genotyping	30
3.2.2 RNA isolation	31
3.2.3 Reverse transcription and quantitative real-time PCR	31
3.3 Protein biochemistry methods.....	32
3.3.1 Preparation of cell lysates	32
3.3.2 SDS-PAGE and Western Blot	32
3.4 Functional assays	33
3.4.1 Flow cytometry analysis and cell sorting.....	33
3.4.2 Apoptosis assay	34
3.4.3 Cell cycle analysis.....	34
3.4.4 Proliferation assay.....	35
3.4.5 Comet assay	35
3.5 Statistical analysis.....	36
4. Results.....	37
4.1 The influence of Miz-1 deficiency on T cell populations in the Vav-Cre x Miz-1 ^{fl/fl} mouse model	37
4.1.1 Targeting strategy at the <i>Zbtb17</i> locus	37
4.1.2 Functional Miz-1 deletion results in a decline in peripheral T cell populations.	37

4.1.3	Loss of functional Miz-1 and aging decline the naïve T cell pool.....	41
4.2	Phenotyping of the T cell compartment in the CD4-Cre x Miz-1 ^{fl/fl} mouse model ...	46
4.2.1	Thymic development is not perturbed using CD4-Cre-mediated recombination of the Miz-1 POZ domain	46
4.2.2	Miz-1 deficiency and aging influence peripheral T cell populations.....	48
4.2.3	Miz-1 deficiency and aging influence memory T cell populations.....	53
4.3	Miz-1 deficiency does not alter cell cycle progression of T cells	57
4.4	Functional deletion of Miz-1 alters T cell proliferation	60
4.5	Deletion of Miz-1 affects T cell survival after activation	63
4.5.1	Miz-1 has no impact on survival of unstimulated T cells	63
4.5.2	Miz-1 deficiency results in a strong induction of apoptosis after activation.....	64
4.5.3	Miz-1 deficiency provokes extrinsic apoptosis induction after T cell activation	65
4.6	The role of Miz-1 in T cells in response to irradiation.....	67
4.6.1	Analysis of irradiation-induced apoptosis induction of activated T cells	67
4.6.2	Upregulation of pro-apoptotic genes after irradiation of T cells	68
4.6.3	DNA repair in T cells is independent of the transcription factor Miz-1	71
5.	Discussion	72
5.1	Miz-1 is crucial for peripheral T cell populations	72
5.2	A critical role of Miz-1 in T cell apoptosis.....	77
5.2.1	Miz-1 regulates p53-independent apoptosis after T cell activation.....	77
5.2.2	Miz-1 and DNA damage in T cells	79
5.3	Miz-1 is a novel regulator of immune aging	82
5.4	Conclusions	89
6.	Supplemental figures	90
7.	References	97
	Declaration of independent assignment – Ehrenwörtliche Erklärung.....	XVII

List of figures

Figure 1: Overview of T cell development and T cell-mediated immunity.	4
Figure 2: Overview of the DNA damage response pathway.	14
Figure 3: Structure and functions of Miz-1.....	16
Figure 4: Loss of functional Miz-1 declines splenic T cells.	38
Figure 5: Miz-1 controls T cell subset composition of CD4 ⁺ and CD8 ⁺ T cells.	39
Figure 6: Miz-1 depletion affects CD4 ⁺ and CD8 ⁺ cells in aged mice.....	40
Figure 7: Miz-1 deficiency increases CD4 ⁺ effector memory T cell frequencies.....	42
Figure 8: Miz-1 deficiency results in depletion of naïve CD4 ⁺ T cells in aged mice.....	43
Figure 9: Deletion of functional Miz-1 increases CD8 ⁺ central memory T cells.	44
Figure 10: Functional Miz-1 deletion depletes naïve CD8 ⁺ T cells in aged mice.....	45
Figure 11: Thymic T cell development is not perturbed in CD4-Cre x Miz-1 ^{fl/fl} mice.....	48
Figure 12: Reduction of splenic T cells is caused by Miz-1 deficiency and by aging.....	50
Figure 13: CD4 ⁺ and CD8 ⁺ T cell numbers are altered due to loss of functional Miz-1.	52
Figure 14: Miz-1 deficiency and aging decline the CD4 ⁺ naïve T cell pool.....	54
Figure 15: Miz-1 deficiency increases frequencies of CD8 ⁺ memory T cells.....	56
Figure 16: Cell cycle progression of unstimulated T cells.	58
Figure 17: T cell activation induces cell cycle progression independent of Miz-1.	59

Figure 18: Miz-1-deficient CD4 ⁺ T cells proliferate faster.....	61
Figure 19: Miz-1-deficient CD8 ⁺ T cells show more proliferation.	62
Figure 20: Loss of functional Miz-1 decreases p21 levels after T cell activation.	63
Figure 21: Apoptosis of unstimulated T cells is not altered due to Miz-1 deficiency.....	64
Figure 22: T cell activation induces apoptosis due to Miz-1 deficiency.....	65
Figure 23: Apoptosis-associated gene expression after T cell activation.....	66
Figure 24: Activation of Miz-1-deficient T cells induces caspase 8 cleavage.....	67
Figure 25: T cell response to irradiation.	68
Figure 26: Induction of p53-associated target genes after irradiation of T cells.	70
Figure 27: Repair of DNA damage in T cells is independent of Miz-1.....	71
Figure 28: Schematic overview summarizing key findings.....	88
Figure 29: Targeting strategy of the <i>Zbtb17</i> locus.	90
Figure 30: Deletion of functional Miz-1 decreases naïve T cells in adult mice.	91
Figure 31: Deletion of functional Miz-1 depletes naïve T cells in aged mice.	92
Figure 32: Thymic characterization of Miz-1-deficient mice.	93
Figure 33: Reduction of Miz-1-deficient T cells in blood.	94
Figure 34: Analysis of apoptosis after T cell activation and irradiation.....	95
Figure 35: Apoptosis-related gene expression is not altered in Miz-1-deficient T cells.	96

List of tables

Table 1: List of mice strains.	23
Table 2: List of chemicals.....	23
Table 3: List of reagents, commercial kits, and enzymes.	25
Table 4: List of antibodies for flow cytometry.	26
Table 5: List of antibodies for Western Blot.....	26
Table 6: List of primers for genotyping.	27
Table 7: List of murine primers used for qRT-PCR.....	27
Table 8: List of used software.	28

List of abbreviations

A	ampere
ACAD	activated cell-autonomous death
AICD	activation-induced cell death
ANOVA	analysis of variance
APAF-1	apoptotic protease-activating factor 1
APC	antigen-presenting cell
APC	allophycocyanin
ARF	alternative reading frame
ATM	ataxia telangiectasia mutated
ATR	ataxia telangiectasia and RAD3-related
ATRIP	ATR-interacting protein
Asp (D)	aspartic acid
BAK	BCL-2 homologous antagonist/killer
BAX	BCL-2-associated protein X
BCL-2	B cell lymphoma 2
BCR	B cell receptor
BID	BH3-interacting domain death agonist
BER	base excision repair
BH	BCL-2 homology
bHLH	basic helix-loop-helix
BRCA1	breast cancer 1
BSA	bovine serum albumin
BTB/POZ	Broad complex, Tramtrack, Bric à brac/poxvirus and zinc finger
Caspase	cysteine protease that cleaves after an aspartate residue
CD	cluster of differentiation
cDNA	complementary DNA
CD4 SP	CD4 single-positive
CD8 SP	CD8 single-positive
Cebpd	CCAAT/enhancer-binding protein delta
CFSE	Carboxyfluorescein succinimidyl ester
CHK1	checkpoint kinase 1
cl.	cleaved

c-MYC	cellular myelocytomatosis oncogene
Ct	cycle threshold
CTD	C-terminal domain
C-terminal	carboxy-terminal
CTL	cytotoxic T lymphocyte
Da	Dalton
DAPI	4',6-Diamidino-2-phenylindole
DBD	DNA-binding domain
DC	dendritic cell
DDR	DNA damage response
DISC	death-inducing signaling complex
DMSO	Dimethyl sulfoxide
DN	double-negative
DNA	deoxyribonucleic acid
DNase	deoxyribonuclease
DNA-PK	DNA-dependent protein kinase
DNMT1	DNA methyltransferase 1
dNTP	deoxynucleotide triphosphate
DP	double-positive
DR4	death receptor 4
DSB	double-strand break
E	embryonic (day)
E-box	enhancer box
ECL	enhanced chemiluminescence
EDTA	Ethylenediaminetetraacetic acid
ELP	early lymphoid progenitor
ER	endoplasmic reticulum
et al.	et alii
ETP	early thymic progenitor
FACS	fluorescence-activated cell sorting
FADD	Fas-associated protein with death domains
FasL	Fas ligand
FCS	fetal calf serum
FITC	fluorescein isothiocyanate

fl	flanked by loxP sites, floxed
FSC	forward scatter
GAPDH	Glyceraldehyde-3-phosphate dehydrogenase
GEF	guanine nucleotide exchange factor
GFI-1	growth factor independent 1
GG-NER	global genome NER
GRB2	growth factor receptor-bound protein 2
Gy	Grey
h	hour
HAT	histone acetyltransferase
HDAC	histone deacetylase
HEPES	4-(2-Hydroxyethyl)-1-piperazineethanesulfonic acid
hi	high
Hox	homeobox
HR	homologous recombination
HRP	horseradish peroxidase
HSC	hematopoietic stem cell
IFN- γ	interferon γ
IgG	immunoglobulin G
INR	initiator
ITAM	immunoreceptor tyrosine-based activation motif
JAK	Janus kinase
JNK1	c-Jun N-terminal kinase 1
K	lysine
KLF2	Kruppel-like factor 2
KO	knockout
IL-7	interleukin 7
IL-7R	IL-7 receptor
IR	γ -irradiation
LAT	linker for activation of T cells
LCK	lymphocyte-specific protein tyrosine kinase
lo	low
LPS	lipopolysaccharide
LZ	leucine zipper

MAPK	mitogen-activated protein kinase
MAX	Myc-associated factor X
MCL-1	myeloid cell leukemia 1
MDM2	mouse double minute 2
MHC	major histocompatibility complex
miRNA	microRNA
Miz-1	MYC-interacting zinc finger protein 1
MMR	mismatch repair
MPP	multipotent progenitor
MRN	MRE11-RAD50-NBS1
mRNA	messenger RNA
NER	nucleotide excision repair
NFAT	nuclear factor of activated T cells
NF- κ B	nuclear factor kappa-light-chain-enhancer of activated B cells
NHEJ	non-homologous end joining
NK	natural killer
NOXA	Latin for damage
NPM	nucleophosmin
NP-40	Nonidet P40
N-terminal	amino-terminal
OD	oligomerization domain
PAMP	pathogen-associated molecular patterns
PBS	phosphate-buffered saline
PCR	polymerase chain reaction
PE	phycoerythrin
PerCP-Cy5.5	peridinin-chlorophyll-protein complex-Cyanine5.5
PI	Propidium iodide
PIC	protease inhibitor cocktail
POZ	poxvirus and zinc finger
PLC- γ	phospholipase C- γ
PS	phosphatidylserine
PTM	post-translational modification
PRR	pattern recognition receptor
PUMA	p53 up-regulated modulator of apoptosis

PVDF	polyvinylidene fluoride
qRT-PCR	quantitative real-time PCR
RAG1	recombination activating gene 1
RCL	red cell lysis
RPL22	ribosomal protein L22
RNase	ribonuclease
ROS	reactive oxygen species
RPA	replication protein A
RPMI	Roswell Park Memorial Institute
RSS	recombination signal sequences
RT	room temperature
Ser (S)	serine
SD	standard deviation
SDS	Sodium dodecyl sulfate
SDS-PAGE	SDS polyacrylamide gel electrophoresis
SOCS1	suppressor of cytokine signaling 1
SPF	specific-pathogen-free
SP1	specificity protein 1
SSB	single-strand break
SSC	side scatter
STAT5	signal transducer and activator of transcription 5
S1P	sphingosine-1-phosphate
TAD	transactivation domain
T-ALL	T-lineage acute lymphoblastic leukemia
TBE	Tris/boric acid/EDTA (buffer)
tBID	truncated BID
T _{CM} cell	central memory T cell
TC-NER	transcription-coupled NER
TCR	T cell receptor
TEC	thymic epithelial cell
T _{EFF} cell	effector T cell
T _{EM} cell	effector memory T cell
TdT	terminal deoxynucleotidyl transferase
TF	transcription factor

T _{FH} cell	T follicular helper cell
T _H cell	T helper cell
TLR	Toll-like receptor
T _M cell	memory T cell
T _N cell	naïve T cell
TNF	tumor necrosis factor
TNFR	TNF receptor
TopBP1	topoisomerase II β binding protein 1
TP53	tumor protein 53
TPA	12-O-tetradecanoylphorbol-13-acetate
TRAF2	TNF receptor-associated factor 2
T _{REG}	regulatory T cell
TRIS	Tris(hydroxymethyl)aminomethane
T _{RM}	tissue-resident memory T cell
TRP53	transformation-related protein 53
T _{VM} cell	virtual memory T cell
U	Unit
UV	ultraviolet
V	valine
V	Volt
V(D)J	variable, diversity, joining (gene segments)
v/v	volume per volume
WT	wild-type
w/v	weight per volume
XRCC4	X-ray repair cross complementing 4
ZAP70	zeta-chain-associated protein kinase 70
Zbtb17	zinc finger and BTB domain-containing 17
ZnF	zinc finger
Δ	delta; deleted

Summary

A functional immune system is important to protect the organism against various pathogens and to induce an adequate response to vaccinations. However, a deregulated immune system can lead to immune deficiencies, autoimmune diseases, or even cancer. B and T lymphocytes are the main drivers of adaptive immunity. An important regulator of their development is the MYC-interacting zinc finger protein 1 (Miz-1). The transcription factor Miz-1 is highly necessary for adequate T cell development by restricting apoptosis during V(D)J recombination. However, the importance of Miz-1 in mature T cells is yet not fully understood.

To provide new insights into the role of Miz-1 for T lymphocytes, mice possessing a conditional knockout of Miz-1 either in all hematopoietic cells (Vav-Cre x Miz-1^{fl/fl}) or specifically in T cells (CD4-Cre x Miz-1^{fl/fl}) were used. As the POZ domain of Miz-1 is necessary for its transcriptional activity, this domain was targeted by Cre-mediated deletion in both mouse models. Phenotypical analysis of these mice showed severe perturbations of the peripheral T cells, resulting in a reduction of mature T cells in several secondary lymphoid organs. Likewise, this decrease was observed in CD4⁺ as well as in CD8⁺ T cells.

T cell activation experiments showed that Miz-1 controls proliferation as well as apoptosis of peripheral T cells. Miz-1 deficiency resulted in a faster proliferation but also an excessive induction of apoptosis. Furthermore, the process of apoptosis seems to be p53-independent and induced via the extrinsic apoptosis pathway. Moreover, the p53-dependent apoptosis caused by γ -irradiation was not affected by the functional deletion of Miz-1 and the susceptibility of Miz-1-deficient T cells to DNA damage did not alter.

Flow cytometry experiments revealed that Miz-1 is a novel regulator of T cell aging, since young mice possessing a functional Miz-1 deletion exhibited similar distributions of T cell populations as old control mice. Due to Miz-1 deficiency, the numbers of naïve T cells dropped while frequencies of memory T cells were increased. Thus, Miz-1 is necessary to maintain the homeostasis of naïve and memory T cells in the course of aging. The observed premature aging signature in young mice that developed due to functional Miz-1 deletion was even more pronounced in old Miz-1-deficient mice.

The obtained results highlight the important role of Miz-1 in peripheral T cell homeostasis and T cell activation. Furthermore, this thesis improves our understanding of Miz-1 in the context of immunoaging and the generated data could be helpful for pharmacological interventions.

Zusammenfassung

Ein funktionierendes Immunsystem ist wichtig, um den Organismus vor verschiedenen Krankheitserregern zu schützen und um eine angemessene Reaktion auf Impfungen hervorzurufen. Ein dereguliertes Immunsystem kann jedoch zu Immundefizienzen, Autoimmunerkrankungen und sogar zu Krebs führen. B- und T-Lymphozyten sind die Hauptakteure der adaptiven Immunität. Ein wichtiger Regulator für deren Entwicklung ist das MYC-interagierende Zinkfingerprotein 1 (Miz-1). Der Transkriptionsfaktor Miz-1 ist für eine adäquate T-Zell-Entwicklung wichtig, da er die Apoptose während der V(D)J-Rekombination einschränkt. Die Bedeutung von Miz-1 für reife T-Zellen ist jedoch noch nicht vollständig geklärt.

Um neue Einblicke in die Rolle von Miz-1 für T-Lymphozyten zu gewinnen, wurden Mäuse verwendet, welche einen konditionellen Knockout von Miz-1 entweder in allen hämatopoetischen Zellen (Vav-Cre x Miz-1^{fl/fl}) oder spezifisch in T-Zellen (CD4-Cre x Miz-1^{fl/fl}) aufweisen. Da die POZ-Domäne von Miz-1 für dessen Transkriptionsaktivität notwendig ist, wurde diese Domäne in beiden Mausmodellen gezielt durch eine Cre-vermittelte Deletion entfernt. Die phänotypische Analyse dieser Mäuse zeigte schwerwiegende Störungen der peripheren T-Zellen, was zu einer Verringerung der reifen T-Zellen in verschiedenen sekundären lymphatischen Organen führte. Dieser Rückgang wurde sowohl bei CD4⁺ als auch bei CD8⁺ T-Zellen beobachtet.

T-Zell-Aktivierungsexperimente zeigten, dass Miz-1 sowohl die Proliferation als auch die Apoptose von peripheren T-Zellen kontrolliert. Der Verlust von funktionellem Miz-1 führte zu einer schnelleren Proliferation, aber auch zu einer verstärkten Induktion von Apoptose. Außerdem scheint der Apoptoseprozess p53-unabhängig zu sein und über den extrinsischen Apoptoseweg induziert zu werden. Darüber hinaus wurde die durch γ -Bestrahlung induzierte, p53-abhängige Apoptose durch die funktionelle Deletion von Miz-1 nicht beeinträchtigt und die Anfälligkeit von Miz-1-defizienten T-Zellen für DNA-Schäden veränderte sich nicht.

Durchflusszytometrische Experimente zeigten, dass Miz-1 einen neuen Regulator der T-Zell-Alterung darstellt, da junge Mäuse mit einer funktionellen Deletion von Miz-1 ähnliche Verteilungen von T-Zell-Populationen wie alte Kontrollmäuse aufwiesen. Aufgrund der Deletion von Miz-1 sank die Anzahl der naiven T-Zellen, während die Häufigkeit der Gedächtnis-T-Zellen zunahm. Somit ist Miz-1 notwendig, um die Homöostase von naiven und Gedächtnis-T-Zellen im Verlauf des Alterns aufrechtzuerhalten. Die bei jungen Mäusen beobachtete vorzeitige Alterung, die sich

aufgrund der Deletion von funktionellem Miz-1 entwickelte, war bei alten Miz-1-defizienten Mäusen noch ausgeprägter.

Die erzielten Ergebnisse unterstreichen die wichtige Rolle von Miz-1 bei der Homöostase peripherer T-Zellen und bei der T-Zell-Aktivierung. Darüber hinaus trägt diese Arbeit zu einem besseren Verständnis von Miz-1 im Zusammenhang mit der Alterung des Immunsystems bei und die gewonnenen Daten könnten für pharmakologische Interventionen hilfreich sein.

1. Introduction

1.1 Immune system

The immune system of mammals is a complex host defense entity to protect the organism against pathogens such as viruses, bacteria, fungi, and parasites, which can cause severe diseases if not eliminated. To recognize and fight these pathogens, the immune system comprises innate and adaptive immunity, both being necessary for an entire defense (Murphy and Weaver, 2018).

The innate or non-specific immune system is the first defense mechanism usually being activated immediately or within minutes after pathogen exposure. Its recognition and response against the infection are antigen-independent. In the first place, pathogens attacking an organism have to overcome anatomical and physiological barriers, for instance, the epithelium of the skin, a low pH in the stomach, or mucus layers in the respiratory tract (Turvey and Broide, 2010). After successfully entering these barriers, a chemical defense exists, for instance, consisting of complement factors, cytokines, and chemokines (Nauta et al., 2004). The activation of the complement induces a cascade that leads to pathogen lysis or their opsonization for cellular uptake (Zipfel and Skerka, 2009). The cellular component of innate immunity is composed of several immune cells that are attracted by cytokines and chemokines (Nauta et al., 2004). Mast cells and basophils secrete histamine or other inflammatory mediators to induce inflammation (Borriello et al., 2017). Macrophages and dendritic cells (DCs) express so-called pattern recognition receptors (PRRs) to sense invading pathogens that possess specific molecules or defined pathogen-associated molecular patterns (PAMPs). The receptor family of PRRs includes, for example, toll-like receptors (TLRs) that recognize PAMPs such as bacterial lipopolysaccharide (LPS) or nucleic acids originating from viruses (Gordon, 2002; Kawasaki and Kawai, 2014). Receptor activation leads to a subsequent signaling cascade, which can induce the elimination of pathogenic microorganisms by phagocytosis or macropinocytosis. The presentation of antigens by innate immune cells and the production of cytokines activate the adaptive immune system (Murphy and Weaver, 2018).

In contrast to the innate immune system, adaptive immunity is antigen-specific, the response starts hours after contact of the host with the pathogen and takes from several days up to weeks. Activation of the adaptive immune response starts with the presentation of antigens by antigen-presenting cells (APCs) like DCs. After pathogen uptake and digestion, APCs present them as antigens on their cell surface to activate the adaptive

immune system. The mediators of adaptive immunity can be classified into B and T lymphocytes, both being characterized by the expression of highly variable and specific receptors on their surface. This variability of the so-called B cell receptors (BCRs) and T cell receptors (TCRs) is a result of a random rearrangement of gene segments (somatic recombination) and it is important to recognize antigens with a high specificity. Lymphocytes get activated upon antigen recognition and differentiate to execute their effector functions. B cells become plasma cells and produce soluble antibodies, similar to the BCR on their surface, to neutralize the antigens. The effector functions of T cells after antigen encounter are more diverse and will be discussed in the following chapter. An important feature of the adaptive immune system is the immunological memory. Memory cells exist for the B and T cell lineage and they exhibit a faster, stronger, and more effective response after a potential reinfection (Bonilla and Oettgen, 2010; den Haan et al., 2014; Murphy and Weaver, 2018).

1.2 T lymphocytes

1.2.1 Development of T cells

T lymphocytes undergo a complex process of maturation to assure an adequate pathogen response (**Figure 1**). Similar to cells of the bloodline, T cells develop from multipotent and self-renewing hematopoietic stem cells (HSCs) that are placed in the bone marrow. After the generation of multipotent progenitors (MPPs), they leave this niche and undergo multiple differentiation steps during their migration to the thymus. The thymus is a central lymphatic organ where T cells are generated. It declines with age and consists of 4 compartments of which the cortex is the place where T cell development starts and the medulla where this maturation terminates (Aspinall et al., 2010; Koch and Radtke, 2011; Porritt et al., 2003).

Early lymphoid progenitors (ELPs) enter the thymus via the bloodstream and develop into early thymic progenitors (ETPs) (Allman et al., 2003; Igarashi et al., 2002). These ETP cells belong to the double-negative (DN) 1 compartment, which is characterized by the absence of the surface markers cluster of differentiation (CD) 4 and CD8. Moreover, these cells are negative for the expression of CD25 and positive for CD44 (CD25⁻, CD44⁺) (Godfrey et al., 1993; Porritt et al., 2004; Shortman and Wu, 1996).

Importantly, developing thymocytes are highly dependent on signaling via the NOTCH1 receptor that is expressed on their surface. Binding to NOTCH ligands, which are expressed on thymic epithelial cells (TECs), and the activation of the intracellular

NOTCH1 signaling cascade are important for the commitment to the T cell lineage and determination of the T cell fate (Felli et al., 1999; Radtke et al., 1999; Wilson et al., 2001). However, deregulated signaling via NOTCH1 can contribute to the development of T cell acute lymphoblastic leukemia (T-ALL) (Ellisen et al., 1991; Pear et al., 1996). Another important regulator of early T cell development is the cytokine interleukin (IL)-7 and the downstream pathway activated by its binding to the respective IL-7 receptor α -chain (IL-7R α). The expression of IL-7R α is, in turn, transcriptionally regulated by NOTCH1 (Bolotin et al., 1996; González-García et al., 2009; von Freeden-Jeffry et al., 1997).

By receiving signals from the thymic environment, DN1 cells progress to differentiate into DN2 cells that are defined by CD44⁺ and CD25⁺ surface expression (Godfrey et al., 1993). The DN2 compartment can be further subdivided into the early DN2a subset with a high expression of CD117 (c-kit) and the late DN2b cells with an intermediate expression of CD117 (Godfrey et al., 1992; Masuda et al., 2007). While DN2a cells can still give rise to other cell lineages, for instance, DCs, cells in the DN2b stage have lost their potential to develop into DCs (Masuda et al., 2007; Moore and Zlotnik, 1995). These cells continue to differentiate into cells of the DN3 stage, which is characterized by a CD44⁻ and CD25⁺ surface expression profile (Godfrey et al., 1993). This DN3 stage is further subdivided into DN3a cells possessing a low expression of CD27 and DN3b cells expressing high levels of CD27 (Taghon et al., 2006). The transition from DN3a to DN3b depends on functional signaling through the pre-TCR, which is composed of the rearranged TCR β -chain and a non-rearranged pre-TCR α -chain (Falk et al., 2001; Taghon et al., 2006; von Boehmer, 2005). This process is controlled at the β -selection checkpoint and will be discussed in more detail in the next chapter. Cells progress from the DN3b stage to the DN4 stage, which is characterized by a CD44⁻ and CD25⁻ surface expression pattern (Godfrey et al., 1993). Developing T cells continue their maturation in the thymus by upregulating the surface markers CD4 and CD8, and therefore become double-positive (DP) cells (Ceredig et al., 1982; Wilson et al., 1989). At this stage, rearrangement of the α -chain of the TCR is initiated. Afterward, the α -chain is expressed on the surface together with the β -chain, both forming the newly assembled $\alpha\beta$ TCR (Malissen et al., 1992; Nikolic - Zugic and Moore, 1989; Petrie et al., 1993). In the last step of thymic development, DP cells commit either to the CD4 lineage as CD4 single-positive (CD4 SP; CD4⁺, CD8⁻) cells, or to the CD8 lineage as CD8 SP (CD4⁻, CD8⁺) cells (Fowlkes et al., 1985; Germain, 2002). Several selection processes assure an appropriate binding of the functional TCR and eliminate auto-reactive cells. Finally, T cells upregulate the sphingosine-1-phosphate receptor 1 (S1P₁), which leads to an egression of mature T cells from the thymus and homing to the periphery (Matloubian et al., 2004).

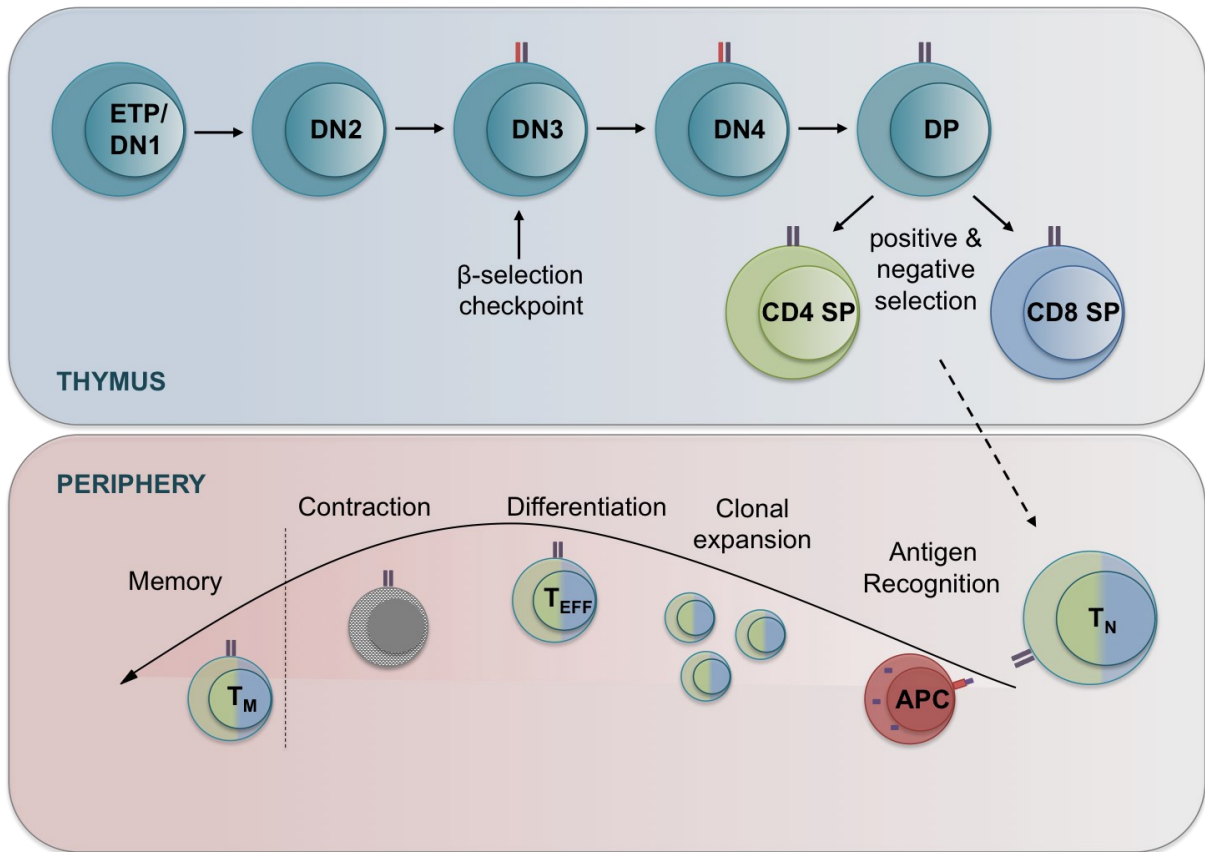


Figure 1: Overview of T cell development and T cell-mediated immunity.

T cell development takes place in the thymus and starts with an early thymic progenitor (ETP) that belongs to the double-negative (DN) 1 population, further developing into the DN2 and DN3 population. Here, the β -selection checkpoint assures proper rearrangement of the T cell receptor (TCR) β -chain, forming a pre-TCR (bicolored) with a non-rearranged TCR α -chain. Cells then progress through DN4 and become double-positive (DP) by the upregulation of CD4 and CD8. They are further characterized by the expression of the mature $\alpha\beta$ TCR (single-colored). Commitment to either CD4 single-positive (CD4 SP) or CD8 SP cells is the last developmental step in the thymus. Several positive and negative selection processes assure proper TCR binding and check for auto-reactiveness. Unprimed, naïve T (T_N) cells then migrate to the periphery where they check for matching antigens, presented on antigen-presenting cells (APCs). T cell-mediated immunity starts with antigen recognition, followed by clonal expansion of the T cells and the differentiation into effector T (T_{EFF}) cells. These cells show a fast and efficient response to the pathogen. After antigen clearance, a contraction phase is initiated where a substantial amount of cells undergo apoptosis. A small subset of memory T (T_M) cells survive, forming the immunological memory of the T cell lineage. Adapted from (EITanbouly and Noelle, 2021; Kaech et al., 2002; Koch and Radtke, 2011).

1.2.2 Selection mechanisms of T cells

T cell development needs to be tightly regulated to assure adequate T cell responses to antigens and simultaneously prevent reactions to self-antigens. Thus, several checkpoints and selection mechanisms exist to control the developmental processes. T cells execute effector functions via the TCR, which is located on the cellular surface. The antigen-binding α - and β -chains of a TCR form a complex that is associated with invariant chains of the CD3 complex, involved in intracellular signaling. Cells with these receptors are called $\alpha\beta$ T cells and form the major part of the T cell lineage (Murphy and Weaver, 2018). Their development will be described in the following. Another small group is formed by the so-called $\gamma\delta$ T cells, characterized by a TCR that is composed of a γ - and a δ -chain. These cells develop from the same progenitor in the thymus as $\alpha\beta$ T cells do, but they exhibit differences in their maturation (Ciofani et al., 2006; Petrie et al., 1992). Importantly, $\gamma\delta$ T cells are transcriptionally programmed in the thymus, meaning that discrete subsets can acquire effector functions already in the thymus (Muñoz-Ruiz et al., 2017).

The TCR of $\alpha\beta$ T cells is generated in several steps, starting with deoxyribonucleic acid (DNA) rearrangement of the β -chain predominantly in the DN3 stage (Godfrey et al., 1994; Masuda et al., 2007). The process of somatic rearrangement of the chain gene segments is called V(D)J recombination. Firstly, diversity (D) and joining (J) segments are rearranged together. Later, variable (V) segments are added (Chi et al., 2020; Nemazee, 2000). This process starts with the cleavage of DNA by the recombination activating genes 1/2 (RAG1/2) at recombination signal sequences (RSSs). Consequently, a hairpin structure is formed (McBlane et al., 1995; Roth et al., 1992). A complex of DNA-dependent protein kinase (DNA-PK) and Artemis binds and resolves this hairpin (Ma et al., 2002). To increase the diversity of the TCR, random nucleotides are added by members of the polymerase family Pol X such as the terminal deoxynucleotidyl transferase (TdT) (Lieber et al., 1988). Subsequently, DNA ends are joined by the non-homologous end joining (NHEJ) repair process including the enzymes Ku70, Ku80, DNA ligase IV, and the X-ray repair cross complementing 4 (XRCC4) (Critchlow et al., 1997; Gu et al., 1997; Nussenzweig et al., 1996; Schatz and Swanson, 2011; Taccioli et al., 1993). The process of rearrangement induces cell-intrinsic DNA breaks that have to be tolerated by developing T cells. The successfully rearranged β -chain of the TCR binds a surrogate α -chain, pT α , forming a pre-TCR with CD3 on the surface of DN3 cells (von Boehmer, 2005). The adequate TCR rearrangement is controlled at the so-called β -selection checkpoint at the transition of DN3a to DN3b cells. Signaling via the pre-TCR is required to pass through this checkpoint for the development into DN4 cells and the induction of proliferation (Falk et al., 2001; Koch and Radtke, 2011). The rearrangement of

the α -chain subsequently leads to the expression of a mature TCR on DP cells. This is accompanied by expression of the co-receptor proteins CD4 and CD8 that facilitate enhanced binding to major histocompatibility complex (MHC) molecules (Koch and Radtke, 2011).

All nucleated cells express MHC I, which presents intracellular antigens of these cells. In contrast, MHC II is found on B cells, DCs, and macrophages, exposing extracellular antigens to the immune system (den Haan et al., 2014). Developing T cells interact with a complex consisting of self-antigens and MHC class I or II molecules that are presented on cortical epithelial cells in the cortex of the thymus. The avidity between these interactions determines the further development of T cells. If signaling upon the TCR engagement with the complex is not strong enough, these cells do not receive proper survival signals to sustain viability and die (Klein et al., 2009). Thus, during this positive selection step, interactions with self-peptide-MHC complexes are crucial for T cell survival (Kisielow et al., 1988; MacDonald et al., 1988; von Boehmer et al., 1989). In contrast, the negative selection checks for high-affinity interactions between T cells and self-antigen-MHC complexes to remove auto-reactive T cells. On the contrary, T cells with an intermediate avidity to these complexes and an appropriate level of signaling via the TCR get positively selected, which assures their further maturation (Klein et al., 2009; Stritesky et al., 2013).

At the end of these selection processes, DP cells have to commit either to the CD4 or the CD8 lineage by silencing the transcription of one of these two co-receptors (Ellmeier et al., 1999; Hostert et al., 1997; Sawada et al., 1994). The CD4 molecule can bind pan-MHC class II complexes and CD4 SP cells are considered T helper (T_H) cells. On the contrary, CD8 binds pan-MHC class I complexes and CD8 SP cells are regarded as cytotoxic T lymphocytes (CTLs) (Germain, 2002). The committed SP T cells migrate to the medulla of the thymus where they undergo a second wave of negative selection. They encounter once again a high variety of self-antigens and high-affinity interactions induce cell death to avoid the development of auto-reactive T cells (Koch and Radtke, 2011; Kurd and Robey, 2016; Stritesky et al., 2013).

1.2.3 Receptor signaling in T cells

Signaling via the TCR ensures proper maturation and is necessary for executing responses to pathogen infestation. The TCR is a heterodimer composed predominantly of α - and β -chains that are transmembrane receptors with extracellular and intracellular domains. This heterodimeric complex can attach to peptides that are bound by MHC, but it is unable to transduce the incoming signals, as it lacks signal-transducing activity

(Ngoenkam et al., 2018). Therefore, the TCR is associated with a CD3 complex, which consists of γ -, δ -, two ϵ -polypeptide chains, and mostly two ζ -chains. All CD3 polypeptides possess so-called immunoreceptor tyrosine-based activation motifs (ITAMs), which get phosphorylated during activation and induce signal transduction (Gaud et al., 2018). This process requires the interaction of the co-receptors CD4 or CD8 with the appropriate MHC molecule, thereby bringing the intracellular receptor-associated lymphocyte-specific protein tyrosine kinase (LCK) into close proximity to the TCR (Barber et al., 1989; Burgess et al., 1991). Its kinase domain gets auto-phosphorylated and in turn, phosphorylates the CD3-based ITAMs (Barber et al., 1989; Danielian et al., 1989). The phosphorylation sites of ITAMs build a platform for the SH2 domain-containing zeta-chain-associated protein kinase 70 (ZAP70), which gets activated by a conformational change and by phosphorylation (Chan et al., 1992; Iwashima et al., 1994). ZAP70 activates the linker for activation of T cells (LAT) through phosphorylation, which subsequently acts as a signaling hub, recruiting multiple adaptor proteins and activating several downstream pathways (Bunnell et al., 2000; Zhang et al., 1998). Adaptors, for instance, growth factor receptor-bound protein 2 (GRB2) or phospholipase C- γ (PLC- γ), bind to these docking sites and allow various signaling responses (Sieh et al., 1994; Zhang et al., 2000). Overall, 3 major signaling pathways get activated. On the one hand, PLC- γ gets stimulated, leading to a calcium influx from the endoplasmic reticulum (ER) into the cytoplasm (Zhang et al., 2000). Elevated calcium levels induce, via binding to calcineurin, the shuttling of the nuclear factor of activated T cells (NFAT) to the nucleus, where it initiates the transcription of target genes (Jain et al., 1992; Shaw et al., 1988). On the other hand, the mitogen-activated protein kinase (MAPK) pathway, as well as the nuclear factor kappa-light-chain-enhancer of activated B cells (NF κ B) pathway, get activated, leading to the expression of specific target genes (Coudronniere et al., 2000; Finco et al., 1998; Gaud et al., 2018; Liu et al., 2015). The activation of these pathways results in proliferation, production of cytokines, and gain of T cell effector functions (Rudd, 2021). Another important feature of TCR activation is the recruitment and phosphorylation of Vav1, a guanine nucleotide exchange factor (GEF) that is under physiological conditions expressed in hematopoietic cells (Han et al., 1997; Katzav et al., 1989). Activation of Vav1 induces the reorganization of the cytoskeleton, which is required for the stabilization of the immunological synapse (Schuebel et al., 1998; Villalba et al., 2001). Furthermore, co-stimulatory signals that are required for T cell activation and proliferation are provided by the surface receptor CD28. Ligand binding to this homodimeric complex entirely activates the T cells and protects them from undergoing cell death or from going into a state of anergy, where they are resistant to further stimulation (Beyersdorf et al., 2015; Jenkins and Schwartz, 1987; Lai and Tan, 1994; Tan et al., 1993).

1.2.4 T cell-mediated immunity

Unprimed T cells circulate through the blood and the secondary lymphoid organs until they recognize a matching antigen, which is presented as a complex of peptide and MHC molecule on the surface of APCs. After encountering a matching antigen, the T cells get activated via the TCR. However, a further co-stimulatory signal of the APC is necessary to assure survival and proliferation of the T cell (den Haan et al., 2014; Jenkins et al., 1991). The process of antigen recognition is called priming of naïve T cells and it is followed by a clonal expansion phase. Activated T cells further differentiate into effector T (T_{EFF}) cells that show a fast and efficient response. Several T_{EFF} cells exist and their lineage commitment is controlled by specific cytokines and a complex regulatory network (Broere and van Eden, 2019; Wang et al., 2015).

$CD4^+$ T helper cells are important for establishing and maximizing the immune response. Based on the production of signature cytokines, they can be divided into several subgroups of effector cells. T_H1 cells mainly produce interferon γ (IFN- γ), IL-2, and tumor necrosis factor α (TNF- α) to support macrophages that are encountered by pathogens, activate $CD8^+$ T cells and stimulate B cells for the production of opsonizing antibodies. T_H2 cells produce mainly the interleukins IL-4, IL-5, IL-6, IL-10, and IL-13 to support mast cells eliminating extracellular pathogens, and to stimulate immunoglobulin G (IgG), IgA, and IgE antibody production by B cells (Broere and van Eden, 2019; Mosmann and Coffman, 1989). T_H17 cells play a role in autoimmunity and are important for an effective immune response against extracellular bacteria by producing key effector cytokines such as IL-17A and IL-17F (Harrington et al., 2005; Luckheeram et al., 2012; Park et al., 2005). Furthermore, T follicular helper (T_{FH}) cells and regulatory T (T_{REG}) cells have been identified. T_{FH} cells regulate humoral immunity by supporting B cells to produce antibodies and perform isotype switching (Breitfeld et al., 2000; Schaerli et al., 2000). T_{REG} cells maintain peripheral tolerance and help to avoid autoimmunity by negatively regulating the immune response (Groux et al., 1997; Sakaguchi et al., 1995; Sharma and Rudra, 2018). On the contrary, $CD8^+$ CTLs induce cytotoxicity after adhering to their target cells by releasing cytolytic effector molecules such as granzymes or cytokines into the immunological synapse. Granzymes are a family of cell death-inducing serine proteases and are released with the pore-forming molecule Perforin, which can induce membrane permeabilization of the target cell (Cassoli and Baldari, 2022; Jenne and Tschopp, 1988).

1.2.5 T cell memory

A unique characteristic of the adaptive immune system is the ability to create an immunological memory, an important feature used for vaccinations against various pathogen-derived diseases. Following antigen contact, lymphocytes differentiate into effector cells during the clonal expansion phase. After clearance of the infection, effector cells undergo a contraction phase, whereby most cells die due to apoptosis. However, about 5-10 % of the effector cells survive this selection process and mature into memory cells (**Figure 1**) (Pepper and Jenkins, 2011; Pepper et al., 2010; Sallusto et al., 2004). These cells are long-lived and self-renewing. They can rapidly proliferate and re-acquire effector functions upon a second encounter with the same antigen (Fearon et al., 2001; Graef et al., 2014; Rutishauser and Kaech, 2010). Memory cells occur for both, the B and T cell lineage, although memory T cells (T_M) are more heterogenic. They exist for the $CD4^+$ and $CD8^+$ T cell compartments and each is composed of three main subgroups. The first one comprises the central memory T (T_{CM}) cells, which can recirculate through the lymph node and have the potential to differentiate into effector cells. Effector memory T (T_{EM}) cells migrate to the site of inflammation and quickly exhibit effector functions (Sallusto et al., 1999). The last big group is composed of the tissue-resident memory T (T_{RM}) cells that reside in non-lymphoid tissues where they exert their functions (Gebhardt et al., 2009; Steinbach et al., 2018).

T_M cells differ from naïve and effector cells in gene expression profiles, surface markers, and immune responses. An important molecule to distinguish between the different subpopulations represents the cell adhesion molecule L-selectin, also called CD62L. It is expressed on naïve T cells and enables them to enter the lymph node to find a cognate antigen. CD62L expression on naïve T cells is necessary for tethering to the endothelial venules (Bradley et al., 1994; Geoffroy and Rosen, 1989). The surface marker CD44, a glycoprotein for cell adhesion, is absent on naïve cells but highly expressed on memory and effector T cells (Budd et al., 1987; Mackay et al., 1994). The expression profiles of both markers, CD62L and CD44, can be used to distinguish between T_{CM} and T_{EM} cells. As T_{CM} cells can still recirculate, they express the homing factor CD62L and the activation marker CD44. On the other hand, high CD44 levels but a lack of CD62L expression characterize the T_{EM} cell population (Baaten et al., 2012; Sallusto et al., 1999).

1.3 Survival and death of T lymphocytes

1.3.1 Pathways of T cell apoptosis

The survival of T lymphocytes is dependent on multiple signals the cells receive. The main drivers are signals via the TCR, co-stimulatory molecules (such as CD28), adhesion molecules, cytokines (such as IL-2), and other pro- or anti-apoptotic molecules (Krammer et al., 2007). Apoptosis, the programmed cell death (Kerr et al., 1972), is important at several stages during the life of T cells. It is involved in processes such as the development of T lymphocytes in the thymus, TCR repertoire selection, removal of activated T cells, and T cell homeostasis (Brenner et al., 2008).

Apoptosis can either be activated via the extrinsic or the intrinsic apoptosis pathway. Extrinsic apoptosis induction starts with the binding of pro-apoptotic factors such as Fas ligand (FasL, also known as CD95L) to a cell-death receptor such as Fas (also known as CD95). Consequently, complex formation of the death-inducing signaling complex (DISC) is induced. This complex includes Fas-associated protein with death domains (FADD), which is recruited to the receptor, and the pro-caspases 8 and/or 10 (Boldin et al., 1995; Chinnaiyan et al., 1995; Kischkel et al., 1995; Krammer et al., 2007). The intrinsic pathway, on the contrary, can be triggered by several stimuli such as DNA damage, cytokine deprivation, or TCR stimulation and its initiation is dependent on the permeabilization of the outer mitochondrial membrane. The balance between pro- and anti-apoptotic factors of the B cell lymphoma 2 (BCL-2) family is the main driver of this apoptosis pathway (Reed, 2000). The BCL-2 family can be divided into 3 groups, depending on structural characteristics. The first group contains the BCL-2 homology (BH) domains 1-4 and its members, such as BCL-2 and induced myeloid cell leukemia 1 (MCL-1), have anti-apoptotic activity. The members of the second group, such as BCL-2-associated protein X (BAX) and BCL-2 homologous antagonist/killer (BAK), possess the domains BH1-3 and exhibit pro-apoptotic properties. The last group of this family consists of BH3-only proteins like BH3-interacting domain death agonist (BID), which executes pro-apoptotic functions (Brenner et al., 2008; Lam et al., 1994; Reed, 1997). Crosstalk between the extrinsic and intrinsic pathways is possible by the cleavage of BID into truncated BID (tBID) (Li et al., 1998; Yin et al., 1999). During the intrinsic apoptosis initiation, the permeabilization of mitochondria leads to the release of cytochrome c, which binds the apoptotic protease-activating factor 1 (APAF-1). These molecules form the so-called apoptosome, recruit pro-caspase 9 molecules and induce apoptosis (Li et al., 1997; Zou et al., 1997; Zou et al., 1999).

In both activation pathways, inactive forms of cysteine proteases that cleave after an aspartate residue (caspases) get activated and cleave components of the cell. These catalytically inactive forms are called pro-caspases or zymogens. Apoptosis is activated by the cleavage of initiator caspases, whose catalytic domain is initially blocked. Proteolytic activation converts these pro-caspases into active caspases with the presentation of the catalytic domain. Subsequently, they can cleave effector caspases, which digest the cell after being activated. Initiator caspases differ between both apoptosis pathways. Caspase 9 (part of the apoptosome) initiates the intrinsic pathway whereas the extrinsic pathway starts with caspase 8 or 10. Both pathways have the effector caspases 3, 6, and 7 in common (Krammer et al., 2007; Kuida et al., 1998; Varfolomeev et al., 1998). The process of apoptosis is accompanied by the formation of apoptotic bodies and the translocation of phosphatidylserine (PS) from the inner to the outer plasma membrane. The exposed PS enables the recognition by phagocytic cells. The protein Annexin V binds to PS after externalization and can therefore be used as a marker for apoptosis (Fadok et al., 1992; Kerr et al., 1972; Vermes et al., 1995). Other cell death mechanisms of T cells include the caspase-independent pathway. One example is the activation of cathepsins, which are proteases located in lysosomes (Jäättelä and Tschopp, 2003; Perišić Nanut et al., 2014).

1.3.2 A role for p53 in survival and death

An important regulator of T cell survival and death is p53. The tumor suppressor p53, also known as the guardian of the genome, (human: TP53 (tumor protein 53), murine: TRP53 (transformation-related protein 53)) is a transcription factor (TF) that activates but also represses genes involved in various processes, among them, proliferation, DNA repair, senescence, and apoptosis (DeLeo et al., 1979; Fields and Jang, 1990; Kruiswijk et al., 2015; Lane and Crawford, 1979). p53 possesses discrete domains to execute its function as a regulator of gene expression. It is composed of two amino (N)-terminal transactivation domains (TADs), a proline-rich domain, a DNA-binding domain (DBD), an oligomerization domain (OD), and a carboxy (C)-terminal domain (CTD). The latter is a target of many post-translational modifications (PTMs) (Ko and Prives, 1996; Sullivan et al., 2018). Protein stability of p53 is regulated by different E3 ligases of which mouse double minute 2 (MDM2; human: HDM2 (human double minute 2)) plays a pivotal role by linking poly-ubiquitin chains to lysine (K) at position 48 and, thus, labeling it for proteasome-mediated degradation (Haupt et al., 1997; Kubbutat et al., 1997; Niazi et al., 2018). In unperturbed cells, MDM2 targets p53 for constant turnover, while cellular stress

like DNA damage induces phosphorylation of p53, enabling it to evade degradation (Shieh et al., 1997).

The TF p53 possesses pro-survival as well as anti-survival functions. The pro-survival activity of p53 regulates many DNA repair factors directly or enables repair mechanisms by the induction of cycle arrest, mainly through activation of the negative cell cycle regulator p21 (also known as CIP1, or WAF1; encoded by the gene *Cdkn1a*) (el-Deiry et al., 1993; Mohammadzadeh et al., 2019; Stürzbecher et al., 1996). By exerting its anti-survival activity, p53 can initiate the induction of apoptosis via the intrinsic as well as the extrinsic pathway (Yonish-Rouach et al., 1991). As a regulator of the extrinsic apoptosis induction, p53 can induce the expression of genes encoding for Fas or death receptor 5 (DR5) (Owen-Schaub et al., 1995; Wu et al., 1999). On the contrary, direct targets of p53 are genes encoding for BAX, p53 up-regulated modulator of apoptosis (PUMA), and NOXA (Latin for damage), linking p53 function also to the intrinsic pathway of apoptosis (Miyashita and Reed, 1995; Nakano and Vousden, 2001; Oda et al., 2000).

1.3.3 DNA damage response

All cells of the organism, including T lymphocytes, are frequently exposed to genotoxic stressors leading to DNA damage and this requires p53 to maintain genome integrity (Williams and Schumacher, 2016). p53 is a central effector molecule of the DNA damage response (DDR) pathway, which is an important control mechanism to protect the genome. The DDR pathway detects damage, signals its occurrence to the repair machinery, and induces repair pathways (Delia and Mizutani, 2017). Accumulating evidence suggests that low doses of genotoxic stress have beneficial effects, while high doses are known to be harmful, a dose-response phenomenon called hormesis (Calabrese, 2005; Mägdefrau et al., 2019). Genotoxic stressors can be diverse. To name only a few, ultraviolet (UV) light, ionizing radiation, certain chemicals, and reactive oxygen species (ROS) can cause damage to the DNA (Chatterjee and Walker, 2017).

Depending on the type of DNA damage, specific repair signaling pathways get activated. The formation of double-strand breaks (DSBs) can be recognized by the MRE11-RAD50-NBS1 (MRN) complex. It binds the lesion and builds a platform for the kinase ataxia telangiectasia mutated (ATM), which is a key regulator of DDR (Lee and Paull, 2005; Suzuki et al., 1999). Once ATM gets activated, it consequently stimulates a wide spectrum of downstream effectors, e.g., checkpoint kinase 2 (CHK2), breast cancer 1 (BRCA1), and p53 (**Figure 2**) (Chaturvedi et al., 1999; Chehab et al., 2000; Gatei et al., 2000). One of the first PTMs induced after genotoxic stress is the phosphorylation of histone variant H2AX at serine (S) 139, termed γ H2AX (Chatterjee and Walker, 2017; Rogakou et al.,

2000; Rogakou et al., 1998). This modification can be used as a DNA damage marker and is necessary for the recruitment of DNA repair factors to the side of the lesion (Paull et al., 2000). On the contrary, DNA single-strand breaks (SSB) trigger activation of ataxia telangiectasia and RAD3-related (ATR), another key regulator of DDR. These DNA lesions are bound by replication protein A (RPA) and recruit ATR-interacting protein (ATRIP), which directly interacts with ATR. The kinase ATR signals the damage to downstream effectors, for instance, checkpoint kinase 1 (CHK1) and p53 (Awasthi et al., 2015; Cortez et al., 2001; Tibbetts et al., 1999; Zou and Elledge, 2003). Both DDR pathways are tightly interconnected and effectors control the induction of cell cycle arrest, DNA repair, or apoptosis (Smith et al., 2010).

Similar to the repair signaling pathways, distinct repair mechanisms exist for different types of DNA lesions (**Figure 2**). SSBs such as a damaged base induce base excision repair (BER), while base mismatches trigger mismatch repair (MMR). Bulky adducts induce nucleotide excision repair (NER) that is either transcription-coupled (TC-NER) or acting throughout the global genome (GG-NER) (Williams and Schumacher, 2016). On the contrary, DSBs are repaired by homologous recombination (HR). This repair process is restricted to the S phase, where DNA is replicated and sister chromatids can be used as a template. Another repair mechanism of DSBs is NHEJ, a rather error-prone mechanism, which plays a critical role during V(D)J recombination (Burma et al., 2006; Williams and Schumacher, 2016).

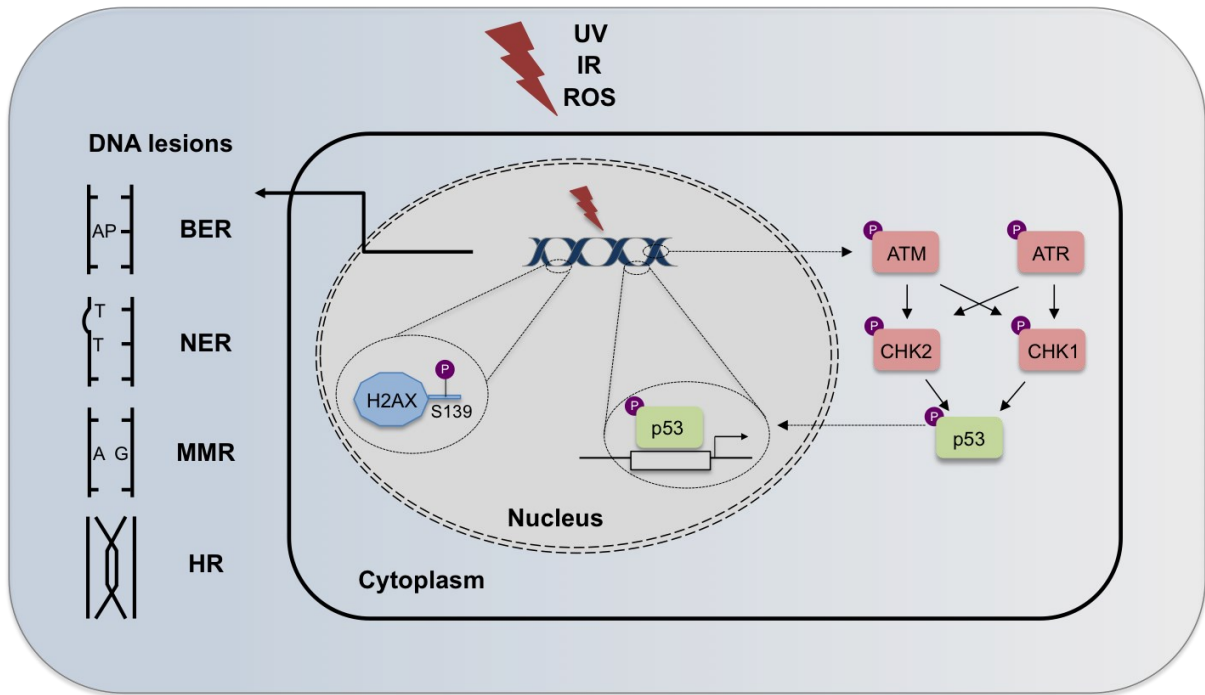


Figure 2: Overview of the DNA damage response pathway.

Genotoxic stressors such as ultraviolet (UV) light, irradiation (IR), or reactive oxygen species (ROS) can trigger DNA damage. The DNA damage response (DDR) ensures the integrity of the genome by detecting, signaling, and repairing these damages. One of the first events of DDR is the phosphorylation of the histone variant H2AX at serine (S) 139 (γ H2AX), serving as a docking site for repair factors. Depending on the type of DNA lesion, the kinases ataxia telangiectasia mutated (ATM) or ataxia telangiectasia and RAD3-related (ATR) get activated and phosphorylate (P) several downstream effectors, e.g., checkpoint kinase 1 (CHK1), checkpoint kinase 2 (CHK2), or p53. The transcription factor p53 can induce cell cycle arrest or apoptosis by the expression of several target genes. Different types of DNA lesions are repaired by specific repair mechanisms, including base excision repair (BER), nucleotide excision repair (NER), mismatch repair (MMR), or homologous recombination (HR). Adapted from (Mägdefrau et al., 2019).

1.4 The transcription factor Miz-1

1.4.1 Biochemistry of Miz-1

An important interaction partner of p53 as well as a regulator of its activity in developing T cells is the TF MYC-interacting zinc finger protein 1 (Miz-1) (Miao et al., 2010; Rashkovan et al., 2014). Originally, Miz-1 was discovered in a yeast two-hybrid screen as a partner protein of the cellular myelocytomatosis oncogene (c-MYC) (Peukert et al., 1997). The domain structure of the TF c-MYC comprises, among others, a basic helix-loop-helix (bHLH) domain and a leucine zipper (LZ). Both are important for dimerization and DNA binding (Conacci-Sorrell et al., 2014).

The murine gene *Zbtb17* (zinc finger and BTB domain-containing 17) encodes for the protein Miz-1, which consists of 794 amino acids (Peukert et al., 1997; Schulz et al., 1995). Miz-1 is composed of a Broad complex, Tramtrack, Bric à brac/poxvirus and zinc finger (BTB/POZ) domain located at the N-terminus and 13 C-terminal zinc fingers (ZnFs) of the C₂-H₂-type (Peukert et al., 1997; Schulz et al., 1995). The interaction with c-MYC was mapped between ZnF 12 and 13 of Miz-1, which build an α -helical structure that binds to the bHLH domain of c-MYC (**Figure 3**) (Peukert et al., 1997). The conserved POZ domain induces dimerization of Miz-1 monomers, followed by the formation of homotetramers (Stead et al., 2007). In addition, heterotetramerization of Miz-1 is possible by binding other POZ domain-containing factors like B cell lymphoma 6 (BCL-6) (Phan et al., 2005). Oligomerization of Miz-1 is required for its stable association with chromatin, assuring its function as a transcriptional regulator (Herold et al., 2002; Kosan et al., 2010). However, direct DNA binding is performed by ZnF motifs. N-terminal ZnFs are needed to scan the DNA for the consensus sequence, while C-terminal ZnFs perform DNA binding itself (Barrilleaux et al., 2014; Bédard et al., 2017). Miz-1 associates to initiator (INR) regions of core promoters that contain a conserved sequence element (Staller et al., 2001; Wolf et al., 2013). However, binding to multiple independent motifs is possible, as other DNA consensus sequences are known for Miz-1 (Barrilleaux et al., 2014).

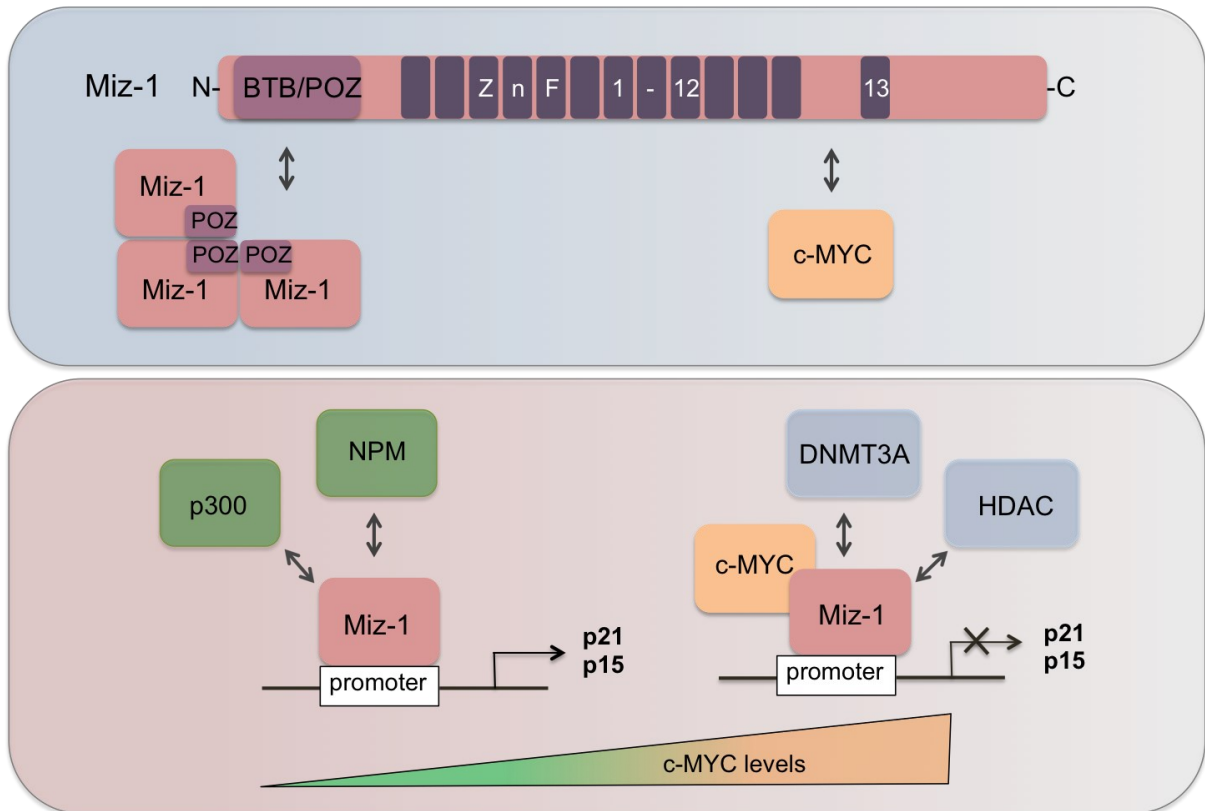


Figure 3: Structure and functions of Miz-1.

The upper panel shows the protein domains of the transcription factor MYC-interacting zinc finger protein 1 (Miz-1). It consists of an N-terminal Broad complex, Tramtrack, Bric à brac/poxvirus and zinc finger (BTB/POZ) domain, necessary for multimerization with Miz-1 itself or other POZ domain-containing factors. Miz-1 contains also 13 zinc finger (ZnF) domains, some of which are important for its DNA binding capacity. An important interaction partner of Miz-1 is the cellular myelocytomatosis oncogene (c-MYC) and the interaction surface is mapped between ZnF 12 and 13 of Miz-1. The lower panel shows two functions of Miz-1 in regulating gene expression. In complex with the co-activators p300 or nucleophosmin (NPM), it activates the transcription of target genes encoding for cell cycle regulators such as p21 and p15. High intracellular c-MYC levels induce transcriptional repression by Miz-1 through their interaction and the replacement of the co-activators. Co-repressors, e.g., DNA methyltransferase 3A (DNMT3A) or several histone deacetylases (HDACs), are recruited and gene expression is repressed. Adapted from (Möröy et al., 2011).

1.4.2 Functions of Miz-1

Depending on the availability of co-factors, the TF Miz-1 can act as a transcriptional activator or repressor. Co-activators, such as the histone acetyltransferase (HAT) p300 or nucleophosmin (NPM), are required for the concerted activation of transcription (**Figure 3**) (Staller et al., 2001; Wanzel et al., 2008). Transcriptional activation by Miz-1 is a c-MYC-independent process. On the contrary, high intracellular levels of c-MYC induce its binding to Miz-1 and trigger transcriptional repression by co-activator replacement and the

recruitment of DNA methyltransferase 3A (DNMT3A) or histone deacetylases (HDACs) (Brenner et al., 2005; Seoane et al., 2002; Staller et al., 2001; Varlakhanova et al., 2011). Importantly, the expression and interaction of Miz-1 and c-MYC are highly relevant in tumorigenesis (Ross et al., 2019; van Riggelen et al., 2010). The TF c-MYC can also form a heterodimer with MYC-associated factor X (MAX), leading to transcriptional activation of target genes in a Miz-1-independent process (Blackwood and Eisenman, 1991). MAX and c-MYC bind the DNA at so-called enhancer (E)-boxes with CACGTG as a consensus sequence and use several co-regulators for sufficient transcriptional regulation (Eilers and Eisenman, 2008).

Physiological levels of *Myc* are crucial for executing lots of cellular functions, for instance, cell growth, proliferation, differentiation, and metabolism (Eilers and Eisenman, 2008). However, an aberrant expression of *Myc* in maturing lymphocytes can lead to malignant transformation and lymphomagenesis (Adams et al., 1985; Korać et al., 2017; Langenau et al., 2003). As the expression and interaction of Miz-1 and c-MYC is highly relevant in tumorigenesis (Ross et al., 2019; van Riggelen et al., 2010), MYC^{V394D} was generated to study the role of their interaction. This variant of c-MYC carries a point mutation at position 394 from valine (V) to aspartic acid (D) and it is deficient in binding Miz-1 (Gebhardt et al., 2006; Herold et al., 2002; Wu et al., 2003). Interestingly, transgenic MYC^{V394D} mice show a delay in the onset of lymphomagenesis (van Riggelen et al., 2010). Moreover, the lack of functional Miz-1 impairs lymphoma development induced by the oncogenic activity of c-Myc (Ross et al., 2019).

Besides complex formation with c-MYC, other inhibitory interactions of Miz-1 can be seen with co-repressors like BCL-6 or growth factor independent 1 (GFI-1) (Basu et al., 2009; Phan et al., 2005). The most prominent targets of Miz-1 are genes encoding for the negative cell cycle regulators p21 and p15, the anti-apoptotic factor BCL-2 or homeobox (Hox) genes (Patel and McMahon, 2007; Seoane et al., 2002; Staller et al., 2001; Varlakhanova et al., 2011).

Miz-1 protein is ubiquitously expressed during mouse embryogenesis, demonstrating its importance for embryonic development. A complete knockout (KO) of Miz-1 induces early embryonic lethality at embryonic day (E) 7.5 due to severe defects during gastrulation (Adhikary et al., 2003). This observation revealed the necessity of mouse models with a conditional KO of Miz-1 by using Cre/loxP systems. Transgenic mice were generated where exons 3 and 4 of *Zbtb17*, encoding for the POZ domain of Miz-1, are flanked by loxP sites (fl) (Kosan et al., 2010). Cre-mediated recombination allows for the specific POZ domain deletion at the genomic level, resulting in a truncated form of Miz-1 termed Miz-1^{ΔPOZ}. As Miz-1^{ΔPOZ} is impaired in stable chromatin binding, the transcriptional function

of Miz-1 is consequently disrupted (Herold et al., 2002; Kosan et al., 2010; Wanzel et al., 2008). Tissue-specific Cre expression revealed various functions of Miz-1, for example in the central nervous system where it regulates autophagy. Miz-1 was shown to maintain the autophagic flux and, thus, prevents neurodegeneration (Wolf et al., 2013). Furthermore, the use of another Cre recombinase revealed an important function of Miz-1 in keratinocytes, controlling hair follicle proliferation and differentiation (Gebhardt et al., 2007). A critical role in keratinocytes was also observed during skin tumorigenesis. The expression of Miz-1^{ΔPOZ} restricted tumor growth in chemically induced, Ras-dependent tumors concomitant with altered p21 levels (Hönnemann et al., 2012). Moreover, Miz-1 was shown to exert an important role in the suppression of LPS-induced inflammation in the lungs. Here, phosphorylation of Miz-1 at S178 was necessary to repress the gene *CCAAT/enhancer-binding protein delta (Cebpd)*, an amplifier of inflammation (Domehara et al., 2013).

Besides its important role in transcriptional regulation, Miz-1 controls cytoplasmic signaling pathways in a transcription-independent manner without the necessity of the POZ domain. Miz-1 is associated with the c-Jun N-terminal kinase 1 (JNK1), a kinase activated by the pro-inflammatory cytokine TNF- α . Activation of JNK1 needs the K63-linked polyubiquitination of TNF receptor-associated factor 2 (TRAF2), which is selectively inhibited by Miz-1 (Liu et al., 2012; Liu et al., 2009). Upon TNF- α stimulation, K48-linked polyubiquitination of Miz-1 is induced by the E3 ligase Mule (Yang et al., 2010). This leads to the subsequent proteasomal degradation and, thus, Miz-1-mediated suppression of JNK1 activation is relieved (Liu et al., 2012; Liu et al., 2009).

1.4.3 Miz-1 in hematopoiesis

The importance of Miz-1 in hematopoiesis is demonstrated by severe developmental defects of hematopoietic cells lacking functional Miz-1 (Kosan et al., 2014; Kosan et al., 2010; Saba et al., 2011b). Miz-1 is expressed in lymphoid organs such as the thymus and the spleen, but also in B and T lymphocytes (Kosan et al., 2010). A critical role of Miz-1 during early hematopoiesis was discovered using a Vav-Cre transgene for the POZ domain deletion of Miz-1 in all hematopoietic cells. B lymphocytes lacking functional Miz-1 show a developmental block during the transition from pre-pro B cells to pro B cells (Kosan et al., 2010). Similarly, T lymphocytes lacking functional Miz-1 exhibit developmental defects at the ETP/DN1/DN2 stage and the DN3 stage of differentiation, leading to a strong reduction of thymic cellularity (Saba et al., 2011a; Saba et al., 2011b). Early development of lymphocytes relies on IL-7/IL-7R signaling to assure proliferation and survival (Corfe and Paige, 2012; Offner and Plum, 1998). Within this pathway, Miz-1

represses the suppressor of cytokine signaling 1 (SOCS1) and therefore allows the IL-7-mediated activation of Janus kinase (JAK) (Kosan et al., 2010; Saba et al., 2011b). Thereafter, activated JAK phosphorylates signal transducer and activator of transcription 5 (STAT5), leading to an IL-7-dependent expression of target genes such as BCL-2 (Chetoui et al., 2010; Jiang et al., 2005). The upregulation of BCL-2 by Miz-1 is indispensable for early lymphocyte survival as cells lacking functional Miz-1 exhibit increased apoptosis (Kosan et al., 2010; Saba et al., 2011b).

In developing B and T cells, physiological genome alterations occur during V(D)J recombination to produce a large repertoire of antigen receptors (Nemazee, 2000). As DNA damage and the activation of p53 can lead to apoptosis, it has been speculated whether a strong p53 induction needs to be regulated during V(D)J recombination (Dujka et al., 2010; Rashkovan et al., 2014). Interestingly, Miz-1-deficient DN3 T cell precursors exhibit an enhanced p53 response with upregulation of genes encoding for p21, PUMA, and NOXA (Saba et al., 2011a). Further analysis revealed that Miz-1 regulates p53 function and this is mediated via the ribosomal protein L22 (RPL22). Miz-1 activates the expression of *Rpl22* that in turn suppresses the translation of *p53* mRNA to restrict p53-dependent induction of apoptosis (Rashkovan et al., 2014).

Moreover, Miz-1 also controls early developmental steps of erythropoiesis, observed by decreased red blood cells in mice lacking functional Miz-1. Stress-induced erythropoiesis upon hemolysis was impaired in Miz-1-deficient mice, which points to a role of Miz-1 in stress response pathways (Kosan et al., 2014).

1.4.4 Miz-1 in stress response pathways

Cells encounter various stress signals affecting cell fate decisions. Interestingly, Miz-1 was shown to have several implications for the regulation of stress responses (Herold et al., 2002; Miao et al., 2010; Wanzel et al., 2005). Stress signals, for instance, mitogenic stimuli, activate the tumor suppressor alternative reading frame (ARF; human: p14^{ARF}, murine: p19^{ARF}), which stabilizes the tumor suppressor p53 (Kamijo et al., 1998; Vousden and Lu, 2002; Zindy et al., 1998). Both, ARF and p53 were found to interact with Miz-1 by competing for its binding (Miao et al., 2010). A complex of Miz-1 and p53 suppresses p53-mediated functions as its DNA-binding domain is blocked through this interaction (Miao et al., 2010). ARF binding to Miz-1 releases the TF p53 and enables target gene expression, indicating the impact of Miz-1 on the outcome of the p53 response (Miao et al., 2010). Miz-1 can also interfere with p53 function after the induction of physiological DNA damage, which occurs during somatic recombination. By activating *Rpl22* expression through Miz-1, translation of *p53* mRNA is negatively regulated and apoptosis restricted

(Rashkovan et al., 2014). An additional function of the ARF and Miz-1 interaction was elucidated, showing that ARF can disrupt the interaction of Miz-1 with the coactivator NPM. ARF facilitates the sumoylation of Miz-1 and promotes the repressive Miz-1/c-MYC complex formation (Herkert et al., 2010).

Another regulator of DDR is the topoisomerase II β binding protein 1 (TopBP1). AKT phosphorylates TopBP1, which allows its binding to Miz-1 in unperturbed cells (Herold et al., 2002; Liu et al., 2006; Yamane et al., 2002). This complex formation disables Miz-1 to activate target genes like *Cdkn1a* (Herold et al., 2002; Liu et al., 2006). UV exposure restricts the expression of TopBP1 and releases Miz-1 from the interaction, leading to the upregulation of *Cdkn1a* and cell cycle arrest induction (Herold et al., 2002). By c-MYC binding to Miz-1, target genes are repressed, allowing the cell to recover from UV-mediated cell cycle arrest (Herold et al., 2002). Interestingly, Miz-1 recruits a fraction of cellular TopBP1 to chromatin, preventing its degradation and making it accessible for DDR (Herold et al., 2008). Thus, Miz-1 is part of the ATR-dependent DDR pathway (Herold et al., 2008).

After DNA damage, gene expression repertoire has to adapt to fulfill the new demands of the cell. This switch is, among others, realized by AKT kinase-mediated phosphorylation of Miz-1 at position S428 after DNA damage (Wanzel et al., 2005). This PTM enables the interaction of Miz-1 with the phospho-binding protein 14-3-3 η , leading to inhibition of Miz-1 function by blocking its DNA-binding domain (Wanzel et al., 2005). Hence, Miz-1 has two functions after DNA damage: Firstly, it activates genes such as *Cdkn1a*, but later it represses these targets (Wanzel et al., 2005). Interestingly, the cell fate decision between cell cycle arrest and apoptosis is realized by c-MYC (Seoane et al., 2002; Vousden, 2002). Complex formation of Miz-1 with c-MYC represses the gene encoding for p21 and blocks its induction by p53, favoring apoptosis induction after induced DNA damage (Seoane et al., 2002; Vousden, 2002).

Aim of the thesis

Protection of the host against pathogens needs innate and adaptive immunity, whereas the latter is dependent on functional T and B lymphocytes. An important factor for lymphocyte development is the transcription factor Miz-1. Mice lacking the POZ domain of Miz-1 in early hematopoietic progenitor cells display several perturbations during T cell development in the thymus accompanied by developmental blocks and high levels of apoptosis. However, a potential role of Miz-1 in mature, peripheral T cells remains elusive and was, therefore, an aim of this thesis.

For this purpose, immune phenotyping of several T cell populations from secondary lymphoid organs of Miz-1-deficient mice (Vav-Cre x Miz-1^{fl/fl}) should be performed by using flow cytometry. The mentioned function of Miz-1 in lymphocyte development was discovered in this mouse model, which possesses a Vav-Cre-dependent functional deletion of the Miz-1 POZ domain. However, this deletion is already present early during T cell development, thereby affecting progenitor T cells, and also in other immune cells such as B cells. Thus, another mouse model with a T cell-specific deletion should be generated (CD4-Cre x Miz-1^{fl/fl}). After evaluating the efficiency of the POZ domain deletion, immune phenotyping should also be performed using this mouse model. Furthermore, functional analysis of Miz-1-deficient T cells should provide insights into the role of Miz-1 in T cell function. Cell cycle and apoptosis should be examined after the isolation and activation of peripheral T cells. Furthermore, following activation of these T cells, gene expression of Miz-1 target genes or genes relevant for apoptosis should be analyzed to gain a better understanding of the role of Miz-1 in T cell function.

Because Miz-1 is known to have several implications in stress response pathways, it should be investigated whether it plays a role during the DNA damage response in T cells. After applying γ -irradiation to Miz-1-deficient T lymphocytes, apoptosis rates, as well as gene expression analysis, should be performed and compared to controls. To study the potential role of Miz-1 in the process of DNA repair, Comet assays ought to be conducted after DNA damage induction by γ -irradiation.

The immune system is not exempted from alterations occurring due to aging and multiple age-related changes in T cells are known. In sum, these alterations to immune cells lead to a higher vulnerability of the elderly to infectious diseases. Thus, immune phenotyping of Miz-1-deficient T cell populations should also be performed in an aged mouse cohort.

Here, flow cytometry analysis should be utilized to investigate the role of Miz-1 for aged T lymphocytes.

Taken together, the results of this thesis ought to gain a broader understanding of the function of Miz-1 for peripheral T cell homeostasis, T cell activation as well as aging.

2. Materials

2.1 Mice strains

Wild-type (WT) and genetically engineered mice strains (**Table 1**) were housed under specific-pathogen-free (SPF) conditions in the Experimental Biomedicine Unit at the University of Jena (Bioinstrumentenzentrum, Winzerlaer Strasse 2, 07745 Jena). Breeding of mice was carried out according to the registration number 02-053/16. Maintaining of mice was conducted in compliance with the European guideline 2010/63/EU. Mice were sacrificed by cervical dislocation or CO₂ inhalation, depending on the scientific question.

Table 1: List of mice strains.

Strain/Allele Symbol	Source
C57BL/6JRj (wild-type)	Janvier Labs
<i>Commd10</i> ^{Tg(Vav1-icre)A2Kio} (Vav-Cre)	The Jackson Laboratory (de Boer et al., 2003)
Tg(Cd4-cre)1Cwi (CD4-Cre)	The Jackson Laboratory (Lee et al., 2001)
<i>Zbtb17</i> ^{tm1Cksn} (Miz-1 ^{fl/fl})	The Jackson Laboratory (Gebhardt et al., 2007; Kosan et al., 2010)

2.2 Chemicals

Table 2: List of chemicals.

Chemical	Source
Agarose	Merck KGaA
Albumin Fraction V (bovine serum albumin, BSA)	Merck KGaA
Ammonium chloride (NH ₄ Cl)	Carl Roth GmbH
Boric acid (H ₃ BO ₃)	AppliChem GmbH
1-Bromo-3-chloropropane	Merck KGaA
Bromophenol blue	SERVA Electrophoresis GmbH
Carboxyfluorescein succinimidyl ester (CFSE)	Thermo Fisher Scientific Inc.
4',6-Diamidino-2-phenylindole (DAPI)	Merck KGaA

Dimethyl sulfoxide (DMSO)	Merck KGaA
Ethanol	Carl Roth GmbH
Ethidium bromide	Carl Roth GmbH
Ethylenediaminetetraacetic acid (EDTA)	Carl Roth GmbH
Gelatine	Carl Roth GmbH
Gentamicin solution	Merck KGaA
Glycerol	Carl Roth GmbH
Glycine	AppliChem GmbH
Hydrogen chloride (HCl)	Carl Roth GmbH
2-Hydroxyethyl agarose Type VII	Merck KGaA
4-(2-Hydroxyethyl)-1-piperazineethanesulfonic acid (HEPES)	Merck KGaA
Isopropyl alcohol	Carl Roth GmbH
Magnesium chloride (MgCl ₂)	Merck KGaA
2-Mercaptoethanol	Carl Roth GmbH
Milk powder	Saliter
N-Lauroyl sarcosine sodium salt	Merck KGaA
Nonidet P40 (NP-40)	Carl Roth GmbH
Phosphate-buffered saline (PBS)	Merck KGaA
Potassium dihydrogen orthophosphate (KH ₂ PO ₄)	Merck KGaA
Potassium chloride (KCl)	Carl Roth GmbH
Propidium iodide (PI)	Carl Roth GmbH
Sodium bicarbonate (NaHCO ₃) solution (7.5%)	Merck KGaA
Sodium chloride (NaCl)	Carl Roth GmbH
Sodium dodecyl sulfate (SDS), pellets	Carl Roth GmbH
Sodium hydroxide (NaOH) solution, 1N	Carl Roth GmbH
Sodium phosphate dibasic hydrate (Na ₂ HPO ₄ x 2H ₂ O)	Merck KGaA
Trichloromethane (CHCl ₃)	Carl Roth GmbH
Tris(hydroxymethyl)aminomethane (TRIS)	Carl Roth GmbH
Tween®20	Carl Roth GmbH
Xylene cyanole	SERVA Electrophoresis GmbH

2.3 Reagents, kits, and enzymes

Table 3: List of reagents, commercial kits, and enzymes.

Reagent	Source
Annexin V Apoptosis Detection Kit	Thermo Fisher Scientific Inc.
Anti-mouse CD3 (Ultra-LEAF™ Purified), Clone 17A2	BioLegend Inc.
Anti-mouse CD28 (Ultra-LEAF™ Purified), Clone 37.51	BioLegend Inc.
Direct-zol™ RNA MiniPrep	Zymo Research
DNase I	Merck KGaA
dNTP-Mix (10 mM)	Thermo Fisher Scientific Inc.
EasySep™ Mouse T cell Isolation Kit	STEMCELL™ Technologies
EasySep™ Mouse CD4 ⁺ T cell Isolation Kit	STEMCELL™ Technologies
EasySep™ Mouse CD8 ⁺ T cell Isolation Kit	STEMCELL™ Technologies
ECL (enhanced chemiluminescence) Western Blotting Substrate (Pierce)	Thermo Fisher Scientific Inc.
Fetal calf serum (FCS)	Merck KGaA
First Strand cDNA Synthesis Kit	Thermo Fisher Scientific Inc.
GeneRuler DNA Ladder Mix	Thermo Fisher Scientific Inc.
GlycoBlue™ Coprecipitant	Thermo Fisher Scientific Inc.
PageRuler™ Prestained Protein Ladder	Thermo Fisher Scientific Inc.
PowerUp™ SYBR® Green Master Mix	Thermo Fisher Scientific Inc.
Proteinase K	Thermo Fisher Scientific Inc.
RiboLock, RNase Inhibitor	Thermo Fisher Scientific Inc.
RNAPure™, peqGOLD	VWR International Ltd.
RNase A	Thermo Fisher Scientific Inc.
Roswell Park Memorial Institute (RPMI)-1640 medium	Merck KGaA
Roti®-Nanoquant	Carl Roth GmbH
Taq DNA Polymerase	produced in-house, Kosan group
TRI Reagent®	Merck KGaA

2.4 Antibodies

Table 4: List of antibodies for flow cytometry.

Specificity	Conjugate	Clone	Host	Source
CD4	FITC	RM4-5	Rat	BioLegend Inc.
CD8a	PE	53-6.7	Rat	Thermo Fisher Scientific Inc.
CD11b	FITC	M1/70	Rat	BioLegend Inc.
CD44	APC	IM7	Rat	Thermo Fisher Scientific Inc.
CD45R/B220	APC	RA3-6B2	Rat	Thermo Fisher Scientific Inc.
CD62L	PerCP-Cy5.5	MEL-14	Rat	Thermo Fisher Scientific Inc.
CD90.2	APC-Cy7	30-H12	Rat	BioLegend Inc.

APC – allophycocyanine, FITC – fluorescein isothiocyanate, PE – phycoerythrin, PerCP-Cy5.5 - peridinin-chlorophyll-protein complex-Cyanine5.5.

Table 5: List of antibodies for Western Blot.

Specificity	Clone	Host	Source
Cleaved Caspase 8 (Asp 387)	Polyclonal	Rabbit	Cell Signaling Technology Inc.
GAPDH	Polyclonal	Rabbit	Merck KGaA
Phospho-H2A.X (Ser139)	JBW301	Mouse	Merck KGaA
PUMA	Polyclonal	Rabbit	Cell Signaling Technology Inc.
p21	F-5	Mouse	Santa Cruz Biotechnology
α -Tubulin	B-5-1-2	Mouse	Merck KGaA
HRP-linked anti-mouse	Polyclonal	Goat	Merck KGaA
HRP-linked anti-rabbit	Polyclonal	Goat	Merck KGaA

Asp – aspartic acid, GAPDH - glyceraldehyde-3-phosphate dehydrogenase, HRP - horseradish peroxidase, PUMA - p53 up-regulated modulator of apoptosis, Ser – serine.

2.5 Primers

Table 6: List of primers for genotyping.

Primer	Sequence 5'-3'	Product
Miz-1_P1	GTATTCTGCTGTGGGGCTATC	wt: 277 bp
Miz-1_P2	GGCTGTGCTGGGGGAAATC	fl: 327 bp
Miz-1_P3	GGCAGTTACAGGCTCAGGTG	Δ POZ: 209 bp
CD4-Cre_For	CCTGGAAAATGCTTCTGTCCGTTT	300 bp
CD4-Cre_Rev	ACGAACCTGGTCGAAATCAGTGCG	
IMR0336	ATAGGTCGGCGGTTTCAT	548 bp
IMR0337	CCCGAGTATCTGGAAGACAG	
mRag1.1	GCTGATGGGAAGTCAAGCGAC	295 bp
mRag1.3	GGGAACTGCTGAACTTTCTGTG	
mVav1.2	GTCACAAAAGAGGAAGTGGTG	490 bp
Cre11	TCCCTGAACATGTCCATCAGG	

fl – flanked by loxP sites (floxed), WT – wild-type.

Table 7: List of murine primers used for qRT-PCR.

Gene	Forward Primer 5'-3'	Reverse Primer 5'-3'
<i>Actb</i> (β -Actin)	CTAAGGCCAACCGTGAAAAG	ACCAGAGGCATACAGGGACA
<i>Bbc3</i> (PUMA)	TTCTCCGGAGTGTTTCATGC	TACAGCGGAGGGGCATCAG
<i>Bcl2</i> (BCL-2)	TCGCTACCGTCGTGACTTC	AAACAGAGGTCGCATGCTG
<i>Bcl2l4</i> (BAX)	TGTTTGCTGATGGCAACTTC	GATCAGCTCGGGCACTTTAG
<i>Cdkn1a</i> (p21)	GACAAGAGGCCAGTACTTC	TAGAAATCTGTCAGGCTGGT
<i>Pmaip1</i> (NOXA)	CAGATGCCTGGGAAGTCG	TGAGCACACTCGTCCTTCAA

BAX - BCL-2-associated protein X, BCL-2 - B cell lymphoma 2, PUMA - p53 up-regulated modulator of apoptosis.

2.6 Consumables and devices

Consumables, such as 15 ml and 50 ml conical tubes, cell culture plates and flasks, as well as pipette tips, were purchased from Greiner Bio-One International GmbH. Round bottom tubes for flow cytometry and 1.5 ml reaction tubes were purchased from Sarstedt Inc. Syringes were used from BD Bioscience Inc. and needles were purchased from B. Braun Melsungen AG.

2.7 Software

Table 8: List of used software.

Software	Source
BD FACSDiva™ v8.0.1	BD Biosciences Inc.
CometScore™ v1.5	Tritek Corp
FlowJo® 9.9.6	FlowJo, LLC
FusionCapt Advance™ 17.04	Vilber Lourmat GmbH
ModFit LT™ v4.1	Verity Software House
NIS Element AR v4.5	Nikon Corporation
Photoshop® CS6	Adobe Inc.
Prism 8.0.0	GraphPad Software Inc.
StepOne™ v2.3	Life Technologies

3. Methods

3.1 Cell culture methods

3.1.1 Isolation of primary T cells

Isolation of splenic cells was performed by using spleens of young and old mice. After sacrificing mice, spleens were collected, covered in PBS, and passed through a 70 µm strainer for generating single-cell suspensions. A centrifugation step at 700 g for 5 min followed and the supernatant was aspirated. Cells were resuspended in RCL buffer and incubated for 5 min at room temperature (RT) for erythrocyte lysis. The reaction was stopped with ice-cold PBS and a second centrifugation step was applied (700 g, 5 min). For isolation of primary T cells, pelletized splenic cells were resuspended in PBS supplemented with 1% FCS and isolation was done by using the EasySep™ Mouse T cell Isolation Kit. According to the manufacturer's protocol, T lymphocytes were isolated via negative selection using biotinylated antibodies directed against non-T cells. Therefore, the antibody cocktail was added to the single-cell suspension and incubated for 10 min at RT to enable antibody binding. Afterward, streptavidin-coated magnetic particles were added for 2.5 min and the tube containing the mixture was placed for another 2.5 min into the EasySep™ magnet. Primary T cells were poured off into a fresh tube while all non-T cells were retained in the magnet. Also, CD4⁺ and CD8⁺ T cells were isolated by using the EasySep™ Mouse CD4⁺ T cell Isolation Kit and the EasySep™ Mouse CD8⁺ T cell Isolation Kit, respectively.

Isolation of cells from lymph nodes was performed as described for spleens but with an erythrocyte lysis step of 2 min only. For isolation of thymocytes, thymuses were resuspended in RCL buffer for 5 min. Peripheral blood collection was done by cardiac puncture post-partum. The blood was transferred into EDTA-containing tubes. Erythrocyte lysis of blood was performed twice, each with a 5 min incubation time and with PBS washing steps in between.

RCL buffer: 8.3 g/l ammonium chloride, 0.01 M Tris-HCl (pH 7.4)

3.1.2 Cultivation of primary T cells

For T cell cultivation, isolation was performed under sterile conditions. After negative isolation, cells were resuspended in RPMI-1640 medium with particular supplements. For

proper activation of T cells, optimal concentrations of anti-CD3 and anti-CD28 antibodies were determined. 12-well plates were pre-coated overnight with anti-CD3 (5 µg/ml) diluted in PBS. The next day, PBS was aspirated and plates were washed once with PBS. T lymphocytes were seeded in a 12-well plate at a density of 10^6 cells per 1 ml of medium and anti-CD28 (2 µg/ml) was added for a complete activation. Cells were grown in incubators under sterile conditions with 5 % CO₂ and at 37 °C until harvested for subsequent experiments.

T cell medium: RPMI-1640, 10 % (v/v) FCS, 0.5 % (v/v) gentamicin, 10 mM HEPES, 50 µM β-mercaptoethanol

3.1.3 Irradiation experiments

Depending on the scientific question, isolated T cells were irradiated to induce DNA damage. For this purpose, the Gammcell GC40 irradiation chamber at the FLI Jena was used. Cells were exposed to 2 Gy of γ-radiation, before further cultivation at 37 °C followed.

3.2 Molecular biology methods

3.2.1 DNA isolation and genotyping

For DNA isolation, tail biopsies of mice were mixed with 50 µl DNA isolation buffer and 0.5 µl Proteinase K (20 mg/ml) and incubated overnight at 56 °C. Afterward, Proteinase K was inactivated for 5 min at 95 °C followed by a centrifugation step (12,000 g, 5 min) to remove cell debris and hairs. The supernatant contained the extracted DNA. For the DNA isolation from cells, about $1-5 \times 10^6$ cells were used and the same procedure was applied. Polymerase chain reaction (PCR) was used to amplify genomic regions of interest. For this purpose, 2 µl of DNA was mixed with 1x PCR buffer, 0.25 µl Taq polymerase, 0.25 µl dNTP mix (10 mM), and the respective primers (**Table 6**) in a total volume of 25 µl. In genotyping PCRs, primer pairs were included to specifically detect altered genomic regions as well as to amplify WT genes as a control. PCR runs were performed in thermocyclers from Biometra with conventional PCR programs and 35 amplification cycles. Afterward, a DNA loading buffer was added to the PCR products, and samples were loaded onto a 2 % (w/v) agarose gel with 0.5 µg/ml ethidium bromide. Separation of PCR products was performed in an electrophoresis chamber filled with 1x TBE buffer at

100 V. A DNA ladder was included in every electrophoresis run. Visualization of fragments was performed under UV light due to intercalation of the dye ethidium bromide into DNA.

DNA isolation buffer: 1X PCR buffer, 0.05 % (v/v) Tween®20, 0.05 % (v/v) NP-40

PCR buffer (1X): 10 mM Tris (pH 8.3), 50 mM KCl, 1.5 mM MgCl₂, 0.001 % (w/v) gelatine

DNA loading buffer: 50 % (v/v) glycerol, 250 mM EDTA (pH 8.0), 2 mg xylene cyanole

TBE buffer (1X): 89 mM Tris, 89 mM boric acid, 2 mM EDTA (pH 8.0)

3.2.2 RNA isolation

For isolating RNA of T lymphocytes, the cells were lysed in TRI Reagent® and 100 µl of 1-Bromo-3-chloropropane was added per 1 ml of TRI Reagent®. For improved visibility of the RNA during isolation steps, 1 µl of GlycoBlue™ Coprecipitant (15 mg/ml) was added. Samples were shaken vigorously, followed by a centrifugation step for 15 min at 12,000 g and 4 °C. The upper phase was transferred into a fresh tube and the same volume of ice-cold 2-propanol was added. The samples were stored overnight at -20 °C and centrifuged the next day for 10 min at 12,000 g and 4 °C. The supernatant was aspirated, the pellet washed in 1 ml of 75 % ethanol and samples spun down for 3 min at 12,000 g and 4 °C. The supernatant was removed and the washing step with ethanol was repeated. Afterward, the supernatant was removed entirely and the pellet was allowed to air dry for 3 min. RNA was dissolved by adding RNA-free water to the pellet followed by an incubation step for 1 min at 55 °C. The concentration and purity of RNA were measured using the NanoDrop™ 2000c device (Thermo Fisher Scientific Inc.).

3.2.3 Reverse transcription and quantitative real-time PCR

For DNA digestion, 1 µg of RNA was treated according to the manufacturer's protocol with deoxyribonuclease (DNase) I and 0.25 µl ribonuclease (RNase) inhibitor for 20 min. Afterward, RNA was reversely transcribed into complementary DNA (cDNA) by using the First Strand cDNA Synthesis Kit according to the manufacturer's protocol. A combination of oligo (dT)₁₈ and random hexamer primers was used for cDNA priming. Yielded cDNA was diluted in water in a 1:10 ratio.

Gene expression was analyzed using the quantitative real-time PCR (qRT-PCR) technique. For this, Power SYBR® Green PCR Master Mix was combined with cDNA and

specific primer pairs (each 200 pmol) in a MicroAmp™ Fast Optical 96-well reaction plate (Applied Biosystems), sealed with a MicroAmp™ Clear Adhesive Film (Applied Biosystems). The run was performed in a QuantStudio 3 PCR system (Thermo Fisher Scientific Inc.) with an initial denaturation step for 10 min at 95 °C. A two-step cycling protocol was applied with elongation and annealing at 60 °C for 40 cycles. Samples were run in triplicates and a negative control was included for every amplicon. Also, melting curves for each primer pair were generated in every run. Quantification of gene expression was analyzed using the comparative $\Delta\Delta C_t$ method and *Actb* (β -Actin) messenger RNA (mRNA) was used for normalization.

3.3 Protein biochemistry methods

3.3.1 Preparation of cell lysates

For protein isolation, T cells were centrifuged for 5 min at 700 g and washed once in PBS. After another centrifugation step, the supernatant was entirely removed and the pellet was lysed in cell lysis buffer supplemented with a protease inhibitor cocktail (PIC) for 30 min on ice. For entire cell lysis, samples were sonicated for 3 min, followed by centrifugation for 10 min at 12,000 g. The supernatant containing the proteins was transferred into a fresh tube and stored at -20 °C or used immediately for further analysis. Protein concentration was measured using the Roti®-Nanoquant solution according to the manufacturer's protocol. For calculations, a standard curve was generated using different BSA concentrations. 50 μ g of each sample was mixed with 6X Laemmli buffer to a final concentration of 1X and boiled afterward at 95 °C for 5 min.

Cell lysis buffer: 1 M Tris (pH 7.5), 1 M NaCl, 0.5 M EDTA, 10 % (v/v) NP-40

Laemmli buffer (6X): 35 % (v/v) β -mercaptoethanol, 350 mM Tris-HCl (pH 6.8), 30 % (v/v) glycerol, 10 % (w/v) SDS, 0.25 % (w/v) bromophenol blue

3.3.2 SDS-PAGE and Western Blot

Separation of proteins was performed by SDS polyacrylamide gel electrophoresis (SDS-PAGE) using a discontinuous Tris-buffer system. For this, the protein samples were loaded onto gels consisting of a 10-12 % (v/v) polyacrylamide/bisacrylamide separating gel, covered with a 5 % (v/v) stacking gel. In every gel run, a PageRuler™ Prestained Protein Ladder was included to estimate the molecular weight of the proteins of interest.

Electrophoresis was done in electrophoresis chambers filled with 1X SDS running buffer and separation proceeded at 70 V (stacking gel), followed by 100 V (separation gel). Proteins were transferred to a polyvinylidene fluoride (PVDF) membrane, which was activated in ethanol beforehand. The gel and the membrane were placed between sheets of Whatmann® chromatography paper and soaked in 1X Towbin buffer. The Western Blot was performed in a blotting chamber filled with 1X Blotting buffer for 1.5 h at 150 mA per gel. After the protein transfer, the membrane was washed firmly in PBS-T. To block non-specific binding to the membrane, it was incubated in a 5 % (w/v) solution of non-fat dry milk powder (Saliter) dissolved in PBS-T for 1 h at RT. Afterward, the membrane was incubated with the primary antibody in 2 % (w/v) non-fat dry milk solution in PBS-T overnight at 4 °C. The next day, the membrane was washed 3 times for 10 min in PBS-T and incubated with the horseradish peroxidase (HRP)-conjugated secondary antibody for 1 h at RT. Again, 3 washing steps in PBS-T for 10 min each were applied. Visualization of the proteins was done using ECL Western Blotting Substrate and the Fusion Solo 4S system (Vilber Lourmat) with the FusionCapt Advance 17.04 software (Vilber Lourmat). For further analysis of proteins on the same membrane, a step-wise detection was applied by using primary antibodies of different host species.

SDS running buffer (10X):	2.5 M glycine, 250 mM Tris, 1 % (w/v) SDS
Towbin buffer (10X):	1.92 M glycine, 250 mM Tris
Blotting buffer (1X):	1X Towbin buffer, 20 % (v/v) ethanol
PBS (10X):	1.37 M NaCl, 27 mM KCl, 80 mM Na ₂ HPO ₄ x H ₂ O, 14 mM KH ₂ PO ₄
PBST-T (1X):	1X PBS, 0.05 % (v/v) Tween®20

3.4 Functional assays

3.4.1 Flow cytometry analysis and cell sorting

Detection and quantification of different cell populations were performed by using the flow cytometry approach. For immune cell phenotyping, cell suspensions were washed in PBS and centrifuged for 5 min at 700 g. The pellet was resuspended in PBS and staining with the according fluorophore-coupled antibodies (0.1 µg each) was performed for 10 min on ice and in the dark. After another washing step in PBS, cell suspensions were resuspended in PBS and stained with DAPI at a final concentration of 0.1 µg/ml to exclude dead cells. Analysis was done using the LSRFortessa™ system (BD Biosciences

Inc.) and data were acquired with the BD FACSDIVA™ v8.0.1 (BD Biosciences Inc.). Fluorescence of the respective antibodies, as well as forward scatter (FSC, size), and side scatter (SSC, granularity) signals were recorded.

For the separation of certain cell populations, fluorescence-activated cell sorting (FACS) was performed at the Core Facility Flow Cytometry, FLI Jena with the help of Katrin Schubert. Cell suspensions were therefore stained as stated previously, resuspended in 0.5 % (w/v) BSA in PBS, and stained with DAPI before analysis. Sorted cell populations were collected and instantly used for further approaches.

3.4.2 Apoptosis assay

Detection of apoptotic cells was done using the Annexin V Apoptosis Detection Kit (Thermo Fisher Scientific Inc.). Annexin V binds to phosphatidylserine (PS), which translocates to the outer membrane when cells undergo apoptosis. According to the manufacturer's protocol, cell suspensions were stained with 5 µl Annexin V-FITC in 1X Annexin V staining buffer for 15 min in the dark at RT. A centrifugation step for 5 min at 700 g followed and cells were washed once in 1X Annexin V staining buffer. For analysis, cells were resuspended in 1X Annexin V staining buffer and 2 µl PI Staining Solution was added to distinguish between dead and apoptotic cells. Afterward, samples were directly measured in the flow cytometer.

3.4.3 Cell cycle analysis

The cell cycle distribution of T lymphocytes was analyzed using the dye PI, which is known to intercalate into DNA. Single-cell suspensions were washed once in PBS and centrifuged for 5 min at 700 g. The pellet was resuspended in 1 ml ice-cold 70 % (v/v) ethanol while shaking and stored overnight at -20 °C. The next day, 1 ml of PBS was added and another centrifugation step (5 min, 700 g) was applied. The pellet was resuspended in 390 µl PBS mixed with 5 µl RNase A (10 mg/ml) and 5 µl PI (2.5 mg/ml). Incubation at 37 °C for 20 min followed before samples were analyzed directly at the flow cytometer.

3.4.4 Proliferation assay

To track CD4⁺ or CD8⁺ T lymphocyte proliferation, 5 x 10⁶ negatively isolated cells were resuspended in PBS with 5 % (v/v) FCS. Next, 0.5 µl CFSE (10 mM) was added and samples were mixed thoroughly and incubated for 5 min at RT in the dark. In total, 3 washing steps in PBS/FCS were applied with centrifugation steps for 5 min at 700 g. Afterward, cells were resuspended in T cell medium, counted, and seeded in 12-well plates. T cell activation and cultivation were done in 12-well plates pre-coated with anti-CD3 (2 µg/ml). Anti-CD28 (2 µg/ml) was added directly to the medium. For 4-5 days, cells were harvested every 24 h, followed by flow cytometry to monitor CFSE intensity. As the fluorescent dye is equally distributed to daughter cells, the fluorescent intensity can be examined in the flow cytometer to gain information about the number of cell divisions. Data analysis was performed using the software ModFit LT™ v4.1 (Verity Software House).

3.4.5 Comet assay

Comet assays were performed to examine the repair capacity of T cells after IR exposure. For this approach, a 1 % (w/v) agarose (Type VII, low-melting) solution was prepared, frosted microscope slides were covered with 800 µl of this solution and air-dried overnight. On the second day, an alkaline lysis buffer was freshly prepared, the agarose solution was heated up and placed in a water bath at 43 °C. After IR was applied to the cell suspensions (300.000 cells per 1ml medium), challenged cells were either directly used (time point zero) in a Comet assay or were left for a certain time at 37 °C to repair the induced DNA breaks. Next, 30 µl of the sample was mixed with 120 µl PBS. 500 µl of the agarose solution was added and 350 µl of this mixture was rapidly pipetted onto the pre-coated microscope slides. An incubation step for agarose gelling of exactly 3 min on ice followed before the microscope slides were incubated in the alkaline lysis buffer overnight at 4 °C in the dark.

On the third day, slides were carefully washed 3 times for 10 min each by submerging them into rinsing buffer. Afterward, the slides were placed into a leveled electrophoresis chamber filled with rinsing buffer. Electrophoresis was conducted at 25 V for 18 min. Slides were neutralized by rinsing them several times with 400 ml of water. Staining was performed with 1 ml of PI (2.5 mg/ml) solution per slide for 20 min in the dark. Another rinsing step was performed with 400 ml of water to remove the excess dye. Analysis of the comet tails was done using the fluorescence microscope Nikon ECLIPSE Ti and the NIS Element AR v4.5 (Nikon Corporation) software. Every condition was imaged and at least

50 comets per slide were analyzed by using the Comet Score™ software (Tritek Corp) to calculate Tail Moments.

Lysis buffer: 1.2 M NaCl, 0.26 M NaOH, 100 mM EDTA, 1 % (w/v)
N-lauroylsarcosine sodium salt

Rinsing buffer: 0.03 M NaOH, 2 mM EDTA (pH 8.0)

3.5 Statistical analysis

Statistical analysis was performed using Prism software version 8.0.0 (Graphpad Software Inc.). Unless stated differently, results were expressed as arithmetic mean \pm standard deviation (SD). *P* values were calculated using either the Student's *t*-test or two-way analysis of variance (ANOVA), depending on the number of compared groups. Significance was determined at $P < 0.05$ and is indicated in the figures.

4. Results

4.1 The influence of Miz-1 deficiency on T cell populations in the Vav-Cre x Miz-1^{fl/fl} mouse model

4.1.1 Targeting strategy at the *Zbtb17* locus

The transcription factor Miz-1 is an important regulator of hematopoiesis (Möröy et al., 2011). Saba and colleagues showed that Miz-1 plays a crucial role in early T lymphocyte development (Saba et al., 2011b). However, little is known about the function of Miz-1 in mature T cells, so this thesis aims to uncover a possible role of Miz-1 in mature T lymphocytes. Since the complete deletion of Miz-1 induces early embryonic lethality (Adhikary et al., 2003), the Vav-Cre x Miz-1^{fl/fl} mouse model was utilized to achieve a conditional knockout (Kosan et al., 2010). As the POZ domain of Miz-1 is essential for binding target gene promoters, Vav-Cre-mediated recombination was used to delete the transcriptionally relevant POZ domain of Miz-1 in all hematopoietic cells (Kosan et al., 2010). To achieve a conditional deletion of Miz-1 in transgenic mice, exons 3 and 4, encoding the POZ domain, are flanked by loxP sites (floxed, fl) on the *Zbtb17* (Miz-1) locus, resulting in a truncated Miz-1^{ΔPOZ} protein (**Supplemental Figure 29**). Adult mice, carrying the *Zbtb17*^{fl/fl} alleles but lacking the Cre transgene, do not show phenotypic differences to C57BL/6 mice and were therefore used as control mice (Kosan et al., 2010).

4.1.2 Functional Miz-1 deletion results in a decline in peripheral T cell populations

To examine whether the loss of the Miz-1 POZ domain influences peripheral T cell populations, splenic cells of control and Miz-1-deficient mice were analyzed by flow cytometry. B and T cell populations were distinguished by the expression of lineage-specific surface markers. Adult mice showed a slight but not significant reduction in T cell (CD90.2⁺, B220⁻) frequencies from 40 % in controls to 31 % in Miz-1-deficient mice (**Figure 4A**). However, absolute numbers of mature T cells of the spleen were strongly reduced by the Miz-1 POZ domain deletion to about 10 % of control mice (**Figure 4B**). To assess the impact of Miz-1 on T cells in aged mice, two different age cohorts were analyzed. Classification of these cohorts was done according to the suggestions of the Jackson laboratory (Flurkey et al., 2007). Hence, 18 months old mice were regarded as

aged or old animals, whereas young mice between 2 and 4 months were termed as adult or young.

Analysis of the aged mouse cohort revealed no big differences in T cell frequencies of old control mice (31 %) and old Vav-Cre x Miz-1^{fl/fl} mice with 27 % (**Figure 4A**). Aged control mice possessed cell numbers of 1.3×10^7 T cells per spleen while old Miz-1-deficient mice had only 0.1×10^7 splenic T cells (**Figure 4B**).

The strong decline in peripheral T cells due to the loss of functional Miz-1 points to an important role of Miz-1 in the maintenance of the peripheral T cell pool in young and old mice, however, this effect does not increase with age.

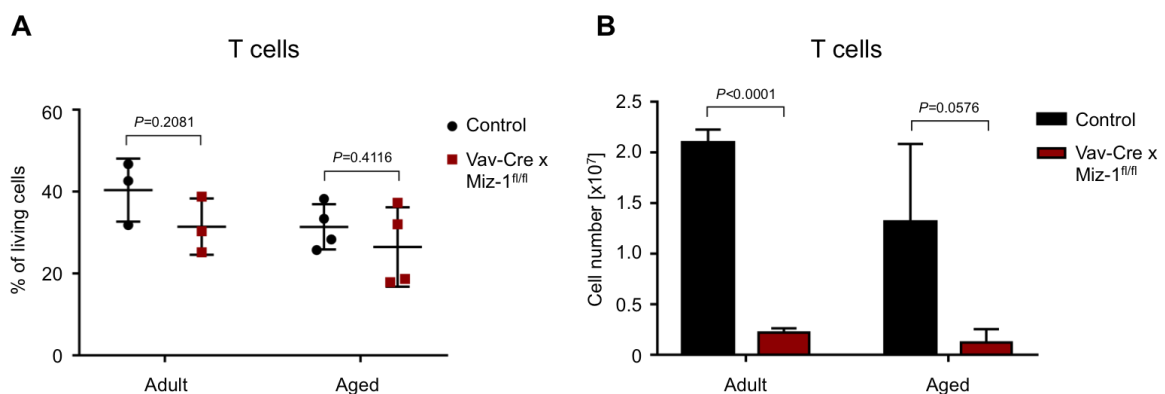


Figure 4: Loss of functional Miz-1 declines splenic T cells.

Splenocytes of control and Vav-Cre x Miz-1^{fl/fl} mice were analyzed with flow cytometry to compare T cell populations in adult (2 - 4 months) and aged (18 months) mouse cohorts. Antibodies against CD90.2 and B220 were utilized for staining lineage-specific surface markers. T cells (CD90.2⁺, B220⁻) were pre-gated on living cells (DAPI⁻) after debris exclusion by FSC/SSC scattering. Depicted are **(A)** T cell percentages as mean \pm SD and **(B)** absolute numbers of splenic T cells as mean + SD. *P* values were calculated using unpaired Student's *t*-test. Data are representative of at least 3 independent experiments.

To examine whether the loss of functional Miz-1 affects the composition of T cell subsets, negatively isolated T cells from spleens of adult control and Vav-Cre x Miz-1^{fl/fl} mice were analyzed by flow cytometry. The two major T cell populations, CD4⁺ T helper (T_H) cells and CD8⁺ cytotoxic T lymphocytes (CTLs), were distinguished by the expression of the surface markers CD4 and CD8, respectively (**Figure 5A**). In adult mice, loss of the Miz-1 POZ domain reduced T_H cell (CD4⁺, CD8⁻) frequencies from 57 % in controls to 25 % (**Figure 5B**). On the contrary, CTLs (CD4⁻, CD8⁺) displayed no significant change in percentages with 37 % in controls and 32 % in Miz-1-deficient mice (**Figure 5B**).

Absolute numbers of CD4⁺ T cells decreased substantially from 7.6×10^6 T_H cells in adult control mice to 0.5×10^6 T_H cells in Vav-Cre x Miz-1^{fl/fl} mice (**Figure 5C**). Likewise, absolute numbers of CD8⁺ T cells declined dramatically from 5.0×10^6 CTLs in control

mice to 0.7×10^6 cells in Vav-Cre x Miz-1^{fl/fl} mice (**Figure 5C**). Of note, a population of unknown origin (CD4⁻, CD8⁻) occurred in splenic T cells of Vav-Cre x Miz-1^{fl/fl} mice after T cell enrichment by negative isolation against non-T cells (**Figure 5A**).

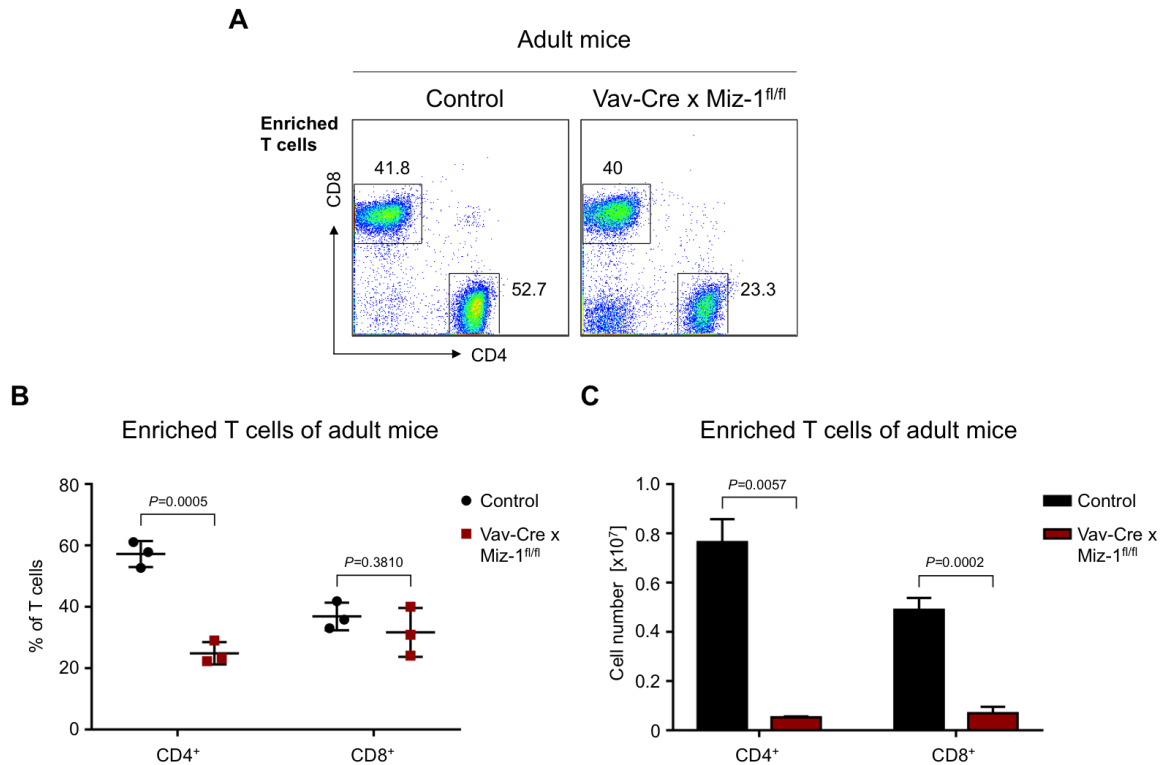


Figure 5: Miz-1 controls T cell subset composition of CD4⁺ and CD8⁺ T cells.

Splenic T cells of control and Vav-Cre x Miz-1^{fl/fl} mice were analyzed with flow cytometry using antibodies against CD4 and CD8. T cells of adult (2 - 4 months) mice were isolated by negative separation prior to flow cytometry analysis. **(A)** Representative plots of adult control and Vav-Cre x Miz-1^{fl/fl} mice after T cell enrichment are shown. Numbers adjacent to gates indicate the percentages of CD4⁺ (CD4⁺, CD8⁻) and CD8⁺ T cells (CD4⁻, CD8⁺) of the corresponding experiment after FSC/SSC debris exclusion. 3 independent experiments were conducted. **(B)** T cell subset composition of CD4⁺ and CD8⁺ cells after FSC/SSC debris exclusion is depicted as mean \pm SD. **(C)** Corresponding absolute numbers of these T cell subsets per spleen are shown as mean + SD. Unpaired Student's *t*-test was used to calculate *P* values indicated in the diagrams. If variances were unequal, unpaired Student's *t*-test with Welch's correction was applied. Data are representative of 3 (B, C) independent experiments.

The impact of Miz-1 on the distribution of T cell subsets was also examined in the aged mouse cohort. Flow cytometry plots illustrate the influence of the Miz-1 POZ domain deletion on the ratio of CD4⁺ and CD8⁺ cells in the spleen of aged mice (**Figure 6A**). The splenic CD4⁺ compartment remained unaffected in aged control and Miz-1-deficient mice and comprised less than 20 % (**Figure 6B**). Also, the frequency of CD8⁺ cells changed only slightly from 12 % in controls to 8 % in old Miz-1-deficient mice (**Figure 6B**).

In addition, aged Vav-Cre x Miz-1^{fl/fl} mice showed an insignificant reduction in absolute numbers of T_H cells to 8 % of control littermates (**Figure 6C**). Likewise, absolute numbers of CTLs declined insignificantly to about 7 % of control mice (**Figure 6C**). However, it should be noted that high variations within the aged cohort arose.

The obtained results show a substantial influence of Miz-1 on the T cell subset composition of CD4⁺ and CD8⁺ cells, with differences between the different age cohorts. Overall, a severe reduction of absolute numbers of T_H cells and CTLs was observed in Miz-1-deficient mice in accordance with the massive drop in peripheral T cells in the Vav-Cre x Miz-1^{fl/fl} mouse model.

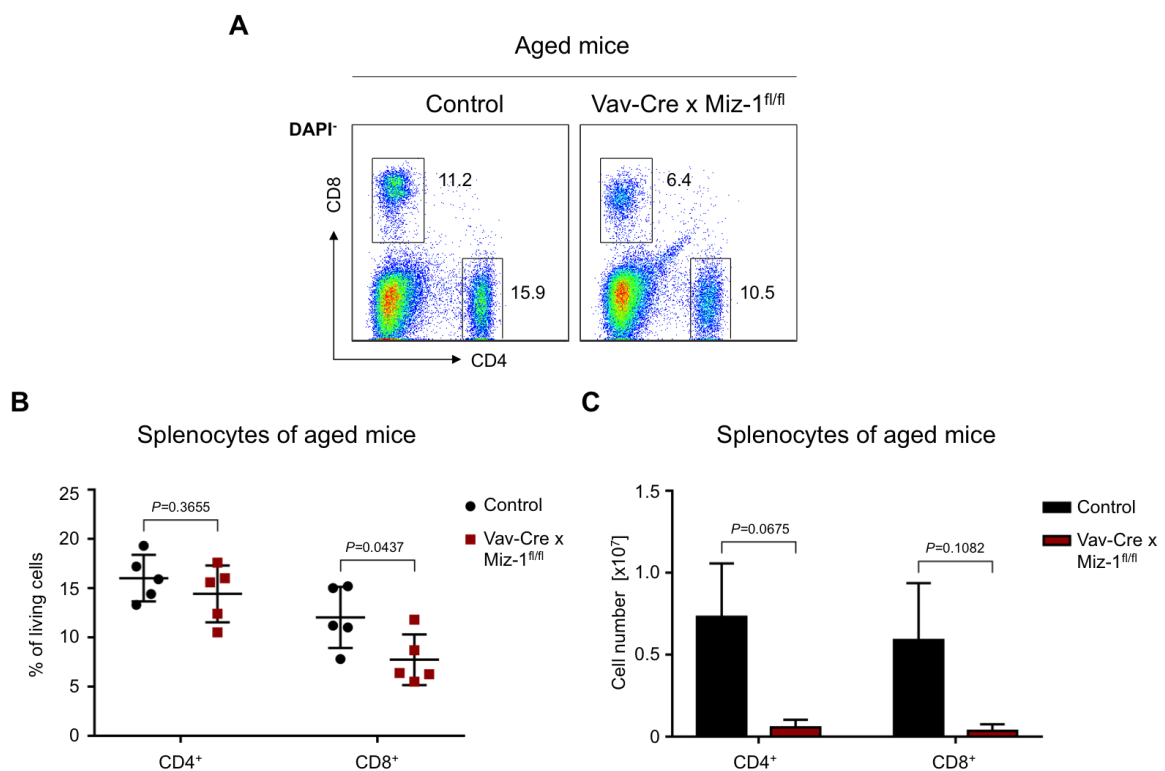


Figure 6: Miz-1 depletion affects CD4⁺ and CD8⁺ cells in aged mice.

Splenocytes of aged (18 months) control and Vav-Cre x Miz-1^{fl/fl} mice were analyzed by flow cytometry using antibodies against CD4 and CD8. **(A)** Representative flow cytometry plots show splenic cells derived from aged mice. Percentages of CD4⁺ (CD4⁺, CD8⁻) and CD8⁺ cells (CD4⁻, CD8⁺) of the represented experiment are indicated as numbers adjacent to gates. Cells were pre-gated on living cells (DAPI⁻) after FSC/SSC debris exclusion. 5 independent experiments were executed. **(B)** Frequencies of CD4⁺ and CD8⁺ cells after FSC/SSC debris exclusion and pre-gating on living cells (DAPI⁻) are shown as mean \pm SD. **(C)** Corresponding absolute numbers of these populations in the spleen are depicted as mean + SD. Unpaired Student's *t*-test was used to calculate *P* values indicated in the diagrams. If variances were unequal, unpaired Student's *t*-test with Welch's correction was applied. Data are representative of 5 (B) or 3 (C) independent experiments.

4.1.3 Loss of functional Miz-1 and aging decline the naïve T cell pool

To further examine the impact of Miz-1 on distinct T cell populations, central memory T (T_{CM}) cell, effector memory T (T_{EM}) cell as well as naïve T cell distributions were studied by flow cytometry. In addition to antibodies for CD4 and CD8, cells were co-stained with antibodies against the activation marker CD44 and the T cell homing factor CD62L to phenotypically distinguish the following subsets: naïve T cells ($CD44^{lo}$, $CD62L^{hi}$), T_{CM} cells ($CD44^{hi}$, $CD62L^{hi}$), and T_{EM} cells ($CD44^{hi}$, $CD62L^{lo}$). These populations were analyzed for the $CD4^+$ and the $CD8^+$ compartment, respectively. All analyses were performed for control and Miz-1-deficient mice of both age cohorts.

Analysis of these T cell populations and their distribution in the $CD4^+$ compartment is shown for adult Vav-Cre x Miz-1^{fl/fl} mice as well as for control mice (**Figure 7A**). Naïve $CD4^+$ T cell frequencies had a 2.5-fold reduction in Vav-Cre x Miz-1^{fl/fl} mice compared to controls (**Figure 7B**). T_{CM} cells of the $CD4^+$ compartment were not changed in adult Miz-1-deficient mice. However, 4-fold increased T_{EM} cell frequencies were observed in the absence of functional Miz-1 relative to controls (**Figure 7B**).

Absolute numbers of naïve, T_{CM} as well as T_{EM} cells had an overall decline in the $CD4^+$ compartment of adult Miz-1-deficient mice compared to controls (**Supplemental Figure 30A**). The observed reduction in absolute cell counts is presumably reasoned in the overall decrease of mature T cells due to loss of functional Miz-1.

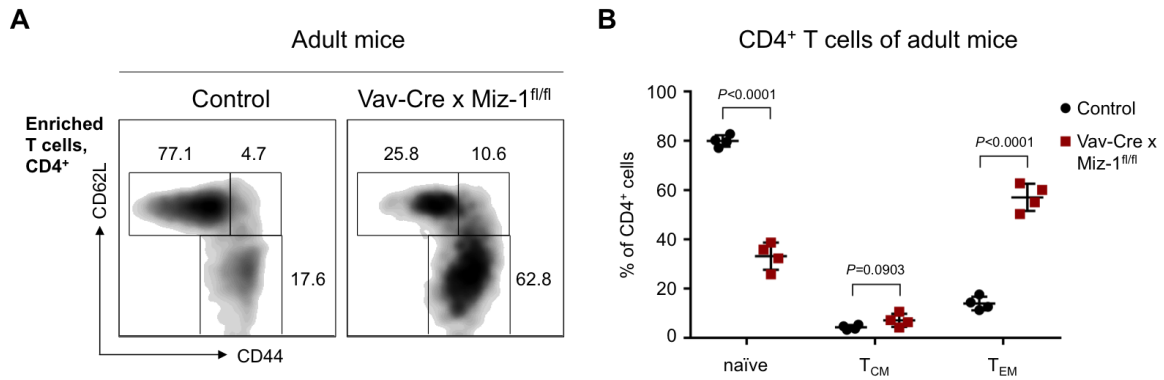


Figure 7: Miz-1 deficiency increases CD4⁺ effector memory T cell frequencies.

Splenic T cells of adult (2 – 4 months) control and Vav-Cre x Miz-1^{fl/fl} mice were used to analyze the distribution of naïve (CD44^{lo}, CD62L^{hi}), central memory (T_{CM}; CD44^{hi}, CD62L^{hi}), and effector memory T cells (T_{EM}; CD44^{hi}, CD62L^{lo}) within the CD4⁺ compartment. The antibodies CD4, CD8, CD44, and CD62L were used to distinguish these subsets by flow cytometry. T cells were enriched by negative selection before staining. Debris was excluded via FSC/SSC scattering. **(A)** Representative plots depict the distribution of T cell subsets in adult mice after FSC/SSC debris exclusion. Numbers next to gates indicate the percentage of these subsets of the corresponding experiment. In total, 4 independent experiments were performed. **(B)** Frequencies of cell populations pre-gated on CD4⁺ T cells are shown for adult mice as mean ± SD. *P* values were calculated using unpaired Student's *t*-test. Results were obtained from 4 independent experiments.

Aging is known to have a strong influence on the immune system, which is displayed, for instance, by a decline of naïve T cells with age (Nikolich-Žugich, 2014). To investigate the effect of the loss of functional Miz-1 in aged mice, splenic single-cell suspensions of the old cohort were analyzed. As described above, the distinct T cell populations of the CD4⁺ compartment were examined for aged Vav-Cre x Miz-1^{fl/fl} mice as well as for control littermates by flow cytometry (**Figure 8A**). The corresponding percentages within the CD4⁺ compartment showed a 9-fold reduction of naïve T cells from 31 % in controls to only 3.6 % in aged Miz-1-deficient mice, whereas minor changes within frequencies of T_{CM} cells were observed (**Figure 8B**). The T_{EM} cell population was increased from 62 % in controls to 91 % due to Miz-1 deficiency (**Figure 8B**). Of note, absolute numbers of the CD4⁺ T_{EM} cell population were decreased due to Miz-1-deficiency in the old mouse cohort compared to old control mice (**Supplement Figure 31A**).

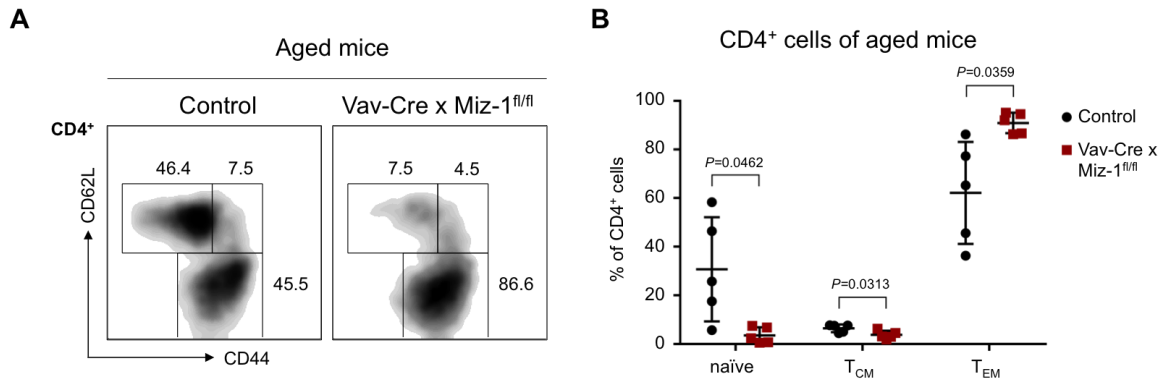


Figure 8: Miz-1 deficiency results in depletion of naïve CD4⁺ T cells in aged mice.

Splenocytes of aged (18 months) control and Vav-Cre x Miz-1^{fl/fl} mice were used to analyze the distribution of naïve (CD44^{lo}, CD62L^{hi}), central memory (T_{CM}; CD44^{hi}, CD62L^{hi}), and effector memory T cells (T_{EM}; CD44^{hi}, CD62L^{lo}) within the CD4⁺ compartment. CD4, CD8, CD44, and CD62L antibodies were used to distinguish these subsets by flow cytometry analysis after debris exclusion via FSC/SSC and pre-gating on living cells (DAPI⁻). **(A)** Representative plots depict the distribution of T cell subsets within the CD4⁺ compartment of aged mice. Numbers indicate the percentage of T cell subsets in the gate of the corresponding experiment. In total, 5 independent experiments were carried out. **(B)** Frequencies of cell populations pre-gated on CD4⁺ T cells are shown as mean ± SD. A Grubbs test ($\alpha=0.05$) did not detect any outliers. *P* values were calculated using unpaired Student's *t*-test. If variances were unequal, unpaired Student's *t*-test with Welch's correction was applied. Data are representative of 5 independent experiments.

Likewise, the CD8⁺ T cell compartment was analyzed for the distribution of naïve, T_{CM}, and T_{EM} cell populations in adult Vav-Cre x Miz-1^{fl/fl} and control mice (**Figure 9A**). The naïve T cell pool decreased highly significantly from 80 % in controls to only 16 % in adult Miz-1-deficient mice, whereas T_{CM} cells increased from 16 % in controls to 78 % in Vav-Cre x Miz-1^{fl/fl} mice (**Figure 9B**). T_{EM} cells constituted only a small fraction within the CD8⁺ compartment and remained unchanged in adult Miz-1-deficient mice (**Figure 9B**). Absolute numbers in adult mice showed a decline of naïve and T_{EM} cells, while T_{CM} cells were not altered in Vav-Cre x Miz-1^{fl/fl} mice in regard to control mice (**Supplemental Figure 30B**).

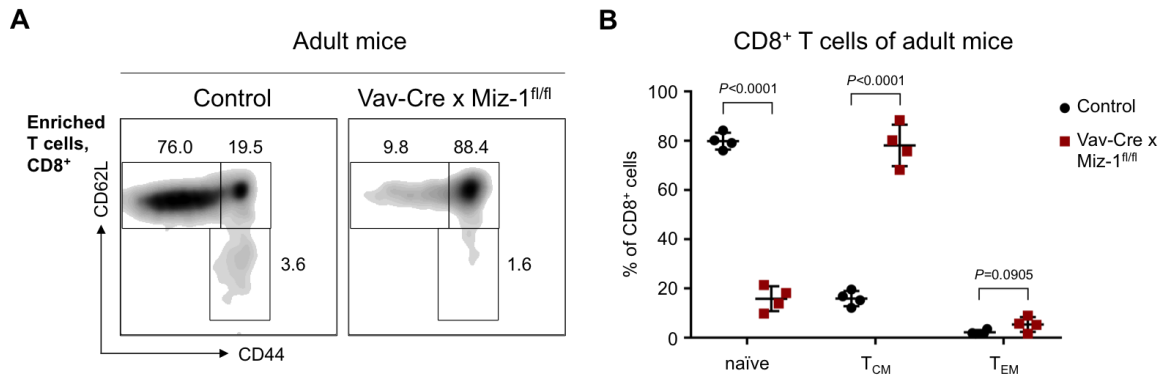


Figure 9: Deletion of functional Miz-1 increases CD8⁺ central memory T cells.

Splenic T cells of adult (2 – 4 months) control and Vav-Cre x Miz-1^{fl/fl} mice were negatively isolated and analyzed by flow cytometry for naïve (CD44^{lo}, CD62L^{hi}), central memory (T_{CM}; CD44^{hi}, CD62L^{hi}), and effector memory T cell (T_{EM}; CD44^{hi}, CD62L^{lo}) populations within the CD8⁺ compartment. Staining was performed with an antibody mixture for the surface markers CD4, CD8, CD44, and CD62L. **(A)** Representative plots depict the distribution of the analyzed T cell subsets in adult mice and numbers adjacent to gates refer to frequencies of cells in the represented experiment. 4 independent experiments were executed. **(B)** Percentages of naïve, T_{CM} and T_{EM} cells pre-gated on CD8⁺ cells are shown as mean ± SD. *P* values were calculated using unpaired Student's *t*-test. Data are representative of 4 independent experiments.

Flow cytometric analysis of the old mouse cohort depicts the distribution of naïve, T_{CM}, and T_{EM} cell populations in the CD8⁺ compartment (**Figure 10A**). Old Miz-1-deficient mice showed only 5.0 % of naïve T cells compared to 46 % in control mice (**Figure 10B**). The T_{CM} cells increased strikingly from 33 % in controls to 80 % in aged Miz-1-deficient mice, while T_{EM} cells were not changed in old Vav-Cre x Miz-1^{fl/fl} mice (**Figure 10B**). Unlike the substantial enrichment of T_{CM} frequencies in the CD8⁺ compartment, the corresponding absolute numbers evinced no increase in old Miz-1-deficient mice with respect to controls (**Supplemental Figure 31B**).

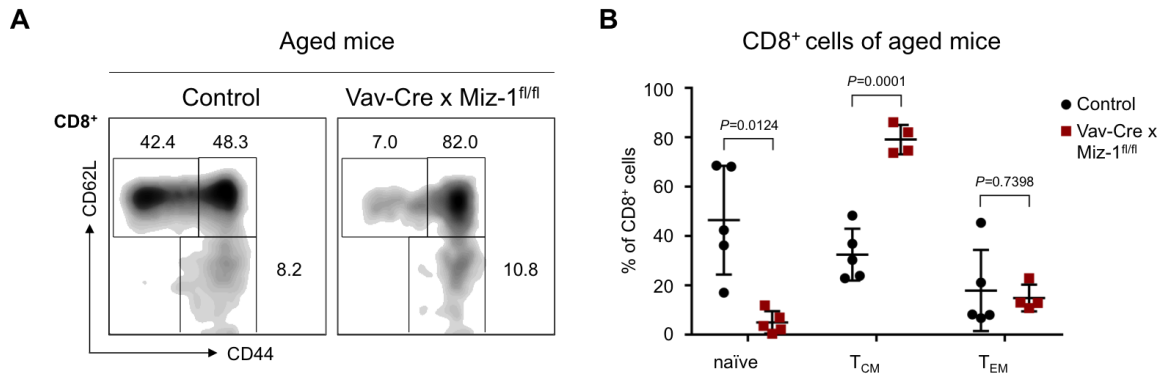


Figure 10: Functional Miz-1 deletion depletes naïve CD8⁺ T cells in aged mice.

Splenocytes of aged (18 months) control and Vav-Cre x Miz-1^{fl/fl} mice were analyzed by flow cytometry for naïve (CD44^{lo}, CD62L^{hi}), central memory (T_{CM}; CD44^{hi}, CD62L^{hi}), and effector memory T cell (T_{EM}; CD44^{hi}, CD62L^{lo}) populations within the CD8⁺ compartment. Splenic cells were stained with an antibody mixture for CD4, CD8, CD44, and CD62L. Beforehand, debris exclusion by FSC/SSC scattering and pre-gating on living cells (DAPI⁻) was performed. **(A)** Plots showing the distribution of T cell subsets in aged mice with the related frequencies of cells in the indicated gates of the represented experiment. In total, 5 independent experiments were conducted. **(B)** Percentages of naïve, T_{CM} and T_{EM} populations after pre-gating on CD8⁺ cells are shown by mean ± SD. Grubbs test ($\alpha=0.05$) was performed and two outliers were detected, which were excluded for statistical analysis and graphic visualization. *P* values were calculated using unpaired Student's *t*-test. If variances were unequal, unpaired Student's *t*-test with Welch's correction was applied. Data are representative of 5 independent experiments.

Taken together, Miz-1 deficiency influences ratios of naïve and memory T cells compared to control mice. The loss of the Miz-1 POZ domain induces a strong decline in the naïve T cell population in adult as well as in aged mice, pointing to enhanced activation of T cells in Vav-Cre x Miz-1^{fl/fl} mice. Consequently, frequencies of T_{CM} and T_{EM} cells are increased, with differences in the CD4⁺ and CD8⁺ T cell compartments.

4.2 Phenotyping of the T cell compartment in the CD4-Cre x Miz-1^{fl/fl} mouse model

4.2.1 Thymic development is not perturbed using CD4-Cre-mediated recombination of the Miz-1 POZ domain

A strong decline in absolute numbers of mature T cells was observed in the Vav-Cre x Miz-1^{fl/fl} mouse model. To overcome this limitation, Miz-1^{fl/fl} mice were crossed with transgenic mice expressing the Cre recombinase under the control of a CD4 minigene (CD4 enhancer, promoter, and silencer sequences) to achieve a T cell-specific deletion (Sawada et al., 1994). The following experiments presented in this thesis were carried out using CD4-Cre x Miz-1^{fl/fl} mice and the terms Miz-1^{ΔPOZ}, Miz-1 deficiency or loss of functional Miz-1 are from here on used to refer to this mouse model only.

To investigate thymic T cell development in this new mouse strain, thymocytes of adult control and Miz-1-deficient mice were analyzed by flow cytometry using antibodies against CD4 and CD8. Flow cytometry analysis in **Figure 11A** depicts the typical distribution of developing T cells in the thymus: double-negative (DN; CD4⁻, CD8⁻), double-positive (DP; CD4⁺, CD8⁺), CD4 single-positive (CD4 SP; CD4⁺, CD8⁻), and CD8 single-positive (CD8 SP; CD4⁻, CD8⁺) cells. Miz-1^{ΔPOZ} mice showed the same distribution of thymic cell populations as observed in control mice (**Figure 11A & B**). Furthermore, absolute numbers of total thymocytes were unaffected due to Miz-1 deficiency by using the CD4-Cre recombinase (**Supplemental Figure 32**).

To monitor the efficiency of the conditional POZ domain deletion of Miz-1 mediated by the CD4-Cre transgene, thymic T cell subsets mentioned above were sorted by fluorescence-activated cell sorting. DNA isolation and a subsequent genomic PCR followed. A mixture of three primers was used to distinguish between full-length *Zbtb17* (with loxP sites) and the truncated *Zbtb17*^{ΔPOZ} locus (Miz-1^{ΔPOZ}) (**Supplemental Figure 29**). The expression of the CD4-Cre commences in thymocytes during the transition from DN to DP T cell progenitors (Lee et al., 2001). The PCR fragment at a height of 327 bp, present in all analyzed thymic cell populations of control mice, refers to the undeleted *Zbtb17*^{fl} locus including the loxP-flanked region of the POZ domain (**Figure 11C**). In the DN population of Miz-1^{ΔPOZ} mice, an additional faint band at 209 bp was observed, indicating the deletion of the POZ domain-encoding exons. However, in DP cells of Miz-1^{ΔPOZ} mice, an almost complete deletion of these exons could be detected. The genomic PCR of the CD4 SP population resulted in a single band, referring to the complete deletion of the floxed segment in Miz-1-deficient mice. Surprisingly, the CD8 SP subset of Miz-1^{ΔPOZ} mice showed, besides a band for *Zbtb17*^{ΔPOZ}, a band for the floxed *Zbtb17* allele, indicating an

incomplete deletion of the Miz-1 POZ domain-encoding exons in the CD8 SP cell population (**Figure 11C**).

As further validation of the CD4-Cre x Miz-1^{fl/fl} mouse model, the efficiency of Miz-1 deletion was examined also in mature T cells. Therefore, DNA of splenic T cells from control and Miz-1^{ΔPOZ} mice was isolated and the PCR on the genomic *Zbtb17^{fl}* locus was performed. T cells of control mice displayed one PCR fragment at 327 bp referring to the undeleted Miz-1 (**Figure 11D**). Splenic T cells of Miz-1^{ΔPOZ} mice showed a strong PCR signal indicative of the truncated Miz-1^{ΔPOZ} and a weaker band referring to residual Miz-1 protein, pointing to an incomplete deletion (**Figure 11D**).

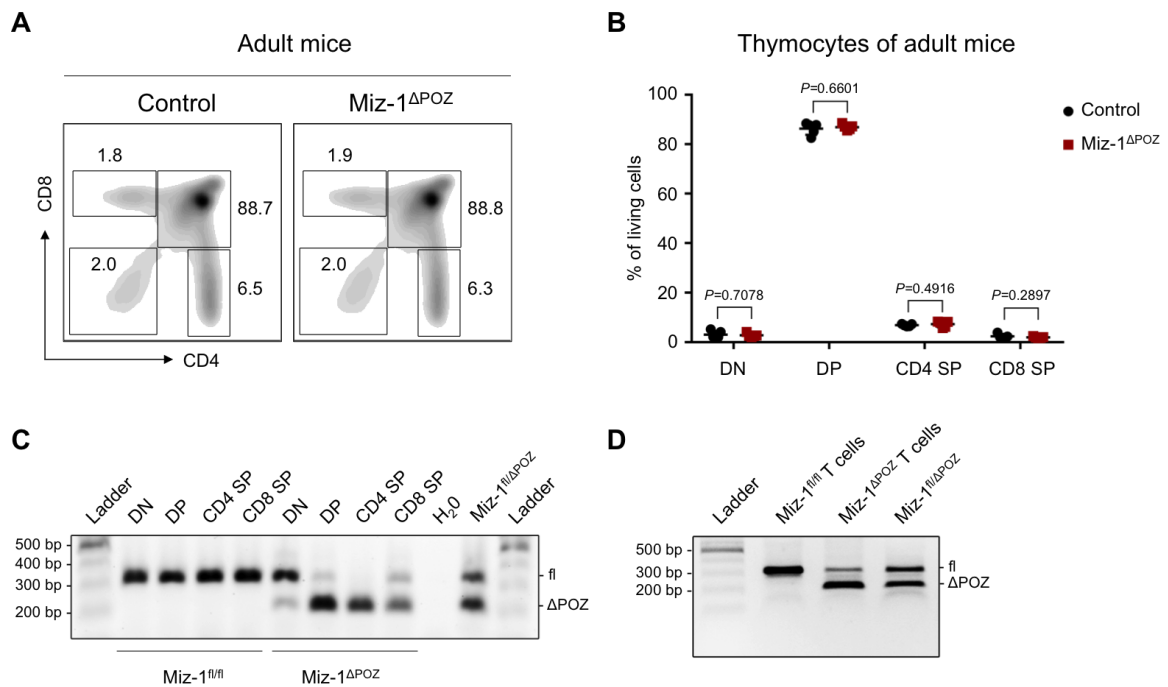


Figure 11: Thymic T cell development is not perturbed in CD4-Cre x Miz-1 $^{fl/fl}$ mice.

(A-B) Thymocytes of adult (2 – 4 months) control and CD4-Cre x Miz-1 $^{fl/fl}$ (Miz-1 Δ POZ) mice were analyzed by flow cytometry using CD4 and CD8 antibodies. **(A)** Numbers adjacent to gates indicate percentage of double-negative (DN; CD4 $^{-}$, CD8 $^{-}$), double-positive (DP; CD4 $^{+}$, CD8 $^{+}$), CD4 single-positive (CD4 SP; CD4 $^{+}$, CD8 $^{-}$), and CD8 single-positive (CD8 SP; CD4 $^{-}$, CD8 $^{+}$) cells of the represented experiment. Cells were pre-gated on FSC/SSC and on living cells (DAPI $^{-}$) to exclude debris and dead cells. 5 independent experiments were performed. **(B)** Frequency of DN, DP, CD4 SP, and CD8 SP thymocyte subsets after pre-gating on living cells (DAPI $^{-}$). Statistical significance is indicated as *P* values and was calculated using unpaired Student's *t*-test. Mean \pm SD is shown. **(C)** Using fluorescence-activated cell sorting, the following subsets of thymocytes were obtained using CD4 and CD8 antibodies: DN, DP, CD4 SP, and CD8 SP cells. DNA of these populations from adult control (Miz-1 $^{fl/fl}$) and Miz-1 Δ POZ mice was isolated. Next, conditional POZ domain deletion was tested by PCR using specific Miz-1 primers (see **Supplemental Figure 29**). Bands at 327 bp represent the loxP-flanked segment encoding the POZ domain at the locus of *Zbtb17 fl* and the 209 bp fragment refers to the deletion of the POZ domain-encoding exons after Cre recombinase activity. A heterozygous mouse (Miz-1 $^{fl/\Delta$ POZ) was used as a positive control and water was used as a negative control. **(D)** Negatively isolated T cells from spleens of adult control (Miz-1 $^{fl/fl}$) and CD4-Cre x Miz-1 $^{fl/fl}$ (Miz-1 Δ POZ) mice were used for DNA isolation and genotyped by PCR for the deletion efficiency of the exons encoding the POZ domain of the *Zbtb17 fl* (Miz-1) locus as described in (C). A heterozygous mouse (Miz-1 $^{fl/\Delta$ POZ) was used as a positive control. Data are representative of 5 (B), 3 (D), and 2 (C) independent experiments.

4.2.2 Miz-1 deficiency and aging influence peripheral T cell populations

Flow cytometry approaches were used to study distributions of T cell populations in CD4-Cre x Miz-1 $^{fl/fl}$ mice. Splenocytes of adult control and Miz-1 Δ POZ mice were analyzed by using antibodies for the T cell marker CD90.2 and the B cell marker B220

(**Figure 12A**). Mature T cells in the spleen were significantly reduced from 31% in control mice compared to 22 % in adult Miz-1-deficient mice (**Figure 12C**). In addition, peripheral T cell populations from blood were significantly decreased from 29 % to 13 % due to Miz-1 deficiency, while T cells in LNs declined insignificantly from 79 % in control mice to 67 % in CD4-Cre x Miz-1^{fl/fl} mice (**Supplemental Figure 33**).

Next, the function of Miz-1 for the peripheral T cell pool was also studied in aged mice. The same experimental setup of flow cytometric analysis was performed in adult as well as in aged mice. By assessing peripheral T cell populations of old control and old Miz-1^{ΔPOZ} mice (**Figure 12B**), a reduction of T cells from 23 % in controls to 16 % in old mice with the Miz-1 POZ domain deletion was identified (**Figure 12C**). Interestingly, T cell percentages of old control mice (23 %) were comparable to T cell frequencies of young Miz-1-deficient mice (22 %) (**Figure 12C**).

Analysis of absolute T cell numbers in adult mice revealed a reduction from 2.2×10^7 cells in controls to 1.3×10^7 in Miz-1^{ΔPOZ} mice (**Figure 12D**). However, aged Miz-1-deficient mice showed a slight but not significant reduction in peripheral T cells relative to aged controls (**Figure 12D**).

Overall, the results support the hypothesis of an important role of Miz-1 in the maintenance of the peripheral T cell pool.

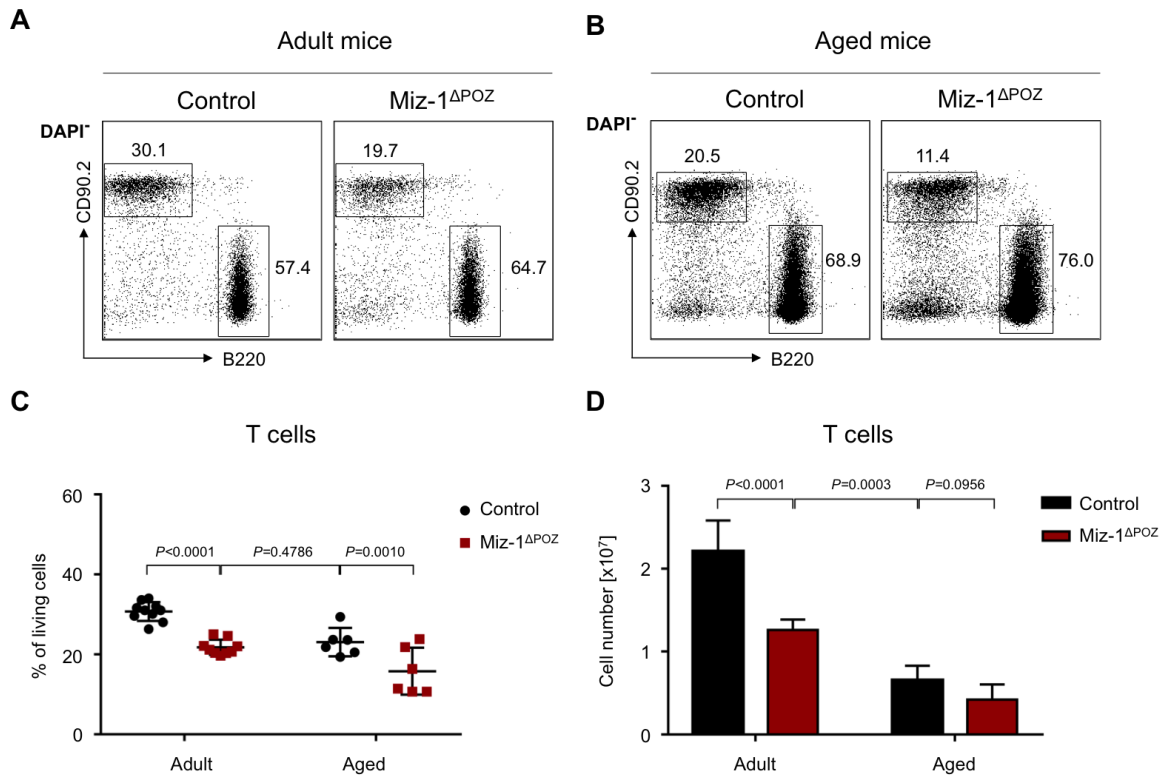


Figure 12: Reduction of splenic T cells is caused by Miz-1 deficiency and by aging.

Splenocytes of adult (2 – 4 months) or aged (18 months) control and CD4-Cre x Miz-1^{fl/fl} (Miz-1^{ΔPOZ}) mice were analyzed by flow cytometry using antibodies against CD90.2 and B220 to distinguish between T and B cells, respectively. Populations were pre-gated on living cells (DAPI⁻) after FSC/SSC debris exclusion. **(A-B)** Representative plots show the distribution of T cells (CD90.2⁺, B220⁻) and B cells (CD90.2⁻, B220⁺) after pre-gating on living cells (DAPI⁻) for (A) adult and (B) aged mice. Numbers adjacent to gates indicate population frequencies of the representative experiments. **(C)** T cell frequencies of adult and aged control and Miz-1^{ΔPOZ} mice after pre-gating on DAPI⁻ cells are depicted as mean ± SD. Grubbs test ($\alpha=0.05$) was performed and one outlier in (C) was excluded from the diagram and for statistical analysis. **(D)** Adult and aged mice were analyzed for absolute numbers of T cells in the spleen. Mean + SD is shown. *P* values were calculated using two-way ANOVA (post-hoc Fisher's LSD). Data are representative of at least 5 experiments.

Due to the reduction of T cells in the periphery of Miz-1^{ΔPOZ} mice, the ratios of T_H cells and CTLs in the spleen of young and old mice were examined by flow cytometry. Two distinct populations for CD4⁺ T_H (CD4⁺, CD8⁻) and CD8⁺ CTLs (CD4⁻, CD8⁺) were observed for adult **(Figure 13A)** or aged **(Figure 13B)** control and Miz-1^{ΔPOZ} mice. In the adult cohort, splenic CD4⁺ T cells of Miz-1-deficient mice were unaffected compared to controls, while CD8⁺ T cells declined significantly from 36 % in controls to 30 % in Miz-1^{ΔPOZ} mice **(Figure 13C)**.

More importantly, T_H cells and CTLs had an overall decrease in absolute numbers due to Miz-1 deficiency. In the adult mouse cohort, T_H cells declined 2-fold with 1.5 x 10⁷ cells in

controls and 0.7×10^7 cells in Miz-1 $^{\Delta\text{POZ}}$ mice (**Figure 13E**). CTLs displayed as well a 2-fold decrease due to Miz-1 deficiency (0.9×10^7 in controls to 0.4×10^7 in Miz-1 $^{\Delta\text{POZ}}$ mice) (**Figure 13E**).

Analysis of the old mouse cohort showed a decline of the CD4 $^+$ compartment from 44 % in controls to 30 % in Miz-1 $^{\Delta\text{POZ}}$ mice and an enrichment of the CD8 $^+$ compartment from 49 % in controls to 58 % in Miz-1-deficient mice (**Figure 13D**). Accordingly, Miz-1 deficiency in the old mouse cohort declined absolute numbers of the CD4 $^+$ population from 3.5×10^6 cells in controls to 1.4×10^6 (**Figure 13F**). Absolute numbers of the CD8 $^+$ population were insignificantly decreased in the aged mouse cohort from 4.0×10^6 in controls to 2.6×10^6 in Miz-1 $^{\Delta\text{POZ}}$ mice (**Figure 13F**).

Summarizing these results, a decline in absolute numbers of CD4 $^+$ and CD8 $^+$ T cells was observed due to the Miz-1 POZ domain loss and ratios between T_H cells and CTLs showed alterations in Miz-1 $^{\Delta\text{POZ}}$ mice.

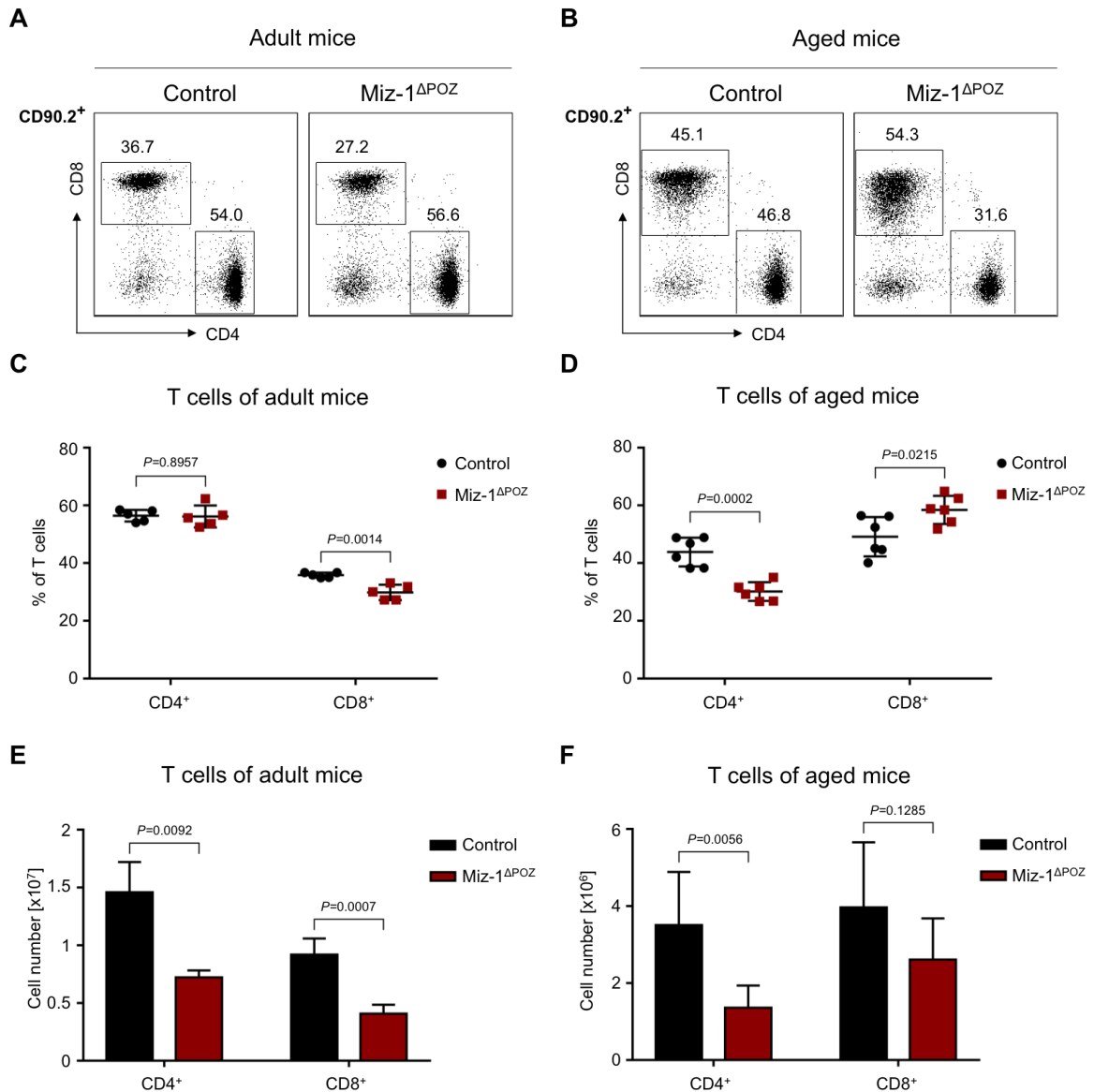


Figure 13: CD4⁺ and CD8⁺ T cell numbers are altered due to loss of functional Miz-1.

Depicted are representative plots of splenic CD4⁺ and CD8⁺ T cell subsets of **(A)** adult (2 – 4 months) or **(B)** aged (18 months) control and CD4-Cre x Miz-1^{fl/fl} (Miz-1^{ΔPOZ}) mice. Subsets were analyzed by flow cytometry using CD4, CD8, and CD90.2 antibodies. Populations were pre-gated on CD90.2⁺ T cells. FSC/SSC gating for debris exclusion and pre-gating on living cells (DAPI⁻) was done prior to T cell gating. Numbers adjacent to gates indicate percentages of CD4⁺ T cells (CD4⁺, CD8⁻) and CD8⁺ T cells (CD4⁻, CD8⁺) of the represented experiments. At least 5 independent experiments were conducted. **(C-D)** Mean ± SD of CD4⁺ and CD8⁺ T cell frequencies of **(C)** adult and **(D)** aged mice are presented. Each data point represents one analyzed mouse. Quantifications of absolute numbers of T cell subsets of **(E)** adult and **(F)** aged mice in the spleen are shown. Graphs depict mean + SD. Unpaired Student's *t*-test was used to calculate *P* values indicated in the diagrams. If variances were unequal, unpaired Student's *t*-test with Welch's correction was applied. Data represent 6 (D, F), 5 (C) or 4 (E) independent experiments.

4.2.3 Miz-1 deficiency and aging influence memory T cell populations

As reported in 4.1.3, analysis of the Vav-Cre x Miz-1^{fl/fl} mouse model provided evidence of how aging as well as Miz-1 deficiency influence the ratio of naïve and memory T cells. Thus, this question was addressed likewise in the CD4-Cre x Miz-1^{fl/fl} mouse model. The CD4⁺ and CD8⁺ T cell compartments were studied separately in the spleen of control and Miz-1^{ΔPOZ} mice by using flow cytometry.

The distribution of naïve, T_{CM} and T_{EM} cells in the CD4⁺ compartment is depicted for young (**Figure 14A**) and old (**Figure 14B**) mice. In adult Miz-1^{ΔPOZ} mice, the T cell populations of the CD4⁺ compartment were unaffected relative to controls with naïve T cells comprising around 80 %, T_{CM} cells approximately 5 %, and T_{EM} cells about 20 % (**Figure 14C**).

Old control mice had naïve T cell frequencies of 41 % and this was reduced to 20 % in aged Miz-1-deficient mice (**Figure 14D**). Frequencies of T_{CM} cells in old mice were not changed due to Miz-1 deficiency relative to controls, while the T_{EM} cell compartment increased from 48 % in old controls to 69 % in aged Miz-1^{ΔPOZ} mice (**Figure 14D**). Worth mentioning are high variances between data points within populations that occur as a result of aging.

Absolute numbers displayed an overall decrease of cell populations in the CD4⁺ compartment due to loss of functional Miz-1. In the adult cohort, the naïve compartment was reduced from 1.1×10^7 in controls to 0.5×10^7 in Miz-1^{ΔPOZ} mice, T_{CM} cells decreased as well in Miz-1-deficient mice (6.4×10^5 to 3.8×10^5) and the T_{EM} compartment was unaffected with less than 3.0×10^6 cells (**Figure 14E**).

Aged control mice possessed 1.5×10^6 naïve T cells and the loss of functional Miz-1 lead to a further decrease, resulting in 0.3×10^6 naïve T cells in aged mice only (**Figure 14F**). In the old mouse cohort, T_{CM} cells had a 3-fold decline in Miz-1-deficient mice relative to controls and the T_{EM} cell compartment was characterized by a decrease from 1.6×10^6 in controls to 0.9×10^6 in CD4-Cre x Miz-1^{fl/fl} mice (**Figure 14F**).

Summarizing the observations made in the CD4⁺ compartment, absolute numbers of naïve CD4⁺ T cells decline in adult as well as in aged Miz-1^{ΔPOZ} mice compared to control mice.

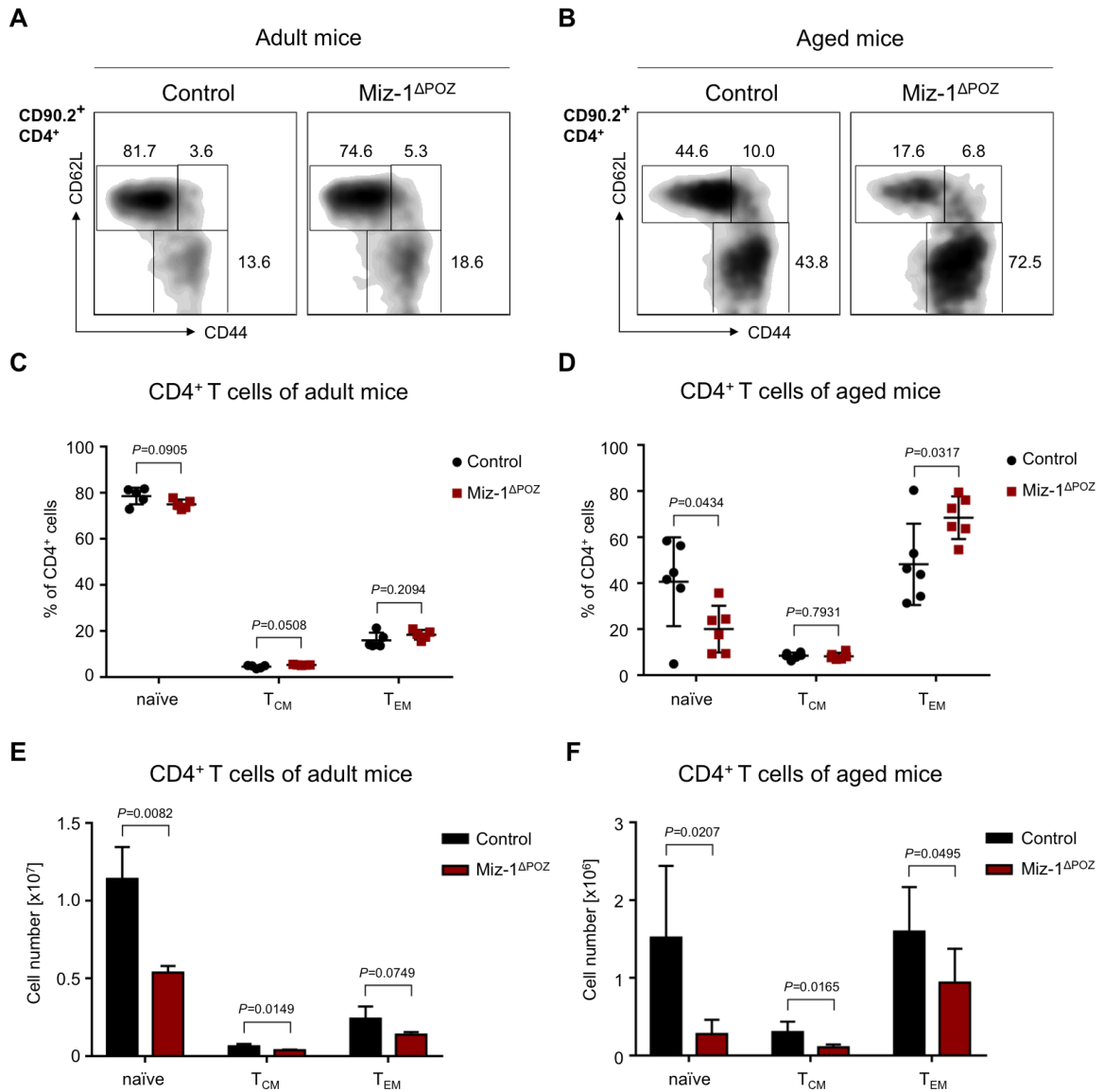


Figure 14: Miz-1 deficiency and aging decline the CD4⁺ naive T cell pool.

Flow cytometry analysis of splenocytes from (A) adult (2 – 4 months) and (B) aged (18 months) control and CD4-Cre x Miz-1^{fl/fl} (Miz-1^{ΔPOZ}) mice. Plots illustrate memory T cell populations by the expression of CD44 and CD62L within the CD4⁺ T cell compartment (CD4⁺, CD8⁻, CD90.2⁺) of the representative experiments. Naïve (CD44^{lo}, CD62L^{hi}), central memory (T_{CM}; CD44^{hi}, CD62L^{hi}), and effector memory T cells (T_{EM}; CD44^{hi}, CD62L^{lo}) were distinguished by their respective surface marker expression. FSC/SSC scattering was used for debris exclusion and populations were pre-gated on living cells (DAPI⁻). Numbers in quadrants refer to the frequencies of cells within these gates of the represented experiments after pre-gating on the CD4⁺ population. At least 5 independent experiments were carried out. (C-D) Corresponding percentages of CD4⁺ naive and memory T cell subsets in (C) adult and (D) aged mice are shown for all analyzed experiments as mean ± SD. Each symbol refers to one individual mouse. Grubbs test ($\alpha=0.05$) did not detect any outliers. Analysis of absolute numbers of CD4⁺ T cells in spleens of (E) adult and (F) aged control and Miz-1^{ΔPOZ} mice is depicted. Diagrams show mean + SD. P values were calculated using unpaired Student's *t*-test. If variances were unequal, unpaired Student's *t*-test with Welch's correction was applied. Data are representative of 6 (D, F), 5 (C), or 4 (E) independent experiments.

The influence of Miz-1 deficiency on the balance between naïve and T_M cells was also investigated within the CD8⁺ compartment and naïve, T_{CM}, and T_{EM} cell subsets are depicted for adult (**Figure 15A**) and aged (**Figure 15B**) mice.

In the adult mouse cohort, frequencies of naïve T cells dropped from 86 % in controls to 75 % in Miz-1-deficient mice (**Figure 15C**). T_{CM} cells doubled from 11 % to 22 % due to Miz-1 deficiency, while T_{EM} cells did not change (about 3 %) (**Figure 15C**).

In aged mice, the naïve T cells declined significantly from 42 % in controls to 17 % in Miz-1-deficient mice (**Figure 15D**). T_{CM} cells increased from 32 % in old controls to 63 % in old Miz-1^{ΔPOZ} mice while T_{EM} cells were not changed (less than 20 %) (**Figure 15D**).

In adult mice, absolute numbers of naïve T cells in the CD8⁺ compartment revealed a decline from 8.0 x 10⁶ in controls to 3.0 x 10⁶ in Miz-1^{ΔPOZ} mice (**Figure 15E**). Absolute numbers of CD8⁺ T_{CM} cells and CD8⁺ T_{EM} cells were unaffected due to Miz-1 deficiency in adult mice with about 1 x 10⁶ and 1 x 10⁵ cells, respectively (**Figure 15E**).

In aged mice, the CD8⁺ naïve T cell compartment comprised only 1.8 x 10⁶ cells in controls and this declined further to 0.4 x 10⁶ naïve T cells in aged Miz-1^{ΔPOZ} mice (**Figure 15F**). On the contrary, absolute numbers of CD8⁺ T_{CM} cells were unaffected in the aged cohort due to Miz-1 deficiency (**Figure 15F**). Old Miz-1^{ΔPOZ} mice showed a reduction in absolute numbers of CD8⁺ T_{EM} cells to 50% of control mice (**Figure 15F**).

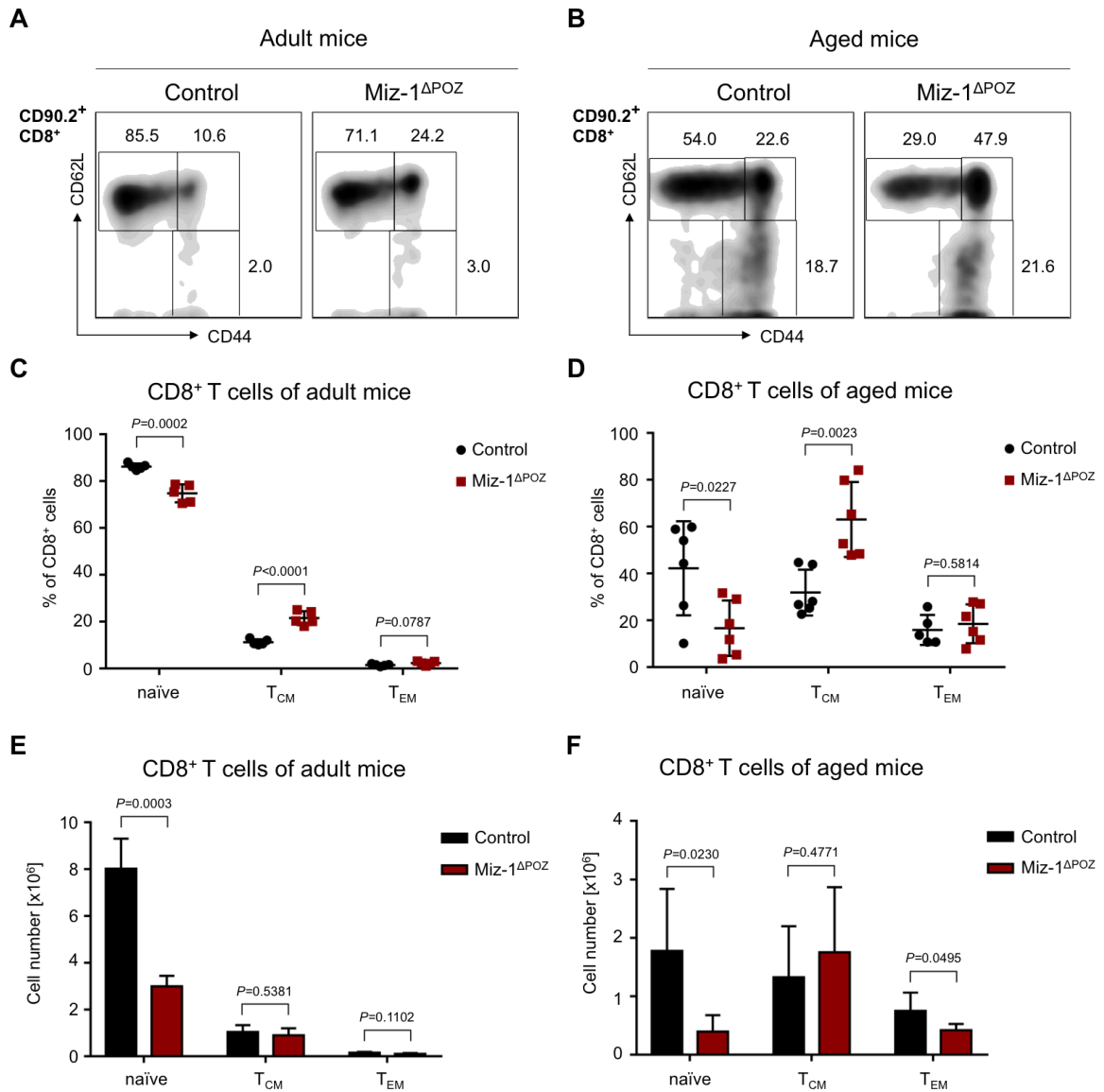


Figure 15: Miz-1 deficiency increases frequencies of CD8⁺ memory T cells.

Flow cytometry analysis of **(A)** adult (2 – 4 months) and **(B)** aged (18 months) control and CD4-Cre x Miz-1^{fl/fl} (Miz-1^{ΔPOZ}) splenocytes. Representative plots depict naïve and memory T cell populations by the expression of CD44 and CD62L within the CD8⁺ T cell compartment (CD4⁻, CD8⁺, CD90.2⁺). Naïve (CD44^{lo}, CD62L^{hi}), central memory (T_{CM}; CD44^{hi}, CD62L^{hi}), and effector memory T cells (T_{EM}; CD44^{hi}, CD62L^{lo}) were distinguished by their respective surface marker expression. FSC/SSC scattering was used for debris exclusion and populations were pre-gated on living cells (DAPI⁻). Numbers in quadrants refer to frequencies of cells within these gates of the represented experiments after pre-gating on the CD8⁺ population. **(C-D)** Corresponding percentages of CD8⁺ naïve and memory T cell subsets in **(C)** adult and **(D)** aged mice are shown for all analyzed experiments as mean ± SD. Each symbol refers to one individual mouse. Outliers were identified using the Grubbs test ($\alpha=0.05$). One outlier was detected in **(D)** that was eliminated in the diagram and for statistical analysis. **(E)** Adult and **(F)** aged control and Miz-1^{ΔPOZ} mice were analyzed for absolute numbers of CD8⁺ T cell subsets in the spleen. Diagrams show mean + SD. *P* values were calculated using unpaired Student's *t*-test. If variances were unequal, unpaired Student's *t*-test with Welch's correction was applied. Data are representative of 6 (**B, D, F**), 5 (**A, C**), or 4 (**E**) independent experiments.

Summarizing the observations, absolute numbers of naïve T cells declined in the CD4⁺ and the CD8⁺ compartment due to Miz-1 deficiency as well as in the course of aging. In aged mice, the CD4⁺ compartment had an increase in T_{EM} cell frequencies, while the CD8⁺ compartment showed an increase in frequencies of T_{CM} cells due to the Miz-1 POZ domain deletion. The following experiments were performed to elucidate the underlying mechanisms causing these severe perturbations of naïve and activated memory T cells.

4.3 Miz-1 deficiency does not alter cell cycle progression of T cells

To assess whether differences in cell cycle progression due to Miz-1 deficiency exist, T cells were analyzed without an *in vitro* activation initially. Therefore, isolated T cells from adult control and Miz-1-deficient mice were stained using propidium iodide (PI) and analyzed by flow cytometry. Cell cycle profiles with the corresponding cell cycle phases are depicted in histograms (**Figure 16A**). The frequencies of T cells in the G1/G0 phase were slightly but significantly altered from 99.5 % in controls to 99 % in Miz-1^{ΔPOZ} mice (**Figure 16B**). In addition, the subG1 fraction of control T cells with 0.2 % was slightly increased to 0.5 % in Miz-1-deficient cells, pointing to a possible even though a mild increase in apoptosis rate. Only marginal frequencies of cells with no significant alterations due to Miz-1 deficiency were observed in S and G2M (**Figure 16B**).

The cell cycle progression of unstimulated T cells might therefore be a process controlled independently of the transcriptional activity of Miz-1. Furthermore, T cells are not cycling without *in vitro* activation, which is important for the analysis of T cell stimulation experiments.

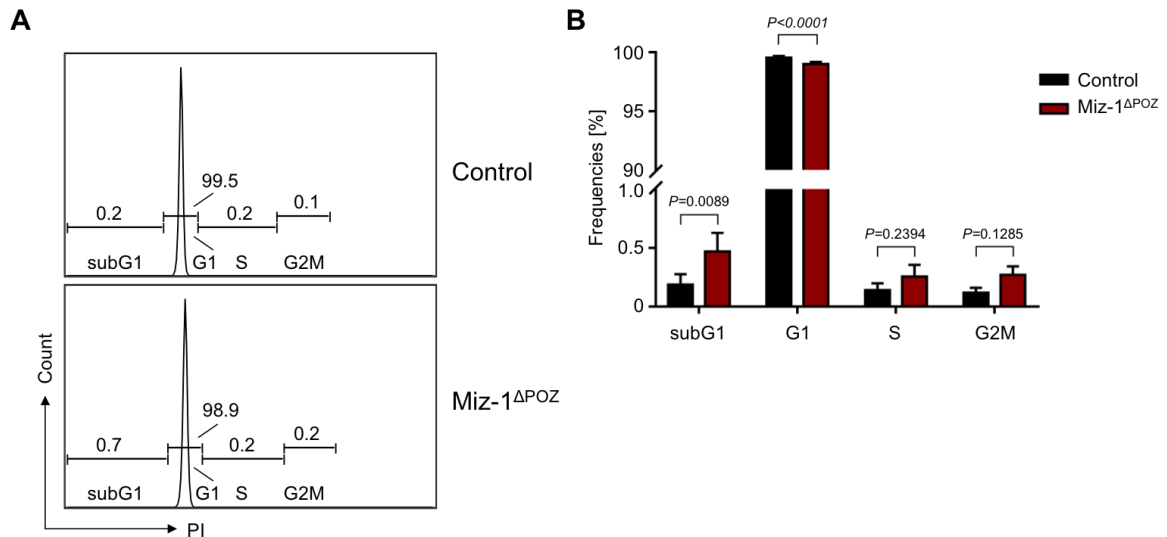


Figure 16: Cell cycle progression of unstimulated T cells.

Splenic T cells of adult (2 – 4 months) control and CD4-Cre x Miz-1^{fl/fl} (Miz-1 Δ POZ) mice were obtained by negative isolation and cell cycle was analyzed using propidium iodide (PI) staining. Intensities of PI were measured by flow cytometry. **(A)** Histograms of cell cycle profiles are shown and gates indicate the corresponding cell cycle phases. Frequencies indicate cell cycle distributions of the representative experiment. 3 independent experiments were performed. **(B)** Percentages of T lymphocytes within the cell cycle phases are depicted by mean + SD and statistical significance was compared using two-way ANOVA (post-hoc Fisher's LSD). *P* values are indicated. Data are representative of 3 independent experiments.

The activation of the T cell receptor (TCR) and the downstream response is an important mechanism of T cells in the concerted action of the adaptive immune system to react to external stimuli. To address the response of T cells to an *in vitro* TCR stimulation and to determine whether differences due to Miz-1 deficiency occur, T cell activation experiments were performed. The scheme in **Figure 17A** depicts the general workflow for these activation experiments. Splenic T lymphocytes, isolated from control and CD4-Cre x Miz-1^{fl/fl} mice, were subsequently stimulated with antibodies for the surface receptors CD3 and CD28 to mimic antigen contact and a co-stimulatory signal during T cell cultivation.

As most of the T cells were resting after isolation, cell cycle progression following TCR stimulation was investigated to prove the efficiency of T cell activation initially. Histograms depict the cell cycle progression of control and Miz-1-deficient T cells and gates indicate subG1, G1, and S/G2M phases (**Figure 17B**). The subG1 fraction remained unaffected by Miz-1 deficiency and constituted less than 5% (**Figure 17C**). Approximately 40% of the cells were detected in G1, independent of Miz-1 function. Also, percentages of T cells being in S/G2M were not altered in Miz-1 Δ POZ mice relative to controls, comprising around 55% (**Figure 17C**).

These results prove an adequate activation of T cells with anti-CD3 and anti-CD28 by the induction of cell cycle progression. However, this process is independent of Miz-1 function since no differences were detected between controls and Miz-1^{ΔPOZ} T lymphocytes.

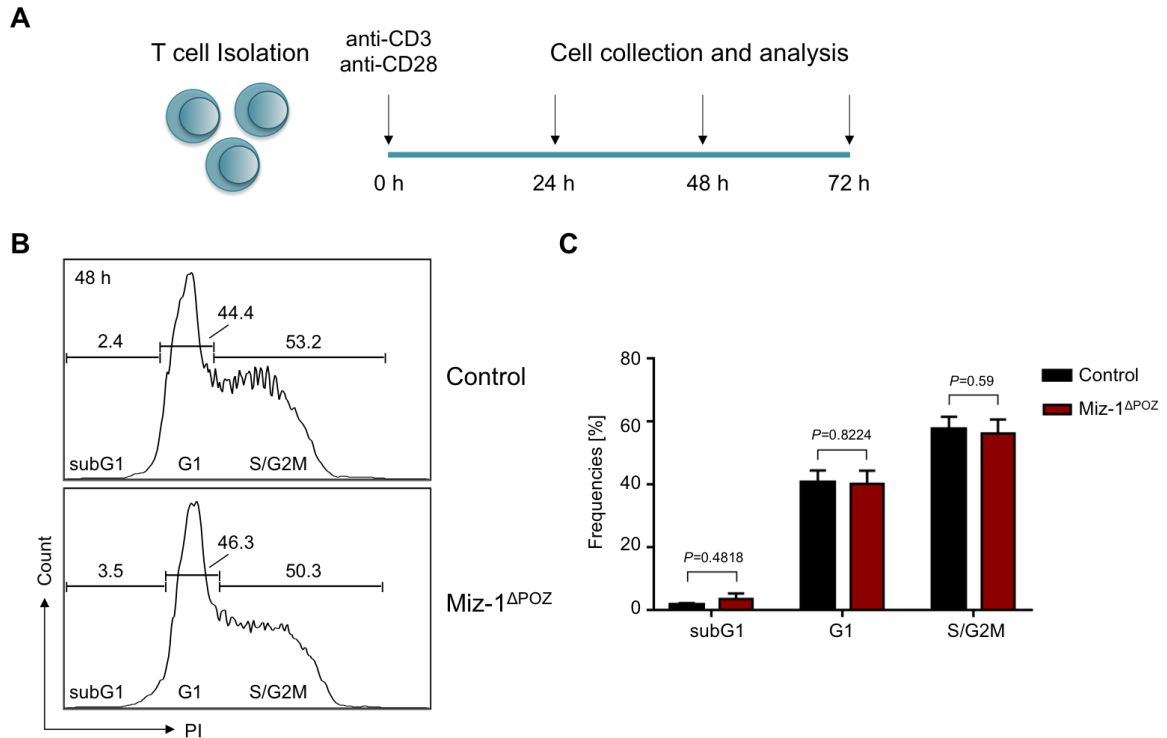


Figure 17: T cell activation induces cell cycle progression independent of Miz-1.

(A) Scheme of the experimental procedure for culturing primary T lymphocytes. Splenic T cells were obtained by negative isolation and cultured with anti-CD3 and anti-CD28 to trigger T cell activation. Sample collection and analysis were carried out after 24 h, 48 h, or 72 h, depending on the subsequent experimental method. **(B, C)** Cell cycle analysis was performed 48 h after T cell isolation and subsequent activation, by using propidium iodide (PI) staining and flow cytometry. **(B)** Cell cycle profiles of T cells from adult (2 – 4 months) control and CD4-Cre x Miz-1^{fl/fl} (Miz-1^{ΔPOZ}) mice are shown as a representative experiment and gates indicate cell cycle phases. Percentages of T cells in the corresponding gates refer to the represented experiment. As distinct G2M peaks were not detected, fractions were combined and analyzed using an S/G2M gate. 4 independent experiments were carried out. **(C)** The corresponding frequencies of control and Miz-1^{ΔPOZ} T cells in the indicated cell cycle phases are depicted. Mean + SD is shown. Two-way ANOVA (post-hoc Fisher's LSD) was used for calculating *P* values. Results were obtained from 4 independent experiments.

4.4 Functional deletion of Miz-1 alters T cell proliferation

Not only the cell cycle but also proliferation is an important process for maintaining cell populations. On this account, cell division of activated CD4⁺ and CD8⁺ T cells was examined by using CFSE staining and by tracking the intensity of the dye over several days with flow cytometry. Within the first 24 h to 48 h, cell division was barely detectable as cells had to convert TCR stimulation and prepare for cell proliferation (data not shown). Histograms in **Figure 18A** show the cell division profiles of CD4⁺ T cells from control and Miz-1^{ΔPOZ} mice 72 h after isolation and subsequent staining. Interestingly, one additional division was observed due to the Miz-1 POZ domain loss (**Figure 18A**). Also, the frequencies of cells in each division highlighted differences. After 72 h, 34 % of control CD4⁺ cells had undergone 3 divisions, which was significantly reduced in Miz-1^{ΔPOZ} mice to 13.3 % (**Figure 18B**). Nearly the same amount of T cells from control and Miz-1-deficient mice divided 4 times (36 % and 34 %). Of note, the biggest difference between control and Miz-1^{ΔPOZ} CD4⁺ cells was observed for 5 cell divisions. While 32 % of the Miz-1 depleted lymphocytes divided 5 times, only 10 % of the control T cells reached this division. Control T cells reached only 5 cell divisions within 72 h, while 7 % of Miz-1-deficient T cells divided 6 times (**Figure 18B**). This points to the tendency of a higher proliferative potential due to Miz-1 deficiency.

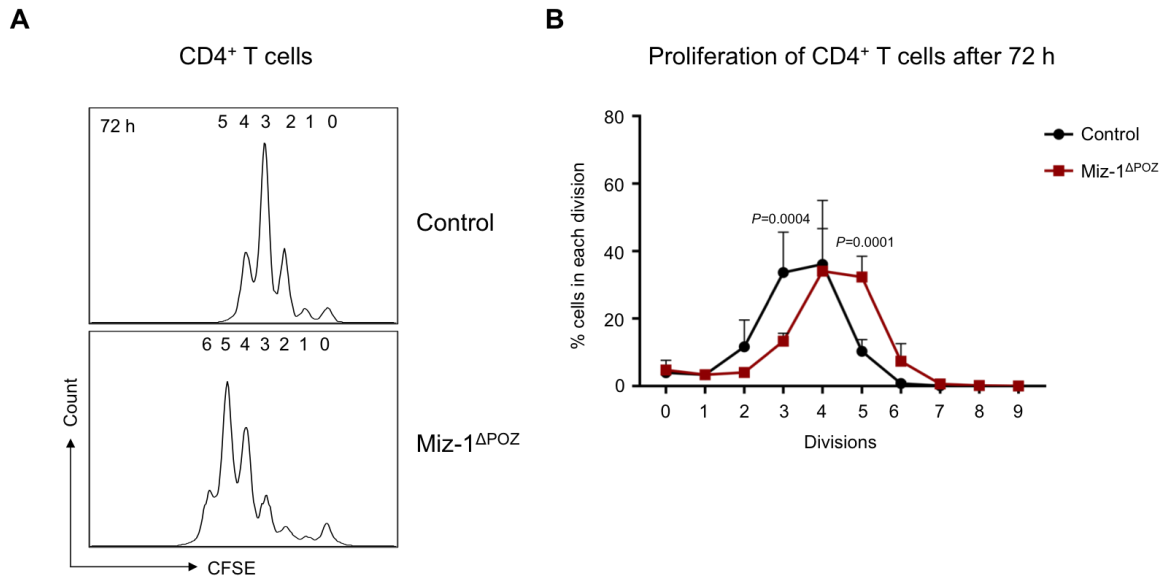


Figure 18: Miz-1-deficient CD4⁺ T cells proliferate faster.

Splenic CD4⁺ T cells of adult (2 – 4 months) control and CD4-Cre x Miz-1^{fl/fl} (Miz-1^{ΔPOZ}) mice were negatively isolated and stained with CFSE for tracking cell proliferation over several days. Cells were cultured with anti-CD3 and anti-CD28 for T cell activation and analyzed by flow cytometry. **(A)** Histograms show CFSE signal 72 h after staining. Numbers in plots refer to the corresponding cell divisions depicted by the respective peak below. Cells were pre-gated on FSC/SSC to exclude debris. **(B)** Diagram represents the frequency of CD4⁺ cells in each cell division after 72 h, calculated by using the ModFit LT™ software. Mean + SD is shown. Significance was calculated using two-way ANOVA (post-hoc Fisher's LSD). For clarity, only significant *P* values are indicated in the diagram. Data are representative of 3 independent experiments. CFSE – carboxyfluorescein succinimidyl ester.

Proliferation was also assessed for the CD8⁺ T cell compartment. Of particular note is a high peak of the undivided fraction of CD8⁺ T cells in comparison to the CD4⁺ T cell pool (**Figure 18A** & **Figure 19A**). This becomes apparent with 52 % of control T cells but only 24 % of Miz-1^{ΔPOZ} T cells showing no division after 72 h (**Figure 19B**). Both, T cells of control and Miz-1^{ΔPOZ} mice showed up to 6 cell divisions within 72 h. Miz-1-deficient T cells tended to have increased frequencies in each division relative to control T cells, however with no significance (**Figure 19B**).

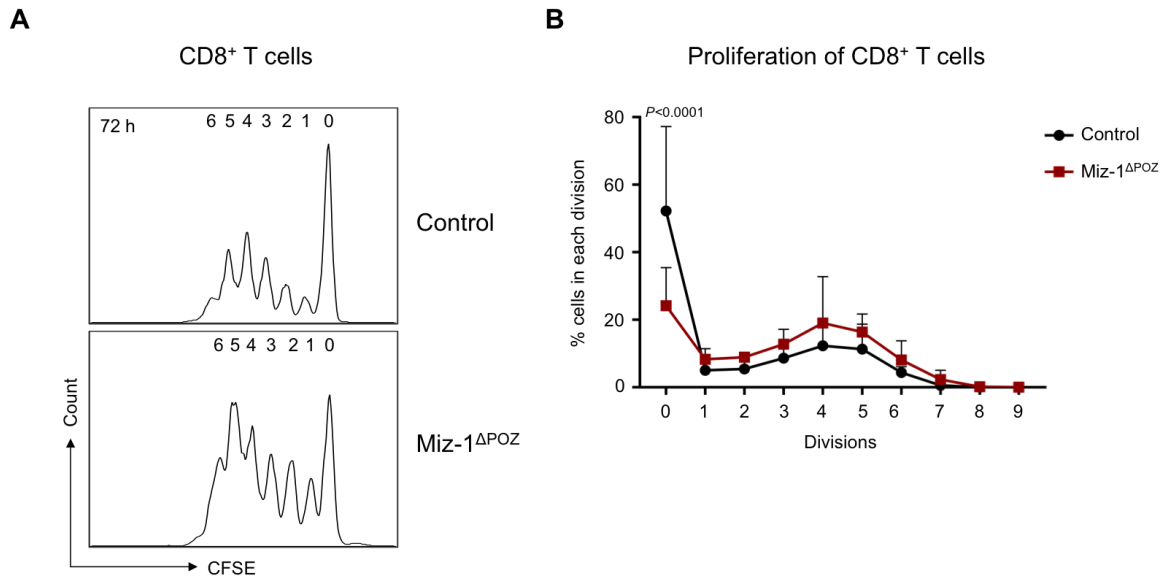


Figure 19: Miz-1-deficient CD8⁺ T cells show more proliferation.

Spleens of adult (2 – 4 months) controls and CD4-Cre x Miz-1^{fl/fl} (Miz-1^{ΔPOZ}) mice were used for CD8⁺ T cell isolation by negative selection. Isolated cells were stained with the dye CFSE to trace proliferation. CD8⁺ T cells were cultured and activated with anti-CD3 and anti-CD28 for several days. Analysis was done by flow cytometry. **(A)** Histograms depict the CFSE signal 72 h after staining of CD8⁺ T cells. Numbers indicate cell divisions and refer to the respective CFSE peaks below. Cells were pre-gated on FSC/SSC for debris removal. **(B)** The frequency of cells in each division 72 h after staining with CFSE was analyzed with the ModFit LT™ software and is depicted by mean + SD. Results were obtained from 3 independent experiments. Statistical analysis was done using two-way ANOVA (post-hoc Fisher's LSD). For clarity, only significant *P* values are indicated. CFSE – carboxyfluorescein succinimidyl ester.

The cell cycle regulator p21 can inhibit cell cycle progression and thus influences proliferation. As the gene encoding for p21 (*Cdkn1a*) is a major target of the Miz-1/c-MYC complex (Seoane et al., 2002) and differences in T cell proliferation due to Miz-1 deficiency were observed, it seemed to be an interesting regulator to analyze. Thus, the relative expression of *Cdkn1a* was investigated in T cells 48 h after TCR activation. In every performed experiment, Miz-1 depletion caused a strong decline of *Cdkn1a* expression resulting in a significantly decreased fold change to 0.5 compared to control T cells (**Figure 20A**). To further test whether the reduced gene expression can also be observed at protein level, activated T cells were used for protein isolation 48 h after TCR engagement. In line with the observed gene expression, reduced p21 protein levels were detected in Miz-1^{ΔPOZ} T cells with respect to control T cells (**Figure 20B**).

Summarizing the proliferation experiments, Miz-1-deficient T cells divide faster or more than the corresponding control cells. Furthermore, Miz-1^{ΔPOZ} T cells show a decreased expression of the negative cell cycle regulator p21 after activation, supporting an increased proliferation. These obtained results do not fully uncover the reason for the

decline in the peripheral T cell compartment in Miz-1^{ΔPOZ} mice and this was the aim of further investigations.

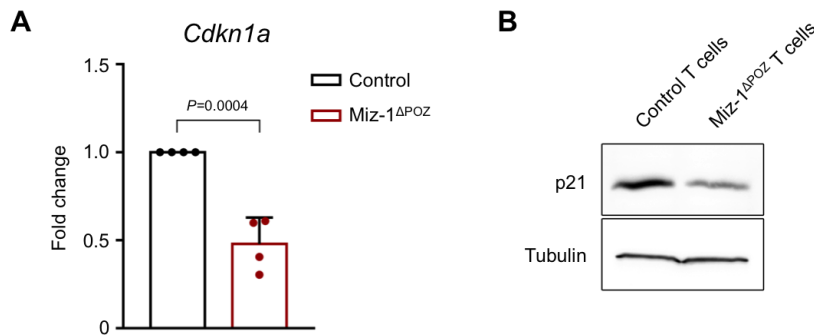


Figure 20: Loss of functional Miz-1 decreases p21 levels after T cell activation.

Negatively isolated, splenic T cells of adult (2 – 4 months) control and CD4-Cre x Miz-1^{fl/fl} (Miz-1^{ΔPOZ}) mice were activated with anti-CD3 and anti-CD28 and cultured for 48 h. **(A)** qRT-PCR was performed to test the relative expression of the gene encoding for p21 (*Cdkn1a*). Fold change over control T cells was calculated using the comparative $\Delta\Delta C_t$ method normalized to *Actin Beta*. The diagram shows mean + SD and each data point depicts one analyzed mouse. *P* value was calculated using unpaired Student's *t*-test. **(B)** Proteins of activated T cells were isolated after 48 h and levels of p21 were detected with immunoblotting. Tubulin was used as a loading control. Data are representative of 4 (A) or 3 (B) independent experiments.

4.5 Deletion of Miz-1 affects T cell survival after activation

4.5.1 Miz-1 has no impact on survival of unstimulated T cells

The results obtained so far imply a considerable perturbation of peripheral T cells and a concomitant decline of this population. The peripheral T cell pool is dependent on the survival of existing and the generation of new T lymphocytes. To further explore the cause of T cell reduction, apoptosis of splenic T cells from adult and aged control and Miz-1^{ΔPOZ} mice was studied by flow cytometry. In the CD4⁺ and the CD8⁺ T cell compartment of adult mice, the apoptosis rates did not change due to Miz-1 deficiency. Frequencies of apoptotic CD4⁺ T cells were 5.1 % in control and 6.5 % in Miz-1^{ΔPOZ} mice, while apoptotic CD8⁺ T cells comprised less than 3 % (**Figure 21A**). In the aged mouse cohort, control mice possessed a higher rate of apoptotic cells with 22 % in the CD4⁺ and 16 % in the CD8⁺ T cell compartment (**Figure 21B**). In old Miz-1^{ΔPOZ} mice, an insignificant increase in apoptosis to 33 % of apoptotic CD4⁺ T cells and 21 % of apoptotic CD8⁺ T cells was determined (**Figure 21B**).

In summary, unstimulated CD4⁺ and CD8⁺ T cells show increasing amounts of apoptosis in aged mice. The survival of T cells seems to be independent of Miz-1 function, however,

CD4⁺ T cells had an insignificant tendency of more Annexin V binding in young and old Miz-1^{ΔPOZ} mice.

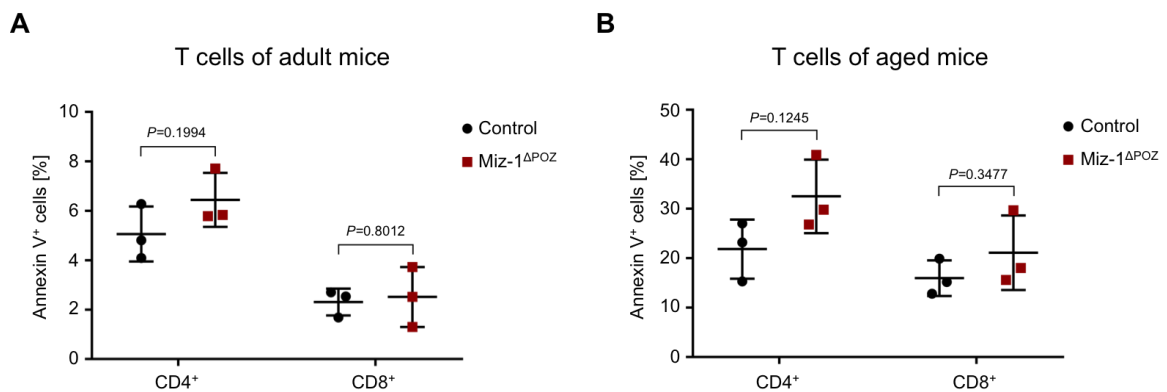


Figure 21: Apoptosis of unstimulated T cells is not altered due to Miz-1 deficiency.

Splenocytes of **(A)** adult (2 – 4 months) or **(B)** aged (18 months) CD4-Cre x Miz-1^{fl/fl} (Miz-1^{ΔPOZ}) and control mice were analyzed for Annexin V binding to T cells using flow cytometry. An antibody mixture for CD4, CD8, CD90.2, and fluorochrome-labeled Annexin V was used to detect apoptosis of CD4⁺ and CD8⁺ T cells. Cells were pre-gated on CD90.2⁺ T cells after FSC/SSC debris exclusion. Annexin V⁺ populations of CD4⁺ and CD8⁺ T cells are indicated as mean ± SD. Statistical analysis was performed using unpaired Student's *t*-test. *P* values are indicated. Data are representative of 3 independent experiments.

4.5.2 Miz-1 deficiency results in a strong induction of apoptosis after activation

To gain insight into a possible role of Miz-1 on the survival of T lymphocytes after TCR stimulation, apoptosis induction after activation was evaluated. Histograms in **Figure 22** depict the intensity of Annexin V binding to control and Miz-1-deficient T cells 48 h after stimulation with anti-CD3 and anti-CD28. After TCR activation, control T cells underwent apoptosis, indicated by 12 % of Annexin V⁺ T cells (**Figure 22**). Surprisingly, Annexin V⁺ T cells increased dramatically to 29 % due to Miz-1 POZ domain deletion in regard to control T cells (**Figure 22 & Supplemental Figure 34**).

These results demonstrate an induction of apoptosis after T cell activation due to Miz-1 deficiency, pointing towards an increase in activation-induced cell death (AICD) in Miz-1-deficient T cells. This could contribute to the observed decline in peripheral T cell populations in Miz-1^{ΔPOZ} mice.

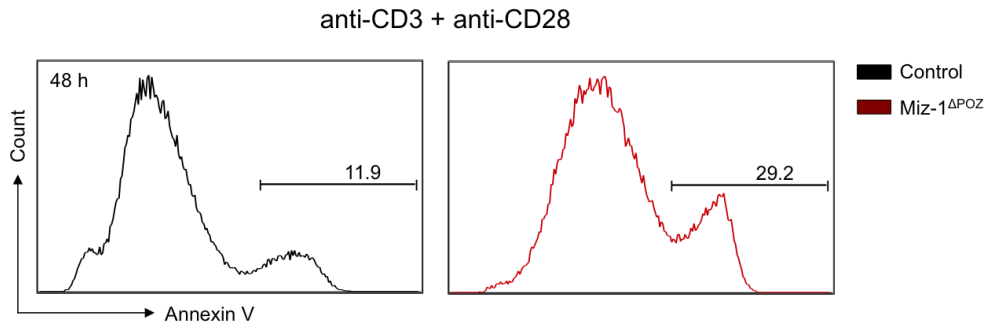


Figure 22: T cell activation induces apoptosis due to Miz-1 deficiency.

Splenic T cells of adult (2 – 4 months) control and CD4-Cre x Miz-1^{fl/fl} (Miz-1^{ΔPOZ}) mice were isolated by negative selection and activated with anti-CD3 and anti-CD28 in culture. After 48 h, apoptosis of T cells was analyzed by flow cytometry using fluorochrome-labeled Annexin V. Debris was excluded using FSC/SSC scattering. Representative histograms of Annexin V binding after T cell activation are shown. Numbers adjacent to gates indicate the percentage of Annexin V⁺ T cells as the mean of 3 independent experiments.

4.5.3 Miz-1 deficiency provokes extrinsic apoptosis induction after T cell activation

Miz-1 regulates p53 by inhibiting the p53-mediated transactivation and apoptosis induction (Miao et al., 2010). Thus, the expression of p53-target genes encoding for PUMA (*Bbc3*), NOXA (*Pmaip1*), BAX (*Bcl2l4*), as well as the gene encoding for the anti-apoptotic factor BCL-2 (*Bcl2*), were determined after T cell activation. Even though an apoptosis induction after TCR triggering was detected (**Figure 22**), none of the pro-apoptotic genes showed a significant increase in Miz-1^{ΔPOZ} T cells relative to control T cells with fold changes of 0.6 for *Bbc3* and 0.8 for *Pmaip1* (**Figure 23**). Interestingly, for the pro-apoptotic *Bcl2l4* transcript a decline to 0.8 was noticeable in Miz-1^{ΔPOZ} T cells in regard to controls (**Figure 23**). Likewise, *Bcl2* expression did not show any significant alterations between control and Miz-1^{ΔPOZ} T cells (**Figure 23**). Expression levels of apoptosis-associated genes were also tested for control and Miz-1-deficient T cells directly after negative isolation and without activation of the TCR. Without being stimulated or challenged, Miz-1-deficient T cells showed no changes in expression levels of the analyzed genes compared to controls (**Supplemental Figure 35**).

These results point towards a p53-independent induction of apoptosis after TCR activation of peripheral Miz-1^{ΔPOZ} T cells.

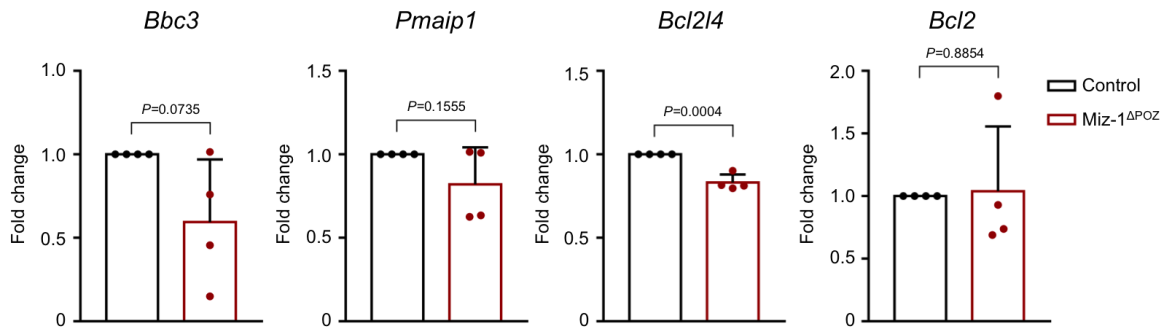


Figure 23: Apoptosis-associated gene expression after T cell activation.

Expression of genes encoding for PUMA (*Bbc3*), NOXA (*Pmaip1*), BAX (*Bcl2l4*), and BCL-2 (*Bcl2*) was measured in T cells of adult (2 – 4 months) CD4-Cre x Miz-1^{fl/fl} (Miz-1^{ΔPOZ}) and control mice after T cell activation. Therefore, T cells were negatively isolated and subsequently activated with anti-CD3 and anti-CD28. After 48 h, cells were harvested for qRT-PCR. Bar diagrams represent fold changes in gene expression of Miz-1^{ΔPOZ} T cells relative to control T cells. Fold changes were calculated using the comparative $\Delta\Delta C_t$ method and normalized to *Actb* (*Actin Beta*). Mean + SD is depicted and each symbol refers to fold change of T cells from one analyzed mouse. Statistics were carried out using unpaired Student's *t*-test and *P* values are indicated in the diagrams. Data are representative of 4 independent experiments.

Apoptosis and DNA damage are accompanied by the phosphorylation of the histone variant H2AX which is necessary for the recruitment of DNA repair factors (Paull et al., 2000; Rogakou et al., 1998). To test for this early posttranslational modification, protein lysates of control and Miz-1^{ΔPOZ} T cells were analyzed after TCR activation with a specific antibody. Interestingly, higher levels of γ H2AX were detected in activated Miz-1-deficient T cells relative to control T cells (**Figure 24A**).

Also, protein levels of Puma, a direct target gene of p53 (Mohammadzadeh et al., 2019), were examined after activation of T cells. However, the expression of the pro-apoptotic factor Puma was unaffected in Miz-1^{ΔPOZ} T cells with respect to control T cells (**Figure 24B**).

An initiator caspase of the extrinsic apoptosis pathway is caspase 8 (Lawen, 2003). The cleavage of caspase 8 is a two-step process that results, among others, in the active subunit p18 (Krammer et al., 2007; Medema et al., 1997). The expression of this subunit was analyzed and interestingly, it was increased in Miz-1^{ΔPOZ} T cells in regard to control T cells (**Figure 24C**).

These results might explain the increased amounts of apoptosis by the induction of the extrinsic apoptosis pathway after TCR engagement in absence of the POZ domain of Miz-1.

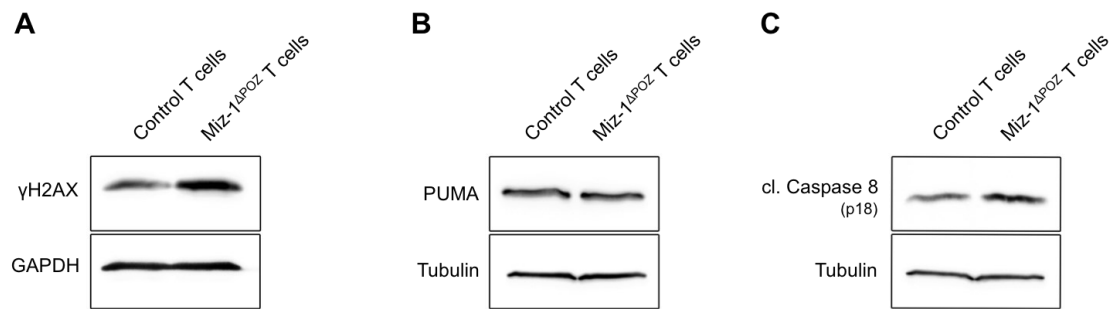


Figure 24: Activation of Miz-1-deficient T cells induces caspase 8 cleavage.

(A-C) Splenic T cells of adult (2 – 4 months) control and CD4-Cre x Miz-1^{fl/fl} (Miz-1^{ΔPOZ}) mice were isolated by negative selection and activated with anti-CD3 and anti-CD28 for 48 h in culture. Protein lysates were obtained and the indicated proteins were visualized with immunoblotting by using specific antibodies. Cleaved (cl.) caspase 8 is detected by the fragment p18. Tubulin or GAPDH was used as a loading control. Representative immunoblots of 3 (B, C) or 2 (A) independent experiments are shown. cl. – cleaved, GAPDH – glyceraldehyde-3-phosphate dehydrogenase.

4.6 The role of Miz-1 in T cells in response to irradiation

4.6.1 Analysis of irradiation-induced apoptosis induction of activated T cells

As Miz-1 is known to have several implications in stress response pathways (Herold et al., 2002; Miao et al., 2010), the influence of DNA damaging stimuli on T cells was investigated. Hence, irradiation experiments were conducted in the CD4-Cre x Miz-1^{fl/fl} mouse model by testing the impact of genotoxic stress on adult T cells. The general workflow for these experiments can be seen in **Figure 25A**. Isolated T cells were activated and after 24 h in culture, 2 Gy γ -irradiation (in the following labeled as IR) was applied.

T cells of control mice showed an increase of Annexin⁺ cells from 12 % after activation to 20 % with combinatorial IR (**Supplemental Figure 34**). Activated Miz-1^{ΔPOZ} T cells had initially high levels of apoptosis with 29 % of Annexin⁺ cells, leading only to an insignificant increase of Annexin⁺ T cells to 42 % after IR (**Supplemental Figure 34**). Comparing IR-induced apoptosis of activated T cells, an almost significant increase ($P=0.0589$) from 20 % in controls to 42 % in Miz-1^{ΔPOZ} T cells was observed (**Figure 25B & Supplemental Figure 34**).

To summarize, activated Miz-1^{ΔPOZ} T cells exhibit a tendency of higher apoptosis following IR-induced DNA damage. However, activation alone sensitized Miz-1-deficient T cells already for increased apoptosis rates.

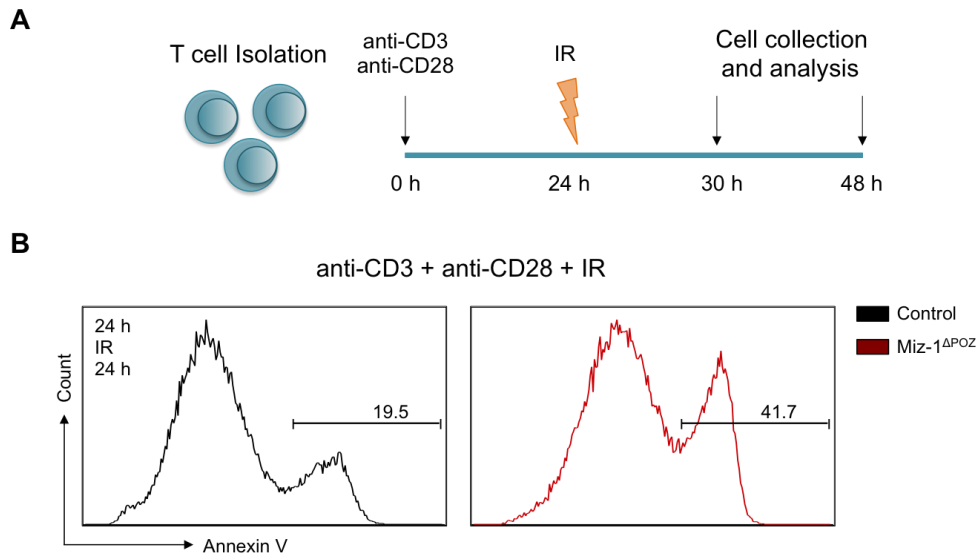


Figure 25: T cell response to irradiation.

(A) Scheme illustrating the experimental setup of T cell activation followed by γ -irradiation (IR). T cells were isolated by negative selection and activated with anti-CD3 and anti-CD28. After 24 h, cells were irradiated with 2 Gy and cultured further. Analysis of T cells was performed in total 30 h or 48 h after isolation, depending on the subsequent experimental method. **(B)** Representative histograms show Annexin V binding to T cells of adult (2 – 4 months) control (black) and CD4-Cre x Miz-1^{fl/fl} (Miz-1 ^{Δ POZ}, red) mice. T cells were activated with anti-CD3 and anti-CD28 and IR (2 Gy) was applied after 24 h. In total, apoptosis of T cells was analyzed 48 h after T cell isolation. Numbers adjacent to gates indicate the percentage of Annexin V⁺ T cells as the mean of 3 independent experiments after FSC/SSC debris exclusion.

4.6.2 Upregulation of pro-apoptotic genes after irradiation of T cells

Expression levels of apoptosis-associated genes were analyzed to assess the genotoxic stress response of T cells in dependency of Miz-1. Hence, transcript levels of BCL-2 (*Bcl2*), as well as the p53-target genes coding for p21 (*Cdkn1a*), PUMA (*Bbc3*), NOXA (*Pmaip1*), and BAX (*Bcl2l4*), were investigated 6 h after the irradiation of activated T cells. Non-irradiated but activated T cells of either control or Miz-1 ^{Δ POZ} mice were used as a reference for calculating the fold change after IR.

As mentioned above, control T cells showed a significant increase in apoptosis after IR and Miz-1 ^{Δ POZ} T cells had an insignificant tendency of more apoptosis after IR relative to the unchallenged, activated T cells (**Supplemental Figure 34**). Indicative of apoptosis induction, apoptosis-associated genes were upregulated after IR. The gene expression of *Pmaip1* increased in control T cells 1.7-fold after IR and in Miz-1-deficient T cells to 2.9-fold after IR (**Figure 26A**). Expression of the gene encoding for the pro-apoptotic factor PUMA increased in control T cells insignificantly 2.8-fold, while Miz-1 ^{Δ POZ} T cells had a significant increase to 3.8-fold after IR (**Figure 26B**). After IR, *Bcl2l4* had an enrichment of

1.7-fold in control T cells and an insignificant enrichment of 2.3-fold in Miz-1-deficient T cells (**Figure 26C**). The mRNA levels of the p53-target gene *Cdkn1a* increased after IR to 1.8-fold in control T cells, whereas Miz-1 deficiency caused a strong increase in *Cdkn1a* expression resulting in a fold change of 4.1 after IR (**Figure 26D**). In addition, the expression of the anti-apoptotic factor *Bcl2* remained unaffected in control T cells after IR or was only slightly increased to 1.2-fold in Miz-1^{ΔPOZ} T cells after IR (**Figure 26E**). The gene expression analysis after DNA damage revealed an induction of p53-target genes for control as well as Miz-1^{ΔPOZ} T cells. However, expression levels of the analyzed genes after IR were slightly higher due to Miz-1 deficiency compared to control T cells.

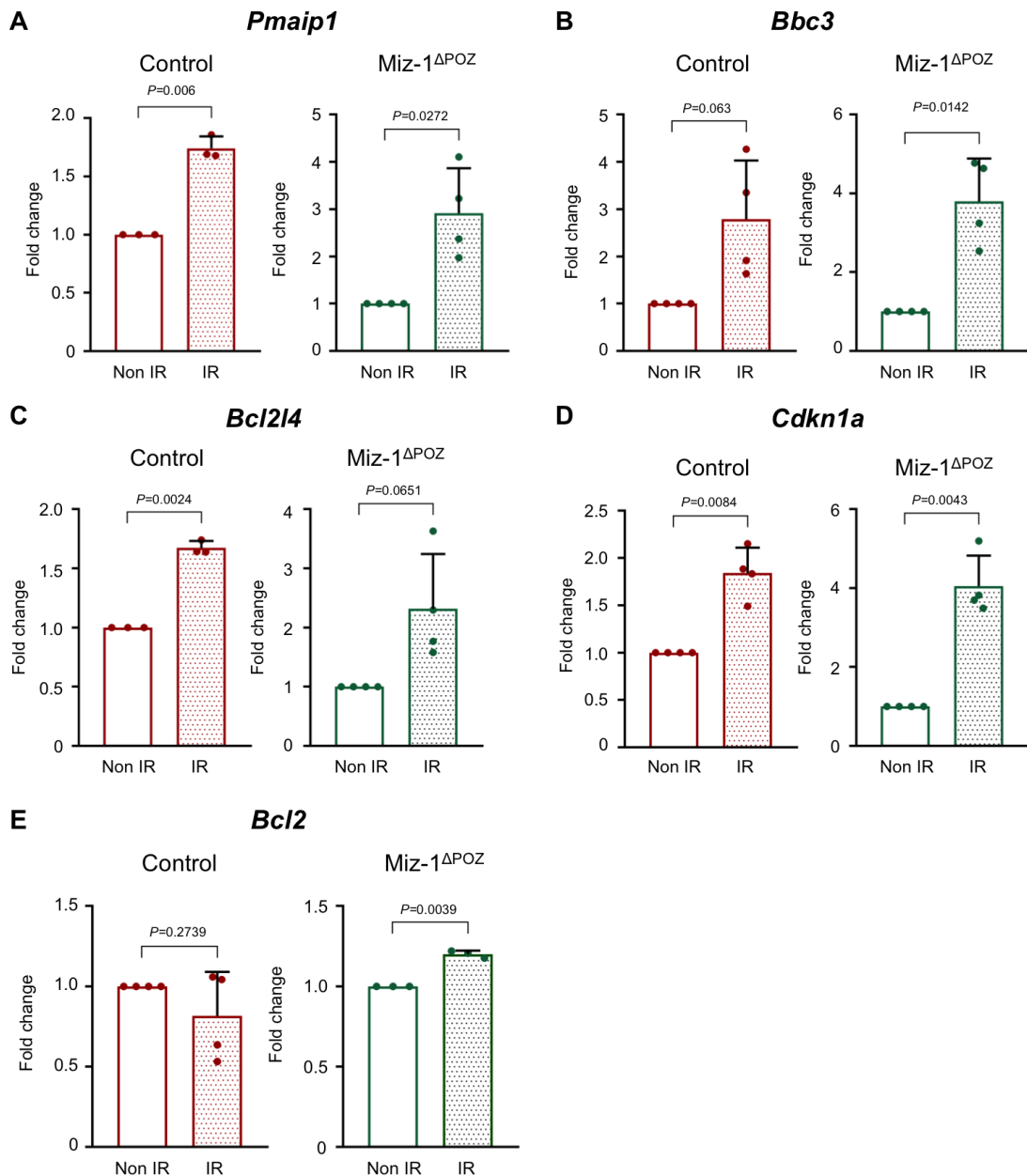


Figure 26: Induction of p53-associated target genes after irradiation of T cells.

Splenic T cells from adult (2 – 4 months) control (red) and CD4-Cre x Miz-1^{fl/fl} (Miz-1 Δ POZ; green) mice were isolated by negative selection and activated in culture with anti-CD3 and anti-CD28. After 24 h, γ -irradiation (IR) of 2 Gy was applied or cells were left untreated (Non IR). After additional 6 h in culture, cells were harvested for qRT-PCR to analyze the expression of genes encoding for (A) NOXA (*Pmaip1*), (B) PUMA (*Bbc3*), (C) BAX (*Bcl2l4*), (D) p21 (*Cdkn1a*), and (E) BCL-2 (*Bcl2*). Fold changes were calculated using the comparative $\Delta\Delta$ Ct method normalized to *Actb* (*Actin Beta*). Gene expression levels of non-irradiated T cells were always set to 1 and compared to the gene expression levels of the corresponding T cells after IR. Results are presented in bar diagrams as mean + SD. One data point represents one individual mouse. Outliers were identified using the Grubbs test ($\alpha=0.05$). Outliers were eliminated in the diagram and for statistical analysis. Statistics were carried out using paired Student's *t*-test and *P* values are indicated in the diagrams. Data are representative of 4 independent experiments.

4.6.3 DNA repair in T cells is independent of the transcription factor Miz-1

An efficient DNA repair is an important feature for the maintenance of cell populations after DNA damage. Thus, a possible effect of Miz-1 on the DNA repair capacity was evaluated by performing Comet assays after challenging isolated T cells of adult mice with 2 Gy IR. Representative pictures are shown, demonstrating the formation of Comet tails after DNA damage and the repair at the indicated time points (**Figure 27A**). The relative Comet Tail Moment of non-irradiated cells with approximately 0.2 in control T cells and 0.1 in Miz-1^{ΔPOZ} T cells corresponds to minor DNA damage in unchallenged cells (**Figure 27B**). After irradiation, cells were left in culture to repair introduced DNA breaks. The relative Tail Moment decreased after 60 min equally in control T cells and Miz-1-deficient T cells to 0.4. After 120 min, the relative Tail Moment declined to approximately 0.2 in control T cells and 0.3 in Miz-1^{ΔPOZ} T cells. Curves for control and Miz-1^{ΔPOZ} T lymphocytes showed no significant differences in their progression, displaying a similar repair capacity (**Figure 27B**).

This clearly shows that the transcription factor Miz-1 does not play a role in DNA damage repair in splenic T cells. Thus, insufficient DNA repair might not be responsible for the decline of the peripheral T cell pool.

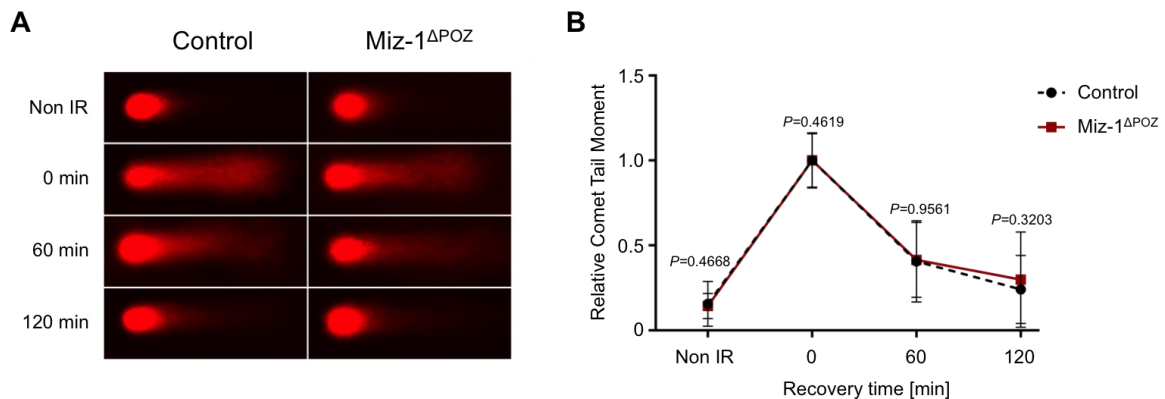


Figure 27: Repair of DNA damage in T cells is independent of Miz-1.

Splenic T cells of adult (2 – 4 months) control and CD4-Cre x Miz-1^{fl/fl} (Miz-1^{ΔPOZ}) mice were irradiated with 2 Gy or left untreated (Non IR). After γ -irradiation (IR), cells could recover and repair for the indicated times, followed by cell lysis and an alkaline Comet assay. **(A)** Representative images of comet tails are shown for the indicated time points. **(B)** Comet Tail Moments were analyzed using the CometScore™ software, relative Comet Tail Moments were calculated based on time point zero and are depicted in the diagram. One of two independent experiments is shown by mean \pm SD. P values were calculated for the represented experiment by using unpaired Student's t-test.

5. Discussion

5.1 Miz-1 is crucial for peripheral T cell populations

An adequate immune response needs adaptive immunity, which is based on functional T and B lymphocytes. The transcription factor Miz-1 is a key player of the early development of these lymphocytes (Möröy et al., 2011). Conditional deletion of the Miz-1 POZ domain in hematopoietic cells revealed a perturbed T lymphocyte development, accompanied by increased p53-dependent apoptosis in the thymus (Rashkovan et al., 2014; Saba et al., 2011a; Saba et al., 2011b). However, little is known about the function of Miz-1 in mature T cells and, therefore, this thesis aimed to elucidate a possible impact.

For this purpose, two mouse models with a conditional Miz-1 POZ domain deletion were used: Vav-Cre x Miz-1^{fl/fl} mice and CD4-Cre x Miz-1^{fl/fl} mice (also termed Miz-1^{ΔPOZ}). The Vav-Cre x Miz-1^{fl/fl} mice possess the deletion in all hematopoietic cells (Kosan et al., 2010), as the Cre-mediated recombination driven by the Vav promoter elements is observed in the entire hematopoietic compartment (de Boer et al., 2003). In CD4-Cre transgenic mice, the Cre expression starts in the double-positive (DP) stage during thymic development (Lee et al., 2001; Sawada et al., 1994). However, it was shown that the CD4-Cre recombinase is already active in the late double-negative 3 (DN3) stage (Wolfer et al., 2001). This could be explained through the accessibility of the *CD4* locus and the start of the expression already in DN3 cells, leading to an active recombinase before developing into DP cells with CD4 surface receptor expression. However, the earliest thymic precursors express low surface levels of CD4 (Wu et al., 1991). This might also explain an early CD4-Cre recombinase expression observed in DN3 cells.

Consistent with this, deletion of the Miz-1 POZ domain was partially detectable already in the thymic DN population when analyzing CD4-Cre x Miz-1^{fl/fl} mice. However, a nearly complete deletion of the POZ domain at the *Zbtb17*^{fl} locus was confirmed in sorted DP cells (**Figure 11C**). While CD4 single-positive (CD4 SP) cells of the thymus exhibited the truncated allele of *Zbtb17* only, the CD8 SP population still showed an incomplete removal of the POZ domain-coding region. This is consistent with the efficiency of the Miz-1 POZ domain deletion in mature T cells of the spleen, showing a similar incomplete deletion (**Figure 11D**). Previously, a deletion efficiency of 85% in enriched peripheral CD8⁺ T cells was shown by using the CD4-Cre transgene (to inactivate the gene encoding NOTCH1), while another study reported a complete deletion in peripheral CD8⁺ T cells with the CD4-Cre (when targeting DNA methyltransferase 1) (Lee et al., 2001; Wolfer et al., 2001). An

explanation for remaining T cells with intact Miz-1 could be a favored survival of CD8 SP thymocytes that did not acquire the POZ domain deletion. A consequence of an incomplete deletion could be the lack of a phenotype, as cells with intact protein might take over the regulatory functions.

It has been reported that Vav-Cre x Miz-1^{fl/fl} mice have a perturbed T cell development with a developmental block at the ETP/DN1/DN2 stage as well as a second block at the DN3 stage. This is concomitant with a 100-fold decrease in thymic cellularity (Saba et al., 2011a; Saba et al., 2011b). These developmental blocks could be avoided by using CD4-Cre x Miz-1^{fl/fl} mice, as an unperturbed thymic development was observed in this mouse model (**Figure 11B**). Furthermore, thymic cellularity was unaffected in CD4-Cre x Miz-1^{fl/fl} mice, yielding absolute cell numbers of thymocytes similar to control. Hence, the impact of a perturbed thymic environment can be mitigated by choosing CD4-Cre x Miz-1^{fl/fl} over Vav-Cre x Miz-1^{fl/fl} mice.

Importantly, CD4-Cre x Miz-1^{fl/fl} mice had considerably fewer mature T cells in the periphery, *e.g.*, the spleen, blood, and, to a lesser extent, the lymph nodes compared to control mice (**Figure 12D**). Differences in absolute T cell numbers were observed between the two mouse models. Both CD4-Cre x Miz-1^{fl/fl} and Vav-Cre x Miz-1^{fl/fl} mice had a drastic reduction in splenic T cells, to 60 % and 10 % compared to controls, respectively. The stronger effect in the Vav-Cre x Miz-1^{fl/fl} mice could be a direct consequence of the defects in early T cell development (Kosan et al., 2010; Saba et al., 2011a; Saba et al., 2011b). Most of the thymocytes have a block in their development, are highly apoptotic, and show altered gene expression profiles. In addition, the hypocellular environment in the thymus and thymic atrophy in Vav-Cre x Miz-1^{fl/fl} mice could affect the maturing T cells (Saba et al., 2011a; Saba et al., 2011b). The reason for decreased peripheral T cells in the CD4-Cre x Miz-1^{fl/fl} mouse model cannot be explained by perturbed thymic development nor by decreased thymic cellularity.

The size of the T cell pool in the periphery is dependent on the survival of T lymphocytes and could be diminished with increased apoptosis. However, apoptosis rates were not significantly induced by Miz-1 deficiency neither in splenic CD4⁺ nor splenic CD8⁺ T cells of young mice (**Figure 21A**). This observation implies that the reduction of the peripheral T cell pool is unlikely the result of a spontaneous occurring apoptosis of unstimulated T cells. The survival of naïve T cells mediated by BCL-2 is strongly dependent on IL-7 signaling (Maraskovsky et al., 1997; Schluns et al., 2000). In line with this, Miz-1 was shown to regulate the IL-7/IL-7R/STAT5/BCL-2 signaling axes in developing pro-T cells, which are also highly dependent on these signals for their survival (Saba et al., 2011b). Therefore, Miz-1 deficiency might induce perturbations in this signaling pathway, which

could account, at least partially, for a reduced peripheral T cell pool. However, expression levels of IL-7R on the surface of peripheral T cells were not altered due to Miz-1 deficiency (data not shown) and further investigations are needed to examine this signaling pathway in mature T cells.

A similar phenotype of fewer peripheral T cells in the spleen and blood was published due to a Vav-Cre-mediated deletion of Kruppel-like factor 2 (KLF2), another transcription factor with zinc finger domains. The KLF2-deficient T cells were homing into non-lymphoid tissue by the upregulation of inflammatory chemokine receptors, accounting for the reduction of the peripheral T cell pool (Sebzda et al., 2008). Hence, the possibility of a false homing was examined in CD4-Cre x Miz-1^{fl/fl} mice by analyzing T cell frequencies in non-lymphoid organs. No differences were observed between Miz-1-deficient mice and controls, thus, an incorrect migration of naïve T cells to the periphery could be excluded (data not shown).

The Miz-1-dependent decrease of peripheral T cells was further supported by flow cytometry data since splenic CD4⁺ and CD8⁺ T cell numbers had a decline by 2-fold in CD4-Cre x Miz-1^{fl/fl} mice (**Figure 13E**). Since the POZ domain deletion in CD8⁺ SP cells was not entire, a stronger phenotype for CD8⁺ T cells could be expected with a higher deletion efficiency. In contrast, absolute numbers of CD4⁺ and CD8⁺ T cells declined more dramatically in Vav-Cre x Miz-1^{fl/fl} mice and this is consistent with the strong decrease in total splenic T cells.

In brief, the CD4-Cre x Miz-1^{fl/fl} mouse model is an effective tool to study how Miz-1 regulates the peripheral T cell pool without the interference of the POZ domain deletion in other cell types, such as B cells and HSCs, and with an unperturbed development of T lymphocytes in the thymus.

Defects in both cell cycle progression and proliferation could cause a reduction of the peripheral T cell pool and were therefore assessed. Freshly isolated splenic T cells of CD4-Cre x Miz-1^{fl/fl} and control mice did not enter the cell cycle and the majority of the cells were in the G1/G0 phase and, hence, in a quiescent state (**Figure 16**). This finding was important for the T cell stimulation experiments because Miz-1-deficient mice showed more post-activation-associated T cell populations. After activation, T cells undergo clonal expansion to form a large pool of effector cells. Following the activation with plate-bound anti-CD3 and soluble anti-CD28, cell cycle progression was observed, but without differences between Miz-1^{ΔPOZ} and control T cells (**Figure 17C**). Moreover, CFSE assays of activated T cells showed that CD4⁺ T cells of Miz-1-deficient mice proliferated faster compared to controls (**Figure 18B**). This is of particular interest since T cells can sense the presence of surrounding T cells and adjust their division rate accordingly.

Consequently, T cells exhibit increased proliferation under lymphopenic conditions (Ernst et al., 1999; Goldrath and Bevan, 1999; Oehen and Brduscha-Riem, 1999). For this thesis, proliferation assays were performed *in vitro*, and equal seeding densities of control and Miz-1^{ΔPOZ} T cells were applied, to exclude the impact of lymphopenia. However, the influence of Miz-1 on the proliferation rate would be interesting to explore also *in vivo*. Furthermore, CFSE assays of CD8⁺ T cells revealed more proliferating cells due to Miz-1 POZ domain loss compared to controls (**Figure 19B**). However, a faster proliferation, as observed for CD4⁺ T cells of Miz-1^{ΔPOZ} mice, was not detected.

An induction in proliferation due to the POZ domain deletion in peripheral T cells seems to contradict a study conducted with keratinocytes lacking functional Miz-1. The proliferation of these Miz-1-deficient cells was reduced in response to treatment with a tumor promoter (12-O-Tetradecanoylphorbol-13-acetate, TPA) (Hönnemann et al., 2012). In addition, increased proliferation was also observed in mature B lymphocytes that carry a functional Miz-1 deletion (Kosan lab, unpublished data), supporting the notion that Miz-1 has a differential role in the proliferation of either tumor tissue or normal, unperturbed cells. One explanation for the differential impact on proliferation could be the overexpression of c-MYC in most cancer cells. These oncogenic expression levels lead to the formation of Miz-1/c-Myc complexes that induce transcriptional changes (Walz et al., 2014; Wiese et al., 2015; Wiese et al., 2013). However, the physiological role of this complex in untransformed cells remains still elusive (Wiese et al., 2013).

Miz-1 is a known activator of the negative cell cycle regulator p21, exerting its function by binding the promoter of *Cdkn1a* (Herold et al., 2002; Hönnemann et al., 2012; Seoane et al., 2002). Induction of p21 negatively modulates cell cycle progression (Gartel and Radhakrishnan, 2005). In line with the observation of increased proliferation, *Cdkn1a* had a reduction in mRNA as well as in protein levels in Miz-1^{ΔPOZ} T cells after TCR activation (**Figure 20**). However, opposite effects were observed in a publication using keratinocytes lacking functional Miz-1. After TPA treatment, levels of *Cdkn1a* were elevated and proliferation was restrained in Miz-1-deficient keratinocytes (Hönnemann et al., 2012). Moreover, upregulation of *Cdkn1a* expression was also observed in Miz-1-deficient DN3 cells of the thymus (Saba et al., 2011a). As mentioned before, differences in cell types and also treatment might account for the different *Cdkn1a* expression levels.

Upon TCR activation, mRNA levels and protein levels of c-Myc are induced and these levels are determined by the strength of the TCR ligand (Preston et al., 2015). The proto-oncogene c-Myc interacts with Miz-1 and replaces co-activators such as nucleophosmin or p300 from the complex (Staller et al., 2001; Wanzel et al., 2008). A repressive complex is formed and the transactivation of genes, *e.g.*, *Cdkn1a*, is blocked (Herold et al., 2002;

Seoane et al., 2002). An expected enhancement of *Cdkn1a* expression as a consequence of Miz-1 deficiency and high c-Myc levels is, however, not in line with decreased *Cdkn1a* levels after TCR stimulation in this thesis.

The regulation of *Cdkn1a* expression is a complex process dependent on many determinants, thus, the expression of *Cdkn1a* in T cells might be indirectly regulated by Miz-1. In line with that, it was previously reported that Miz-1 does not bind directly to the *Cdkn1a* promoter in T cells, however, the lack of promoter binding was here observed in c-Myc-driven T cell lymphomas and it might be different in non-mutated T cells (Walz et al., 2014). The regulation of *Cdkn1a* expression might be via other versatile transcriptional regulators such as specificity protein 1 (SP1), SMADs, or p53 (Gartel and Radhakrishnan, 2005; Karimian et al., 2016). Notably, an involvement of p53 is highly likely, as Miz-1 is a known interaction partner of the tumor suppressor and it regulates the translation of *p53* mRNA via the ribosomal protein L22 (RPL22), controlling both p53 stability and function (Miao et al., 2010; Rashkovan et al., 2014). Besides, histone modifications, post-transcriptional regulation by microRNAs (miRNAs), or alterations in post-translational modifications (PTMs) could account for changes in *Cdkn1a* mRNA as well as protein levels (Kreis et al., 2019). Hence, further investigation is needed to map out the regulation of p21.

Altogether, the first part of this thesis shows that Miz-1 is an important and novel regulator of peripheral T cell populations and it is crucial for their maintenance and homeostasis. The observed defect was not only seen in Vav-Cre x Miz-1^{fl/fl} mice but also in CD4-Cre x Miz-1^{fl/fl} mice, implying a T cell-intrinsic function of Miz-1. Furthermore, the results support the notion that Miz-1 regulates the proliferation of mature T cells after activation but different requirements of Miz-1 for the CD4⁺ and CD8⁺ T cell compartments cannot be excluded.

5.2 A critical role of Miz-1 in T cell apoptosis

5.2.1 Miz-1 regulates p53-independent apoptosis after T cell activation

Programmed cell death is important for T cell development but also T cell homeostasis. Following stimulation with plate-bound anti-CD3 and soluble anti-CD28, T cells of both CD4-Cre x Miz-1^{fl/fl} and control mice showed an induction of apoptosis (**Figure 22**). Importantly, Miz-1 deficiency provoked a much stronger increase in apoptosis than observed for control T cells 48 h post-activation. This result is in line with a previous study observing an apoptosis induction due to Miz-1 deficiency in developing T lymphocytes. Miz-1 was shown to restrict apoptosis by upregulating the gene encoding for the ribosomal protein RPL22, which in turn binds p53 mRNA to inhibit its translation (Rashkovan et al., 2014). Thus, Miz-1 regulates apoptosis induction in the thymus in a p53-dependent manner (Rashkovan et al., 2014).

High levels of apoptosis in activated Miz-1-deficient T cells raised the question of whether this process is mediated via the intrinsic or the extrinsic apoptosis pathway. The extrinsic pathway of apoptosis induction is triggered by the binding of cell-death-receptor ligands such as FasL or TNF to adequate death receptors of the TNFR superfamily, e.g., Fas. The stimulation induces a complex formation of DISC at the inner cell membrane (Chinnaiyan et al., 1995; Kischkel et al., 1995; Krammer et al., 2007). This complex consists, besides oligomerized receptors and adapter molecules, of pro-caspases 8 and pro-caspase 10. These zymogens get cleaved upon activation via the extrinsic pathway and are considered the initiator caspases of the extrinsic apoptosis pathway (Krammer et al., 2007; Varfolomeev et al., 1998). Increased levels of the active subunit of caspase 8 were observed in activated Miz-1^{ΔPOZ} T cells in regard to controls (**Figure 24C**). This leads to the hypothesis of an extrinsic induction of apoptosis. As mentioned beforehand, expression levels of *Cdkn1a* showed a reduction in Miz-1-deficient T cells after activation. Moreover, the observed effects of decreased levels of p21 and induced cleavage of caspase 8 are in line with a publication showing that high levels of p21 could block the cleavage of caspase 8 induced by the death receptor DR4 (Xu and El-Deiry, 2000).

The functional balance of pro- and anti-apoptotic members of the BCL-2 family decides about survival or intrinsic apoptosis induction. Stress stimuli and the increase of pro-apoptotic factors activate the effectors BAX or BAK, leading to a cytochrome c release and apoptosis induction (Li et al., 1997; Opferman and Korsmeyer, 2003; Zhan et al., 2017). The expression of the gene encoding for the anti-apoptotic factor BCL-2, a central player of the intrinsic apoptosis pathway, was unaffected in Miz-1^{ΔPOZ} T cells compared to controls. Altogether, the data suggest the induction of death via the extrinsic rather than

the intrinsic apoptosis pathway, mediating the excessive apoptosis in activated Miz-1^{ΔPOZ} T cells.

To further investigate how the excessive apoptosis due to Miz-1 deficiency is regulated, transcription levels of genes controlling apoptosis were examined after T cell activation. Surprisingly, p53-dependent genes encoding for pro-apoptotic PUMA and NOXA were not upregulated in Miz-1^{ΔPOZ} T cells compared to controls (**Figure 23**). Moreover, the expression of *Bcl2l4*, encoding for the pro-apoptotic effector BAX, was even downregulated in Miz-1^{ΔPOZ} T cells. These data suggest that Miz-1 controls the induction of apoptosis after activation of peripheral T cells in a p53-independent manner. Whether Miz-1 also controls the expression of *Rpl22* in peripheral T cells to restrict apoptosis after activation remains unclear and would be necessary to study to fully understand the function of Miz-1 in T cell apoptosis in the periphery.

Two main concepts for cell death of activated T cells exist, namely activation-induced cell death (AICD) and activated cell-autonomous death (ACAD) (Brenner et al., 2008). AICD is a process of cell death for activated T cells, which experience a re-stimulation of the TCR. This could be achieved *in vitro* by pre-stimulating T cells via the TCR followed by a re-incubation with the same stimulus (Pargmann et al., 2007). Alternatively, T cells can be pre-treated with IL-2 followed by antigen receptor stimulation, as IL-2 predisposes T cells for induction of cell death. Repetitive immunization could induce cell death *in vivo* due to the production of IL-2 after antigen stimulation (Lenardo, 1991). AICD can involve intrinsic as well as extrinsic apoptosis induction. On the contrary, ACAD, also known as death by cytokine deprivation, is independent of a secondary stimulation and involves the intrinsic pathway solely (Brenner et al., 2008). The observed cleavage of caspase 8 indicates that the excessive apoptosis in Miz-1^{ΔPOZ} T cells is rather AICD than ACAD. If so, AICD would surprisingly be induced in Miz-1-deficient T cells without the necessity of a pre-stimulation. This suggests that activation of the TCR without its re-stimulation is sufficient to increase susceptibility to apoptosis in Miz-1^{ΔPOZ} T cells. Similar observations were made in T cells lacking growth factor independent 1 (GFI-1), an interaction partner of Miz-1, where AICD induction was also observed without a pre-stimulation of the TCR (Pargmann et al., 2007). A possible explanation for inducing AICD with anti-CD3/anti-CD28 only might be the deregulation of genes that have pro-apoptotic characteristics due to the loss of Miz-1's transcriptional activity. Fas and FasL are up-regulated after T cell activation and Fas/FasL-mediated apoptosis contributes to AICD of the peripheral T cell pool (Brunner et al., 1995; Eischen et al., 1997; Ju et al., 1995; Trauth et al., 1989). Thus, it would be

insightful to study the influence of Miz-1 deficiency on the expression levels of Fas and FasL after T cell activation.

Summarizing, the data suggest a role for Miz-1 in the regulation of p53-independent apoptosis in peripheral T cells following T cell activation. Miz-1 probably represents an upstream regulator of a particular set of genes, which control proliferation and AICD after TCR activation, however, the exact target genes still have to be mapped out.

5.2.2 Miz-1 and DNA damage in T cells

Studies have established that Miz-1 is necessary for controlling the cell cycle after introducing DNA damage to cells such as fibroblasts and keratinocytes (Herold et al., 2002; Wanzel et al., 2005). Furthermore, Miz-1 was also shown to interfere with p53 function to induce apoptosis after applying DNA-damaging reagents to liver cells (Miao et al., 2010). Besides, the ablation of the Miz-1 POZ domain in combination with a chemotherapeutic drug treatment (cytarabine) delayed lymphoma progression in a T-ALL leukemia model and sensitized tumor cells towards apoptosis (Ross et al., 2019). However, it remains elusive whether Miz-1 has also an impact on non-mutated T lymphocytes after treating them with DNA-damaging stimuli. To research this hypothesis, T cells of control mice were irradiated with γ -irradiation (IR) and the effect on survival and apoptosis was studied. After activation, control T cells showed increased levels of apoptosis when irradiated compared to T cell activation solely (**Supplemental Figure 34**). In line with the increase in apoptosis, expression levels of apoptosis-associated genes were induced in control T cells after IR. More precisely, the p53-target genes encoding for NOXA, BAX, and PUMA were upregulated after IR (**Figure 26**). This supports the notion that this effect after IR treatment of control T cells is a p53-dependent process.

Investigating expression levels of *Zbtb17* after DNA damage would help to elucidate whether Miz-1 plays a role in the regulation of T cell function after IR. Importantly, the irradiation of control T cells showed that neither mRNA levels nor protein levels of *Zbtb17* were altered in their expression (Bachelor's Thesis of Linda Klaus, unpublished). Miz-1 executes functions in the cytoplasm as well as transcriptional functions in the nucleus (Möröy et al., 2011). Shuttling between these compartments due to IR might be possible and preliminary results point to a slight increase in nuclear localization of Miz-1 protein after γ -irradiation (Bachelor's Thesis of Linda Klaus, unpublished). Moreover, PTM's play a central role in the regulation of the DNA damage response (DDR) pathway (Dantuma and van Attikum, 2016). Miz-1 is a known target of several PTM's such as ubiquitination,

which enables inflammatory signaling, or sumoylation, that induces complex formation concomitant with gene repression (Herkert et al., 2010; Liu et al., 2012). A PTM of Miz-1 linked to DNA damage is the phosphorylation by AKT at position S428 that enables the binding of 14-3-3 η to the DNA-binding domain of Miz-1, resulting in an altered target gene expression (Wanzel et al., 2005). Therefore, Miz-1 might be a target to PTM's after IR and further studies elucidating the exact PTM's would give new insight into the role of Miz-1 in the DDR of T cells.

Interestingly, activated Miz-1 ^{Δ POZ} T cells exhibited after IR the tendency of increased apoptosis levels compared to control T cells. Notably, the observed increase in apoptosis after IR from 20 % in control T cells to 42 % in Miz-1-deficient T cells is almost significant (**Supplemental Figure 34**), which could be due to the high variances observed between the experiments. Due to high apoptosis levels, gene expression analysis of apoptosis-associated genes was conducted. Following irradiation, expression levels of genes encoding for NOXA, BAX, and PUMA were increased in control T cells as well as Miz-1 ^{Δ POZ} T cells (**Figure 26**). The expression of these pro-apoptotic genes was slightly higher in Miz-1-deficient T cells, supporting the observed tendency of increased apoptosis. Interestingly, gene expression levels of *Cdkn1a* (p21) showed the biggest difference, resulting in approximately 2 times more *Cdkn1a* mRNA in Miz-1 ^{Δ POZ} T cells than in control T cells. This appears to contradict previous work stating that upregulation of p21 after ultraviolet (UV) radiation is blunted in Miz-1 knock-down cells (Wanzel et al., 2005). In addition, already T cell activation caused altered levels of p21 due to Miz-1 deficiency, hypothesizing a regulatory relationship between Miz-1 and p21 in T cells.

An efficient DNA repair after IR is important to promote cell survival following DNA damage. GFI-1, a zinc finger transcription factor and interaction partner of Miz-1, was shown to be necessary for an effective DNA repair of thymocytes after IR (Vadnais et al., 2018). Due to this observation and high levels of apoptosis after IR in Miz-1-deficient T cells, I hypothesized that Miz-1 plays a role in DNA repair following IR exposure. Comet assays under alkaline conditions, which detect DNA single-strand as well as DNA double-strand breaks (Olive and Banáth, 2006), revealed no differences in the repair capacity of T cells lacking functional Miz-1 (**Figure 27**). Thus, Miz-1 does not regulate IR-induced DNA repair, at least not in peripheral T cells.

The present results show that the apoptosis induction in control and Miz-1 ^{Δ POZ} T cells after DNA damage is a p53-dependent process. Activated Miz-1-deficient T cells exhibit a higher tendency of IR-induced cell death compared to controls. However, T cell activation

alone sensitized Miz-1^{ΔPOZ} T cells already for increased apoptosis. It could be possible that other DNA damaging stimuli such as UV light, reactive oxygen species (ROS), or DNA damaging drugs show a different impact on shifting the balance between survival and apoptosis in dependency of functional Miz-1.

5.3 Miz-1 is a novel regulator of immune aging

Aging is characterized by a time-dependent accumulation of damage and the progressive deterioration of cellular processes (Gems and Partridge, 2013; López-Otín et al., 2013). Age-related changes can also be observed in the immune system, which is commonly termed immunosenescence. Immune aging leads to an increased susceptibility to infectious diseases in the elderly and altered responsiveness to vaccinations with an insufficient generation of immune memory (Nikolich-Zugich, 2005). Studies have established that Miz-1 is required for the development and function of immune cells (Möröy et al., 2011), but it has remained elusive whether Miz-1 has also an impact on T lymphocytes during aging.

As anticipated, absolute numbers of splenic T cells from control mice declined with age relative to young counterparts (**Figure 12D**), as the size of the thymus decreases during aging and thymopoiesis declines (Weiskopf et al., 2009). Comparing young and old control mice, a mild decline was also observed in T cell frequencies (**Figure 12C**). These results are similar to those obtained in a study showing that splenic T cells of old C57BL/6 mice have an overall reduction in frequencies and absolute numbers (Ron-Harel et al., 2018). As discussed before, the T cell compartment of young mice was reduced due to Miz-1 deficiency. These results show that the functional loss of Miz-1 as well as aging result in decreased mature T cells in the periphery and this phenotypical similarity could indicate that Miz-1 plays a role in T cell aging.

When comparing young and old control mice, an age-related drop in CD4⁺ and CD8⁺ T cell numbers became obvious. While CD4⁺ T cells declined 4-fold, CD8⁺ T cells decreased only 2-fold (**Figure 13E/F**). This is similar to young Miz-1-deficient mice, where absolute numbers of CD4⁺ as well as CD8⁺ T cells declined (both twofold) compared to young controls.

Remarkably, ratios of CD4:CD8 cell frequencies changed in old control as well as in old Miz-1-deficient mice compared to their respective young counterparts. A similar effect was observed in aged wild-type mice in several publications (Barrat et al., 1997; Berzins et al., 1999; Boersma et al., 1985). As a consequence of altered ratios, absolute numbers of CD8⁺ T cells had the tendency of higher numbers than CD4⁺ T cells in old control mice. This effect was more pronounced in old mice with functional loss of Miz-1. However, Ron-Harel and colleagues described no alterations in CD4⁺ or CD8⁺ T cell frequencies when comparing young and old mice, indicating that there are at least variations in aging effects in different mouse cohorts (Ron-Harel et al., 2018). Additionally, sex differences are known to affect the immune system (Klein and Flanagan, 2016) and could perhaps lead to

these phenotypical differences. In this thesis, mice of both genders were analyzed and only the particular age of the mouse cohorts was considered.

The CD4:CD8 ratio alterations in this thesis could be due to higher apoptosis rates of CD4⁺ T cells compared to CD8⁺ T cells. Indeed, apoptosis rates in young and old control mice were slightly higher for CD4⁺ than for CD8⁺ T cells. In addition, Miz-1 deficiency in old mice elevated the apoptosis rates of CD4⁺ T cells more than that of CD8⁺ T cells, which could account for the detected phenotype (**Figure 21B**). The observed results are in line with a previous study estimating average lifespans of peripheral T cells from deuterium-labeling experiments and fitting them into a mathematical model. It was demonstrated that the expected life span of naïve CD8⁺ T cells is longer than of naïve CD4⁺ T cells (den Braber et al., 2012). Interestingly, the average lifespan of naïve CD4⁺ T cells did not alter significantly during aging, while the expected lifespan of naïve CD8⁺ T cells increased even further in aged mice compared to adult mice (den Braber et al., 2012).

In addition, an incomplete deletion of the Miz-1 POZ domain was observed in mature, peripheral T cells. The CD8 SP population of the thymus possessed partially the undeleted *Zbtb17^{fl}* locus, while CD4 SP had only the truncated *Zbtb17^{fl}* locus. Therefore, it is likely that CD8⁺ T cells mainly account for the incomplete deletion observed in the periphery of CD4-Cre x Miz-1^{fl/fl} mice (**Figure 11C/D**). As mentioned before, the considerable role of Miz-1 in the apoptosis of CD4⁺ T cells relative to CD8⁺ T cells could therefore be justified by the deletion efficiency in peripheral CD8⁺ T cells. However, this could not be the explanation for altered CD4:CD8 ratios in old control mice relative to young control mice. Hence, studying expression levels of Miz-1 in both T cell populations separately would give insight into a differential role of Miz-1 for these subsets. However, protein expression levels of diverse targets are hard to detect with immunoblotting, because freshly isolated T cells are in a quiescent state and exhibit a low rate of protein synthesis.

Moreover, the excessive induction of apoptosis after activation of Miz-1-deficient T cells (**Figure 22**) could also support the aging effect, reflected by reduced T cells and altered ratios, as more T cells might die in the course of aging. Apoptosis induction after activation was only analyzed in young T cells in this thesis. However, further evidence could be collected by performing these experiments with T cells from mice of different age cohorts and by analyzing CD4⁺ and CD8⁺ T cells separately.

An unexpected finding was the observation that T cell populations of young Miz-1^{ΔPOZ} mice exhibited occasionally a premature phenotype similar to old control mice. This was observed, for instance, for frequencies of peripheral T lymphocytes in the CD4-Cre x

Miz-1^{fl/fl} mouse model. Here, splenic T cell frequencies of young Miz-1^{ΔPOZ} mice were indistinguishable from old control mice (**Figure 12C**). Young Miz-1-deficient did not always exhibit the same frequencies or absolute numbers as the 18-month-old control mice. However, T cell patterns of young Miz-1^{ΔPOZ} mice showed often distributions similar to that of aged control mice, e.g., absolute numbers of naïve CD8⁺ T cells were similar in young Miz-1-deficient and old control mice (**Figure 15**). Moreover, young Miz-1^{ΔPOZ} mice possessed even fewer splenic CD4⁺ T cells than old control mice (**Figure 14**). Overall, these observations are in line with a previous publication stating that Miz-1 is a key player of B lymphocyte aging during peripheral maturation (Piskor et al., 2022). In conclusion, functional Miz-1 deletion results in a premature immune aging phenotype. These observations underline the importance of Miz-1 in T cell aging.

A naïve T cell pool with a high diversity of TCRs is important for effective immune reactions but it declines in the course of aging (Ernst et al., 1993; Fagnoni et al., 2000; Utsuyama et al., 1992). Of note, differences between mice and humans exist, as murine naïve T cells decline strongly during aging concomitant with a decreased thymic output, but human naïve T cells decrease only moderately due to homeostatic proliferation (den Braber et al., 2012; Qi et al., 2014). In this thesis, it was observed that aging caused a reduction of naïve CD4⁺ T cell (7-fold) and naïve CD8⁺ T cell (4-fold) numbers in control mice (**Figure 14 & Figure 15**). These observations are in line with previous reviews stating an absolute decrease of naïve T cells with age (Nikolich-Zugich, 2018). Notably, high variances in cell frequencies and numbers were observed when analyzing old control mice of the CD4-Cre x Miz-1^{fl/fl} as well as Vav-Cre x Miz-1^{fl/fl} mouse line. Even though old mice had the same age (18 months) when analyzed, this spreading in variances influences the statistics. Thus, it might be reasonable to repeat this experiment with a bigger mouse cohort.

The functional loss of Miz-1 in CD4-Cre x Miz-1^{fl/fl} mice resulted also in a decrease in naïve T cell numbers and this was observed in the young as well as in the old cohort (**Figure 14 & Figure 15**). Consequently, old Miz-1-deficient mice had barely naïve CD4⁺ and naïve CD8⁺ T cells left. These results pinpoint once again that the inactivation of Miz-1 might induce a premature aging phenotype. While naïve CD8⁺ T cell frequencies decreased in young as well as in old mice due to Miz-1 deficiency, naïve CD4⁺ T cell frequencies declined in Miz-1-deficient mice only in the aged cohort. It might be possible that Miz-1, as a regulator of T cell aging, has a more prominent role for the naïve T cell pool of CD8⁺ rather than of CD4⁺ cells. In general, Miz-1 might control different functions for these two subpopulations, which can be exerted by maintaining different genetic programs in both cell types.

After T cell activation and the subsequent production of large numbers of effector T cells, the clearance of the infection induces the contraction phase. During this process, the majority of T cells die due to apoptosis and only a minority of T cells survive and develop into memory T cells (T_M) (Harty and Badovinac, 2008; McKinstry et al., 2010). Aging is accompanied by the accumulation of T_M cell subsets, hence the ratio of naïve:memory T cells declines (Ernst et al., 1993; Lerner et al., 1989; Quinn et al., 2019; Utsuyama et al., 1992). In line with this, an enlargement of memory T cell frequencies was observed likewise in old control mice compared to young controls for both the $CD4^+$ and $CD8^+$ compartments.

Interestingly, an accumulation of these post-activation-associated subpopulations was also provoked by the functional loss of Miz-1. This included the increased frequency of memory T cells in the $CD8^+$ T cell compartment of young $CD4\text{-Cre} \times \text{Miz-1}^{\text{fl/fl}}$ mice compared to controls. This enlargement was even more pronounced in old Miz-1-deficient mice and this increase was in these aged mice also observed for $CD4^+$ T_M cells (**Figure 14 & Figure 15**). Importantly, differences in $CD44^{\text{high}}$ populations were observed for T_H cells and CTLs. While $CD4^+$ cells had predominantly an expansion in effector memory T cells (T_{EM}), $CD8^+$ cells exhibited an increase in central memory T cells (T_{CM}). These distinct memory cell accumulations are in line with a previous study, stating a conversion from T_{EM} cells into T_{CM} cells in the $CD8^+$ compartment after the clearance of pathogens. The $CD8^+$ T_{CM} cells are designated as the “true” memory cells, while $CD8^+$ T_{EM} cells form an intermediate population (Wherry et al., 2003). In $CD4\text{-Cre} \times \text{Miz-1}^{\text{fl/fl}}$ mice, Miz-1 deficiency expanded the T_{CM} population of the $CD8^+$ compartment in young as well as in old mice, while it increased frequencies of $CD4^+$ T_{EM} cells only in aged mice. In addition, the enlargement of the T_M pool was again more pronounced in the $\text{Vav-Cre} \times \text{Miz-1}^{\text{fl/fl}}$ mice and occurred here in both T cell compartments in young as well as in old mice.

Altogether, the functional loss of Miz-1 favors the generation of an increased T_M cell pool but how this is realized is a matter of speculation. One possibility could be alterations in the epigenome, as Miz-1 is known to interact with chromatin modifiers, e.g., DNMT3A, and HDACs, thereby affecting DNA methylation pattern and histone acetylation (Brenner et al., 2005; Varlakhanova et al., 2011). Thus, Miz-1 function is necessary for an adequate balance of gene activation and gene silencing and, consequently, Miz-1 deficiency could lead to an imbalance of gene expression. Epigenetic modifications occur not only during T cell activation and differentiation but are also a hallmark of T cell aging. In the latter, this is contributing to dysfunctional cellular processes (Goronzy et al., 2018). Especially changes in DNA methylation are a common characteristic of aging (Horvath and Raj,

2018). As Miz-1 is an interaction partner of DNMT3A (Brenner et al., 2005), Miz-1 deficiency could result in alterations of the methylation pattern in Miz-1-deficient T cells. Besides, epigenetic changes of DNA and/or histones in Miz-1-deficient T cells could also lead to altered gene expression of factors that are important to regulate fate decisions of the different T cell subsets. In addition, an altered gene program due to the loss of Miz-1's transcriptional activity might induce an artificial "pseudo-activated" phenotype of T cells. Therefore, the induced memory T cell formation might be a consequence of extensive genetic reprogramming by Miz-1 interfering with several regulatory pathways.

Perturbations of the contraction phase could also lead to an altered memory T cell pool, through the regulation of cell fate decisions for survival and death. Factors such as PUMA and BIM were shown to control the death of T cells after activation (Bauer et al., 2006). However, excessive apoptosis of activated Miz-1-deficient T cells is contradictory to an increase in T_M cells and PUMA was not differentially regulated upon Miz-1 loss-of-function in this study. A faster activation-induced proliferation of Miz-1 $^{\Delta POZ}$ T cells, on the other hand, points towards a pre-activated signature of these cells. It might be interesting to study cell proliferation not only in mixed CD4 $^+$ and CD8 $^+$ T cell populations, but also separately for naïve and T_M cells. Overall, it could be speculated that Miz-1 deficiency leads to a faster clonal expansion phase of activated T cells, resulting in less naïve and more memory T cells.

Increased T_M cell frequencies were also detected in the Vav-Cre x Miz-1 $^{fl/fl}$ mouse model, however, this phenotype could already be observed at young age in these mice (**Figure 7 & Figure 9**). The difference between the two mouse models could be explained by the influence of immune cells surrounding and interacting with T cells. As the CD4-Cre x Miz-1 $^{fl/fl}$ mouse model has a T cell-specific deletion, Miz-1 deficiency in Vav-Cre x Miz-1 $^{fl/fl}$ mice is observed in all hematopoietic cells. Thus, myeloid cells and B cells possess the Miz-1 POZ domain deletion, which affects their phenotype and function as well. The site of T cell activation is the immunological synapse, which is formed by the interaction of a T cell with an antigen-presenting cell (APC) (Yokosuka and Saito, 2009). Therefore, activation of Miz-1-deficient T cells might be altered in Vav-Cre x Miz-1 $^{fl/fl}$ mice due to Miz-1-deficient B cells and monocytes. Since different types of immune cells are affected in this strain, alterations in circulating factors such as chemokines and cytokines might also influence phenotypical differences. Moreover, T cells emigrating from the thymus might be differentially affected, depending on the chosen mouse model. In Vav-Cre x Miz-1 $^{fl/fl}$ mice, the POZ domain deletion of Miz-1 affects early T cell differentiation, which is characterized by developmental blocks and thymic atrophy (Saba et al., 2011b). A "pseudo-activated" signature of surface receptor expression is for instance not unlikely in Vav-Cre x Miz-1 $^{fl/fl}$ mice.

Interestingly, reports have noted a homeostasis-driven proliferation of naïve CD8⁺ T cells independent of cognate antigens in a depleted lymphoid compartment. During this proliferation, the naïve CD8⁺ T cells convert into T cells acquiring a memory-like phenotype, which is characterized by functional adaptations and the upregulation of several surface markers such as CD44 (Goldrath et al., 2000). As mild lymphopenia was observed in spleens of CD4-Cre x Miz-1^{fl/fl} mice and to a stronger extent in Vav-Cre x Miz-1^{fl/fl} mice, the conversion of naïve T cells into memory-like T cells is likely. Naïve T cells would masquerade as T_M cells and this would account for the high frequencies of T_M cells observed in this thesis. The survival of naïve T cells was shown to be dependent on IL-7 and access to this cytokine is diminished in the course of aging, since the microenvironment of lymph nodes undergoes age-related changes (Becklund et al., 2016). Alterations in the maintenance of true naïve T cells are causative for the conversion of some of these cells into memory-like cells, termed virtual memory T (T_{VM}) cells (Nikolich-Zugich, 2018). An increase in T_M frequencies in Miz-1-deficient mice is similar to a previous observation showing that the majority of the CD8⁺ T_{CM} cells, which accumulated in old naïve mice, are not T_M cells but are actually T_{VM} cells that developed without antigenic stimulation (Chiu et al., 2013). For distinguishing between T_{VM} cells and the true antigen-experienced T_{CM} cells, the authors use the marker CD49d, which is not upregulated by T_{VM} cells (Chiu et al., 2013). The use of different antibody panels for flow cytometry could give new insights into the role of Miz-1 in T cell activation and aging. Memory turnover, a process important for the maintenance of T_M cells, is characterized by a basal cytokine-driven proliferation and an equivalent cell death rate (Harty and Badovinac, 2008). Alterations in the memory turnover due to the observed accelerated proliferation of activated Miz-1-deficient T cells could also account for an increase in T_M cells. Contradictory to this hypothesis are the excessive death rates detected for activated Miz-1-deficient T cells. To unravel whether different cell populations possess a distinct responsiveness, proliferation and apoptosis assays for naïve and memory T cells should be performed.

In summary, functional Miz-1 is necessary to control peripheral T cell populations as well as ratios of CD4⁺ and CD8⁺ T cells (**Figure 28**). After T cell activation, Miz-1 is important to control adequate proliferation and apoptosis rates of T lymphocytes. Adult Miz-1-deficient mice exhibit a premature aging phenotype characterized by less naïve and more memory or rather virtual memory T cells (**Figure 28**). This premature aging signature gets even more pronounced in old Miz-1-deficient mice. In conclusion, Miz-1 is suggested to be a novel regulator of T cell aging.

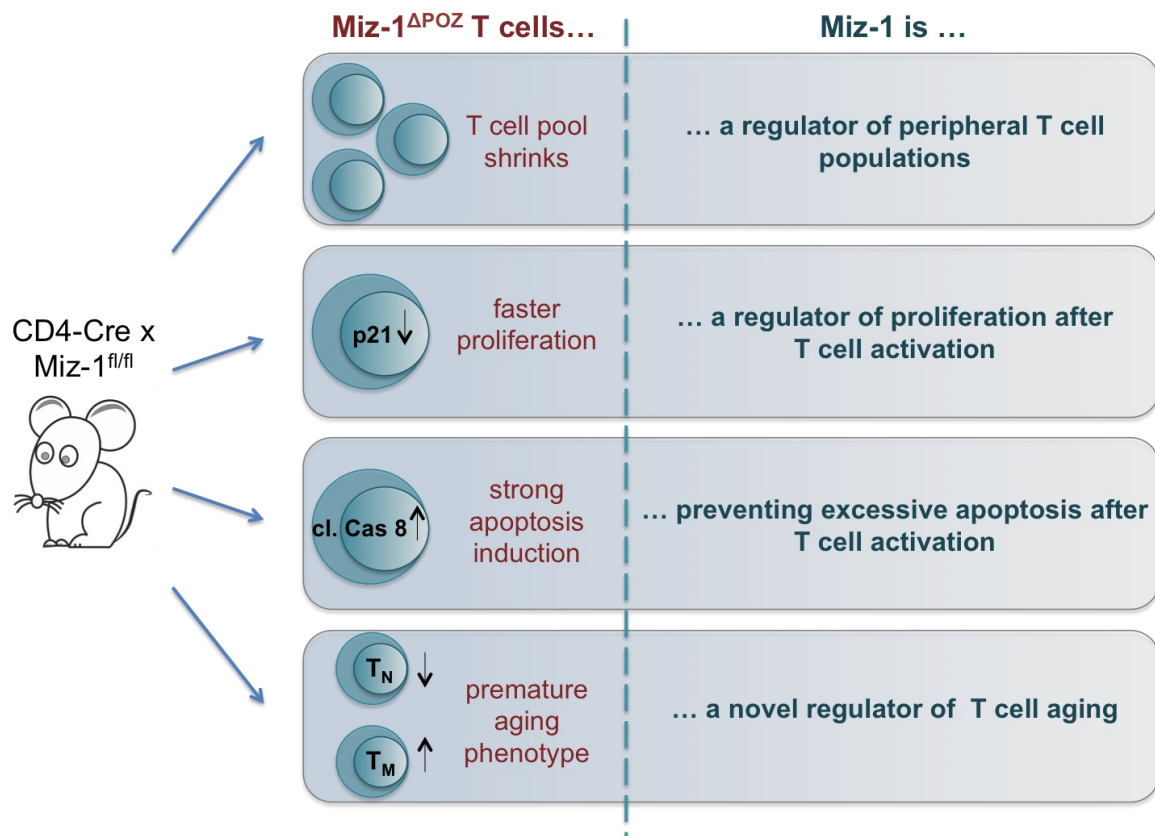


Figure 28: Schematic overview summarizing key findings.

By analyzing CD4-Cre x Miz-1^{fl/fl} (Miz-1^{ΔPOZ}) mice, which possess a T cell-specific deletion of the POZ domain of Miz-1, several new functions of Miz-1 in T lymphocytes were unraveled: (1) Miz-1 is an important regulator for the maintenance of the peripheral T cell pool. (2) Following T cell activation, Miz-1 is necessary to control proper proliferation since Miz-1-deficient T cells proliferate faster concomitant with reduced levels of *Cdkn1a* (p21). (3) Miz-1 prevents an excessive induction of apoptosis after T cell activation. The strong apoptosis induction due to Miz-1 deficiency is accompanied by increased levels of cleaved caspase 8 (cl. Cas 8), an initiator caspase of the extrinsic apoptosis pathway. (4) Miz-1 is suggested to be a novel regulator of T cell aging. Miz-1^{ΔPOZ} T cells exhibit a premature aging phenotype, characterized by a reduced naïve T (T_N) cell pool and increased frequencies of memory T (T_M) cells.

5.4 Conclusions

Altogether, the present thesis unravels a critical role of the transcription factor Miz-1 for T cell maturation and activation. An important observation was the reduction of peripheral T cells due to Miz-1 deficiency. T cells lacking functional Miz-1 showed also multiple defects after activation, e.g., altered proliferation rates and excessive apoptosis.

Interestingly, the deletion of the POZ domain of Miz-1 had a differential impact on CD4⁺ and CD8⁺ T cells and this might reflect different requirements for the immune responses of these cell types. Since *in vitro* experiments with Miz-1-deficient T cells might not reflect their responses *in vivo*, mouse experiments would be helpful to unravel the impact of Miz-1 under more physiological conditions. Meaningful experiments would be adoptive transfer assays to study proliferation and apoptosis *in vivo*. Analyzing this for CD4⁺ and CD8⁺ T cells would give insight into their functionality and responsiveness. In addition, examining the role of Miz-1 in T cell-mediated immune responses by various infection assays and, in addition, observing T cell memory formation after a viral or bacterial infection in a Miz-1-deficient background would reveal the role of Miz-1 in this process.

Excessive apoptosis induction was observed after activation of T cells with a functional Miz-1 deletion and results point towards a p53-independent mechanism. Thus, it would be interesting to cross the utilized mice with another mouse line containing a p53 deletion (Miz-1^{fl/fl} p53^{-/-}) and perform experiments such as apoptosis assays and gene expression analysis. Since Miz-1-deficient T cells showed differences in post-activation-associated populations as well as expression levels of several genes, transcriptome analysis would help to identify target genes of Miz-1, which are differentially expressed in young and old T cells as well as after T cell activation.

Experiments with Miz-1 gain of function approaches in T cells need to be researched to further dissect the role of Miz-1 in lifespan and aging. This would help to understand whether Miz-1 should be considered for pharmacological interventions for immune aging or to achieve a proper immune response after vaccinations. However, the role of Miz-1 in tumor development and progression should be taken into account here. Moreover, *ex vivo* approaches of aged T cells would be helpful to eliminate potential age-related effects of the cellular environment. An important process of unstimulated as well as activated T cells is the metabolism, which was not covered in this thesis so far. Additional experiments need to be performed to map out a possible role of Miz-1 in T lymphocyte metabolism.

6. Supplemental figures

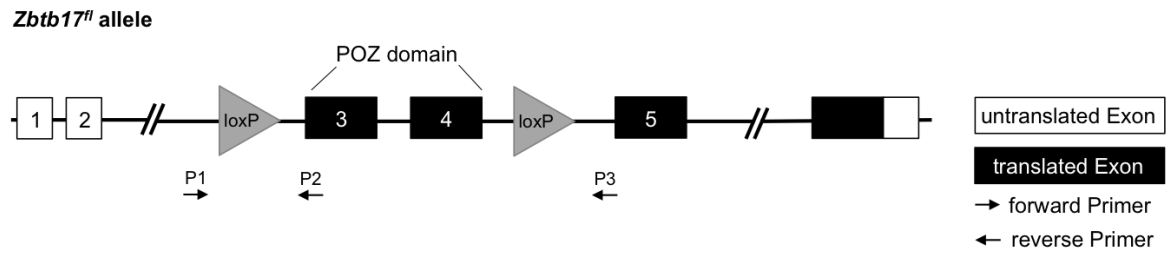


Figure 29: Targeting strategy of the *Zbtb17* locus.

Scheme of the *Zbtb17^{fl}* allele with untranslated exons (white boxes) and translated exons (black boxes) is illustrated. LoxP sites flank exons 3 and 4 to delete the POZ domain of *Zbtb17* by Cre-mediated recombination. Location of primers P1 (Miz-1_P1), P2 (Miz-1_P2), and P3 (Miz-1_P3) used for genotyping the deletion of the POZ domain-encoding exons is indicated.

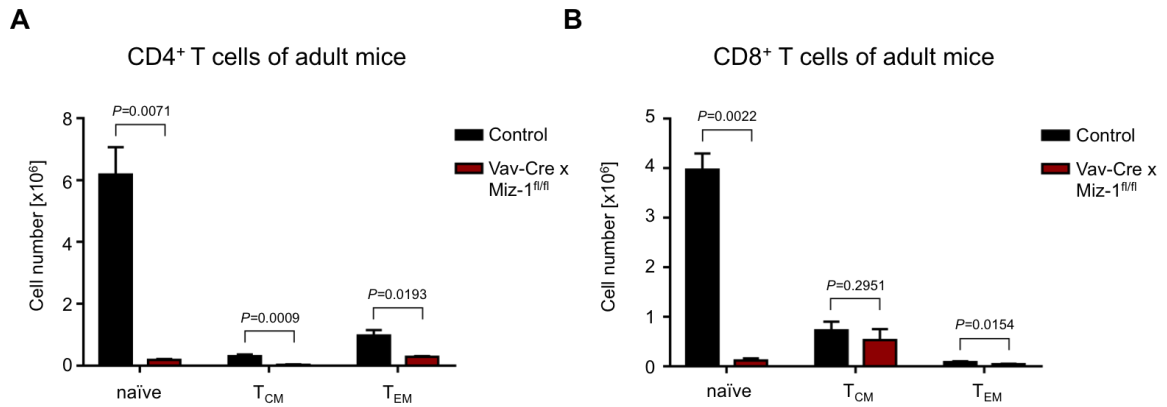


Figure 30: Deletion of functional Miz-1 decreases naïve T cells in adult mice.

Splenocytes of adult (2 – 4 months) control and Vav-Cre x Miz-1^{fl/fl} mice were analyzed for absolute numbers of naïve (CD44^{lo}, CD62L^{hi}), central memory (T_{CM}; CD44^{hi}, CD62L^{hi}), and effector memory T cells (T_{EM}; CD44^{hi}, CD62L^{lo}) within **(A)** the CD4⁺ or **(B)** the CD8⁺ compartment. Splenic cells were used for the negative selection of T cells prior to flow cytometry. The antibodies CD4, CD8, CD44, and CD62L were used to distinguish T cell subsets by flow cytometry after debris exclusion via FSC/SSC scattering. Absolute numbers are depicted in bar diagrams as mean + SD. *P* values were calculated using unpaired Student's t-test. An unpaired Student's t-test with Welch's correction was applied if variances between populations were unequal. Results were obtained from 3 (A, B) independent experiments.

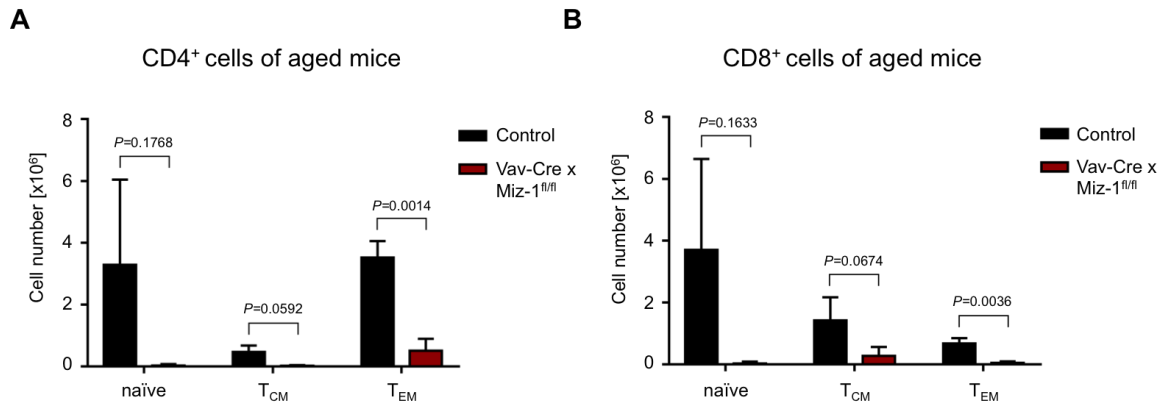


Figure 31: Deletion of functional Miz-1 depletes naïve T cells in aged mice.

Splenocytes of aged (18 months) control and Vav-Cre x Miz-1^{fl/fl} mice were analyzed for absolute numbers of naïve (CD44^{lo}, CD62L^{hi}), central memory (T_{CM}; CD44^{hi}, CD62L^{hi}), and effector memory T cells (T_{EM}; CD44^{hi}, CD62L^{lo}) within **(A)** the CD4⁺ or **(B)** the CD8⁺ cell compartment. Cell suspensions were stained with an antibody mixture of CD4, CD8, CD44, and CD62L. Debris was excluded via FSC/SSC scattering and cells were pre-gated on living cells (DAPI⁻). Absolute numbers are depicted in bar diagrams as mean + SD. *P* values were calculated using unpaired Student's t-test and a Welch's correction was applied if variances between populations were unequal. Results were obtained from 3 (A, B) independent experiments.

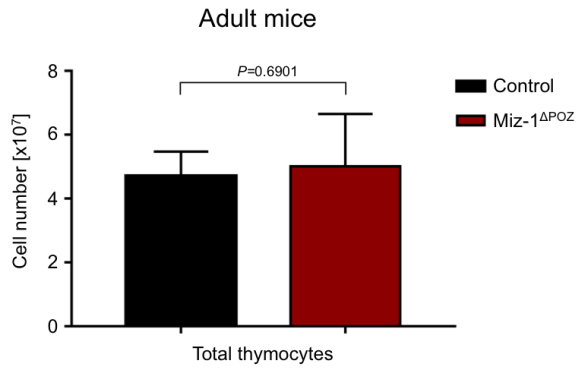


Figure 32: Thymic characterization of Miz-1-deficient mice.

Adult (2 – 4 months) control and CD4-Cre x Miz-1^{fl/fl} (Miz-1 Δ POZ) mice were analyzed for the total amount of thymocytes. Diagram represents cell numbers as mean + SD. Statistical analysis was performed using an unpaired Student's t-test. *P* value is indicated. Data are representative of 6 independent experiments.

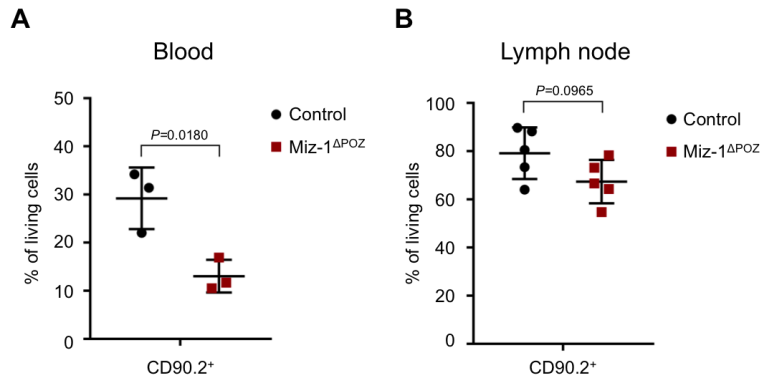


Figure 33: Reduction of Miz-1-deficient T cells in blood.

Adult (2 – 4 months) control and CD4-Cre x Miz-1^{fl/fl} (Miz-1^{ΔPOZ}) mice were analyzed for T cells in different compartments by flow cytometry using B220 and CD90.2 antibodies. Frequencies of T cells (CD90.2⁺, B220⁻) in **(A)** blood and **(B)** lymph nodes after red cell lysis are shown. Cells were pre-gated on FSC/SSC for debris exclusion and living cells (DAPI⁻). Percentages are depicted as mean ± SD. Significances were calculated using unpaired Student's t-test and *P* values are indicated. Data are representative of 5 (B) or 3 (A) independent experiments.

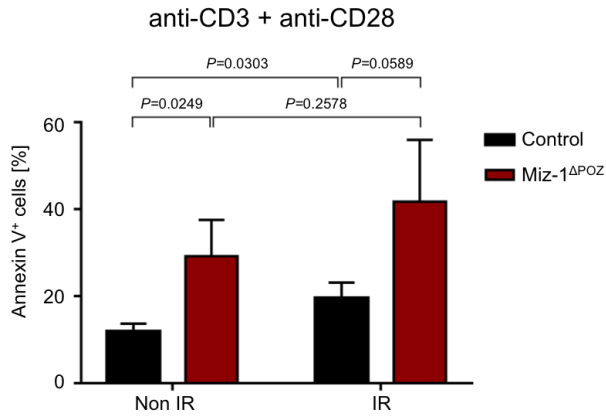


Figure 34: Analysis of apoptosis after T cell activation and irradiation.

Splenic T cells of adult (2 – 4 months) control and CD4-Cre x Miz-1^{fl/fl} (Miz-1^{ΔPOZ}) mice were isolated by negative selection and activated with anti-CD3 and anti-CD28 in culture. T cells were either analyzed 48 h after activation (Non IR) or irradiated after 24 h with 2 Gy of γ -irradiation (IR) and analyzed 24 h post-IR. Apoptosis of T cells was examined by flow cytometry using fluorochrome-labeled Annexin V, after debris exclusion via FSC/SSC scattering. The frequency of Annexin V⁺ cells is depicted as mean + SD. Significances were calculated using unpaired Student's *t*-test. *P* values are indicated. Data are representative of 3 independent experiments.

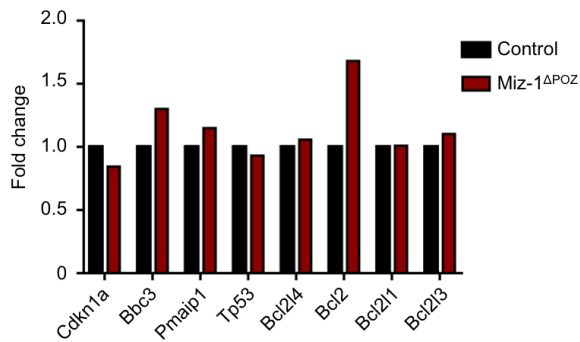


Figure 35: Apoptosis-related gene expression is not altered in Miz-1-deficient T cells.

Spleens of adult (2 – 4 months) control and CD4-Cre x Miz-1^{fl/fl} (Miz-1^{ΔPOZ}) mice were isolated and T cells were obtained by negative separation. Directly after T cell isolation, a qRT-PCR was performed. Gene expression of the indicated transcripts was measured and fold change relative to control T cells was calculated using the comparative $\Delta\Delta C_t$ method and normalized to *Actb* (*Actin Beta*). Data are representative of one experiment performed in technical triplicates.

7. References

- Adams, J.M., Harris, A.W., Pinkert, C.A., Corcoran, L.M., Alexander, W.S., Cory, S., Palmiter, R.D., and Brinster, R.L. (1985). The c-myc oncogene driven by immunoglobulin enhancers induces lymphoid malignancy in transgenic mice. *Nature* **318**, 533-538.
- Adhikary, S., Peukert, K., Karsunky, H., Beuger, V., Lutz, W., Elsässer, H.P., Möröy, T., and Eilers, M. (2003). Miz1 is required for early embryonic development during gastrulation. *Molecular and cellular biology* **23**, 7648-7657.
- Allman, D., Sambandam, A., Kim, S., Miller, J.P., Pagan, A., Well, D., Meraz, A., and Bhandoola, A. (2003). Thymopoiesis independent of common lymphoid progenitors. *Nature immunology* **4**, 168-174.
- Aspinall, R., Pitts, D., Lapenna, A., and Mitchell, W. (2010). Immunity in the elderly: the role of the thymus. *Journal of comparative pathology* **142**, S111-S115.
- Awasthi, P., Foiani, M., and Kumar, A. (2015). ATM and ATR signaling at a glance. *Journal of cell science* **128**, 4255-4262.
- Baaten, B.J., Tinoco, R., Chen, A.T., and Bradley, L.M. (2012). Regulation of Antigen-Experienced T Cells: Lessons from the Quintessential Memory Marker CD44. *Frontiers in immunology* **3**, 23.
- Barber, E.K., Dasgupta, J.D., Schlossman, S.F., Trevillyan, J.M., and Rudd, C.E. (1989). The CD4 and CD8 antigens are coupled to a protein-tyrosine kinase (p56lck) that phosphorylates the CD3 complex. *Proceedings of the National Academy of Sciences of the United States of America* **86**, 3277-3281.
- Barrat, F., Lesourd, B., Louise, A., Boulouis, H., Vincent-Naulleau, S., Thibault, D., Sanaa, M., Neway, T., and Pilet, C. (1997). Surface antigen expression in spleen cells of C57Bl/6 mice during ageing: influence of sex and parity. *Clinical & Experimental Immunology* **107**, 593-600.
- Barrilleaux, B.L., Burow, D., Lockwood, S.H., Yu, A., Segal, D.J., and Knoepfler, P.S. (2014). Miz-1 activates gene expression via a novel consensus DNA binding motif. *PLoS one* **9**, e101151.
- Basu, S., Liu, Q., Qiu, Y., and Dong, F. (2009). Gfi-1 represses CDKN2B encoding p15INK4B through interaction with Miz-1. *Proceedings of the National Academy of Sciences of the United States of America* **106**, 1433-1438.
- Bauer, A., Villunger, A., Labi, V., Fischer, S.F., Strasser, A., Wagner, H., Schmid, R.M., and Häcker, G. (2006). The NF-kappaB regulator Bcl-3 and the BH3-only proteins Bim and Puma control the death of activated T cells. *Proceedings of the National Academy of Sciences of the United States of America* **103**, 10979-10984.
- Becklund, B.R., Purton, J.F., Ramsey, C., Favre, S., Vogt, T.K., Martin, C.E., Spasova, D.S., Sarkisyan, G., LeRoy, E., Tan, J.T., *et al.* (2016). The aged lymphoid tissue environment fails to support naïve T cell homeostasis. *Scientific reports* **6**, 30842.

- Bédard, M., Roy, V., Montagne, M., and Lavigne, P. (2017). Structural Insights into c-Myc-interacting Zinc Finger Protein-1 (Miz-1) Delineate Domains Required for DNA Scanning and Sequence-specific Binding. *The Journal of biological chemistry* 292, 3323-3340.
- Berzins, S., Godfrey, D., Miller, J., and Boyd, R. (1999). A central role for thymic emigrants in peripheral T cell homeostasis. *Proceedings of the National Academy of Sciences* 96, 9787-9791.
- Beyersdorf, N., Kerkau, T., and Hünig, T. (2015). CD28 co-stimulation in T-cell homeostasis: a recent perspective. *ImmunoTargets and therapy* 4, 111.
- Blackwood, E.M., and Eisenman, R.N. (1991). Max: a helix-loop-helix zipper protein that forms a sequence-specific DNA-binding complex with Myc. *Science* 251, 1211-1217.
- Boersma, W., Steinmeier, F., and Haaijman, J. (1985). Age-related changes in the relative numbers of Thy-1-and Lyt-2-bearing peripheral blood lymphocytes in mice: a longitudinal approach. *Cellular immunology* 93, 417-430.
- Boldin, M.P., Varfolomeev, E.E., Pancer, Z., Mett, I.L., Camonis, J.H., and Wallach, D. (1995). A novel protein that interacts with the death domain of Fas/APO1 contains a sequence motif related to the death domain. *The Journal of biological chemistry* 270, 7795-7798.
- Bolotin, E., Smogorzewska, M., Smith, S., Widmer, M., and Weinberg, K. (1996). Enhancement of thymopoiesis after bone marrow transplant by in vivo interleukin-7.
- Bonilla, F.A., and Oettgen, H.C. (2010). Adaptive immunity. *The Journal of allergy and clinical immunology* 125, S33-40.
- Borriello, F., Iannone, R., and Marone, G. (2017). Histamine release from mast cells and basophils. *Histamine and Histamine Receptors in Health and Disease*, 121-139.
- Bradley, L.M., Watson, S.R., and Swain, S.L. (1994). Entry of naive CD4 T cells into peripheral lymph nodes requires L-selectin. *The Journal of experimental medicine* 180, 2401-2406.
- Breitfeld, D., Ohl, L., Kremmer, E., Ellwart, J., Sallusto, F., Lipp, M., and Förster, R. (2000). Follicular B helper T cells express CXC chemokine receptor 5, localize to B cell follicles, and support immunoglobulin production. *The Journal of experimental medicine* 192, 1545-1552.
- Brenner, C., Deplus, R., Didelot, C., Lorient, A., Viré, E., De Smet, C., Gutierrez, A., Danovi, D., Bernard, D., Boon, T., *et al.* (2005). Myc represses transcription through recruitment of DNA methyltransferase corepressor. *The EMBO journal* 24, 336-346.
- Brenner, D., Krammer, P.H., and Arnold, R. (2008). Concepts of activated T cell death. *Critical reviews in oncology/hematology* 66, 52-64.
- Broere, F., and van Eden, W. (2019). T cell subsets and T cell-mediated immunity. In *Nijkamp and Parnham's Principles of Immunopharmacology* (Springer), pp. 23-35.
- Brunner, T., Mogil, R.J., LaFace, D., Yoo, N.J., Mahboubi, A., Echeverri, F., Martin, S.J., Force, W.R., Lynch, D.H., Ware, C.F., *et al.* (1995). Cell-autonomous Fas (CD95)/Fas-ligand interaction mediates activation-induced apoptosis in T-cell hybridomas. *Nature* 373, 441-444.

- Budd, R.C., Cerottini, J.C., Horvath, C., Bron, C., Pedrazzini, T., Howe, R.C., and MacDonald, H.R. (1987). Distinction of virgin and memory T lymphocytes. Stable acquisition of the Pgp-1 glycoprotein concomitant with antigenic stimulation. *Journal of immunology (Baltimore, Md : 1950)* *138*, 3120-3129.
- Bunnell, S.C., Diehn, M., Yaffe, M.B., Findell, P.R., Cantley, L.C., and Berg, L.J. (2000). Biochemical interactions integrating Itk with the T cell receptor-initiated signaling cascade. *The Journal of biological chemistry* *275*, 2219-2230.
- Burgess, K.E., Odysseos, A.D., Zalvan, C., Druker, B.J., Anderson, P., Schlossman, S.F., and Rudd, C.E. (1991). Biochemical identification of a direct physical interaction between the CD4:p56lck and Ti(TcR)/CD3 complexes. *European journal of immunology* *21*, 1663-1668.
- Burma, S., Chen, B.P., and Chen, D.J. (2006). Role of non-homologous end joining (NHEJ) in maintaining genomic integrity. *DNA repair* *5*, 1042-1048.
- Calabrese, E.J. (2005). Hormetic dose-response relationships in immunology: occurrence, quantitative features of the dose response, mechanistic foundations, and clinical implications. *Critical reviews in toxicology* *35*, 89-295.
- Cassioli, C., and Baldari, C.T. (2022). The Expanding Arsenal of Cytotoxic T Cells. *Frontiers in immunology* *13*, 883010-883010.
- Ceredig, R., Glasebrook, A.L., and MacDonald, H.R. (1982). Phenotypic and functional properties of murine thymocytes. I. Precursors of cytolytic T lymphocytes and interleukin 2-producing cells are all contained within a subpopulation of "mature" thymocytes as analyzed by monoclonal antibodies and flow microfluorometry. *The Journal of experimental medicine* *155*, 358-379.
- Chan, A.C., Iwashima, M., Turck, C.W., and Weiss, A. (1992). ZAP-70: a 70 kd protein-tyrosine kinase that associates with the TCR zeta chain. *Cell* *71*, 649-662.
- Chatterjee, N., and Walker, G.C. (2017). Mechanisms of DNA damage, repair, and mutagenesis. *Environmental and molecular mutagenesis* *58*, 235-263.
- Chaturvedi, P., Eng, W.K., Zhu, Y., Mattern, M.R., Mishra, R., Hurle, M.R., Zhang, X., Annan, R.S., Lu, Q., Faucette, L.F., *et al.* (1999). Mammalian Chk2 is a downstream effector of the ATM-dependent DNA damage checkpoint pathway. *Oncogene* *18*, 4047-4054.
- Chehab, N.H., Malikzay, A., Appel, M., and Halazonetis, T.D. (2000). Chk2/hCds1 functions as a DNA damage checkpoint in G(1) by stabilizing p53. *Genes & development* *14*, 278-288.
- Chetoui, N., Boisvert, M., Gendron, S., and Aoudjit, F. (2010). Interleukin-7 promotes the survival of human CD4+ effector/memory T cells by up-regulating Bcl-2 proteins and activating the JAK/STAT signalling pathway. *Immunology* *130*, 418-426.
- Chi, X., Li, Y., and Qiu, X. (2020). V (D) J recombination, somatic hypermutation and class switch recombination of immunoglobulins: mechanism and regulation. *Immunology* *160*, 233-247.

Chinnaiyan, A.M., O'Rourke, K., Tewari, M., and Dixit, V.M. (1995). FADD, a novel death domain-containing protein, interacts with the death domain of Fas and initiates apoptosis. *Cell* 81, 505-512.

Chiu, B.C., Martin, B.E., Stolberg, V.R., and Chensue, S.W. (2013). Cutting edge: Central memory CD8 T cells in aged mice are virtual memory cells. *Journal of immunology* (Baltimore, Md : 1950) 191, 5793-5796.

Ciofani, M., Knowles, G.C., Wiest, D.L., von Boehmer, H., and Zúñiga-Pflücker, J.C. (2006). Stage-specific and differential notch dependency at the alphabeta and gammadelta T lineage bifurcation. *Immunity* 25, 105-116.

Conacci-Sorrell, M., McFerrin, L., and Eisenman, R.N. (2014). An overview of MYC and its interactome. *Cold Spring Harbor perspectives in medicine* 4, a014357.

Corfe, S.A., and Paige, C.J. (2012). The many roles of IL-7 in B cell development; mediator of survival, proliferation and differentiation. *Seminars in immunology* 24, 198-208.

Cortez, D., Guntuku, S., Qin, J., and Elledge, S.J. (2001). ATR and ATRIP: partners in checkpoint signaling. *Science* 294, 1713-1716.

Coudronniere, N., Villalba, M., Englund, N., and Altman, A. (2000). NF-kappa B activation induced by T cell receptor/CD28 costimulation is mediated by protein kinase C-theta. *Proceedings of the National Academy of Sciences of the United States of America* 97, 3394-3399.

Critchlow, S.E., Bowater, R.P., and Jackson, S.P. (1997). Mammalian DNA double-strand break repair protein XRCC4 interacts with DNA ligase IV. *Current biology : CB* 7, 588-598.

Danielian, S., Fagard, R., Alcover, A., Acuto, O., and Fischer, S. (1989). The lymphocyte-specific protein tyrosine kinase p56lck is hyperphosphorylated on serine and tyrosine residues within minutes after activation via T cell receptor or CD2. *European journal of immunology* 19, 2183-2189.

Dantuma, N.P., and van Attikum, H. (2016). Spatiotemporal regulation of posttranslational modifications in the DNA damage response. *The EMBO journal* 35, 6-23.

de Boer, J., Williams, A., Skavdis, G., Harker, N., Coles, M., Tolaini, M., Norton, T., Williams, K., Roderick, K., Potocnik, A.J., *et al.* (2003). Transgenic mice with hematopoietic and lymphoid specific expression of Cre. *European journal of immunology* 33, 314-325.

DeLeo, A.B., Jay, G., Appella, E., Dubois, G.C., Law, L.W., and Old, L.J. (1979). Detection of a transformation-related antigen in chemically induced sarcomas and other transformed cells of the mouse. *Proceedings of the National Academy of Sciences* 76, 2420-2424.

Delia, D., and Mizutani, S. (2017). The DNA damage response pathway in normal hematopoiesis and malignancies. *International journal of hematology* 106, 328-334.

den Braber, I., Mugwagwa, T., Vrisekoop, N., Westera, L., Mögling, R., de Boer, A.B., Willems, N., Schrijver, E.H., Spierenburg, G., Gaiser, K., *et al.* (2012). Maintenance of peripheral naive T cells is sustained by thymus output in mice but not humans. *Immunity* 36, 288-297.

den Haan, J.M., Arens, R., and van Zelm, M.C. (2014). The activation of the adaptive immune system: cross-talk between antigen-presenting cells, T cells and B cells. *Immunology letters* 162, 103-112.

Do-Umehara, H.C., Chen, C., Urich, D., Zhou, L., Qiu, J., Jang, S., Zander, A., Baker, M.A., Eilers, M., Sporn, P.H., *et al.* (2013). Suppression of inflammation and acute lung injury by Miz1 via repression of C/EBP- δ . *Nature immunology* 14, 461-469.

Dujka, M.E., Puebla-Osorio, N., Tavana, O., Sang, M., and Zhu, C. (2010). ATM and p53 are essential in the cell-cycle containment of DNA breaks during V(D)J recombination in vivo. *Oncogene* 29, 957-965.

Eilers, M., and Eisenman, R.N. (2008). Myc's broad reach. *Genes & development* 22, 2755-2766.

Eischen, C.M., Williams, B.L., Zhang, W., Samelson, L.E., Lynch, D.H., Abraham, R.T., and Leibson, P.J. (1997). ZAP-70 tyrosine kinase is required for the up-regulation of Fas ligand in activation-induced T cell apoptosis. *Journal of immunology (Baltimore, Md : 1950)* 159, 1135-1139.

el-Deiry, W.S., Tokino, T., Velculescu, V.E., Levy, D.B., Parsons, R., Trent, J.M., Lin, D., Mercer, W.E., Kinzler, K.W., and Vogelstein, B. (1993). WAF1, a potential mediator of p53 tumor suppression. *Cell* 75, 817-825.

Ellisen, L.W., Bird, J., West, D.C., Soreng, A.L., Reynolds, T.C., Smith, S.D., and Sklar, J. (1991). TAN-1, the human homolog of the *Drosophila* notch gene, is broken by chromosomal translocations in T lymphoblastic neoplasms. *Cell* 66, 649-661.

Ellmeier, W., Sawada, S., and Littman, D.R. (1999). The regulation of CD4 and CD8 coreceptor gene expression during T cell development. *Annual review of immunology* 17, 523-554.

EITanbouly, M.A., and Noelle, R.J. (2021). Rethinking peripheral T cell tolerance: checkpoints across a T cell's journey. *Nature Reviews Immunology* 21, 257-267.

Ernst, B., Lee, D.-S., Chang, J.M., Sprent, J., and Surh, C.D. (1999). The peptide ligands mediating positive selection in the thymus control T cell survival and homeostatic proliferation in the periphery. *Immunity* 11, 173-181.

Ernst, D.N., Weigle, W.O., Noonan, D.J., McQuitty, D.N., and Hobbs, M.V. (1993). The age-associated increase in IFN-gamma synthesis by mouse CD8+ T cells correlates with shifts in the frequencies of cell subsets defined by membrane CD44, CD45RB, 3G11, and MEL-14 expression. *Journal of immunology (Baltimore, Md : 1950)* 151, 575-587.

Fadok, V.A., Voelker, D., Campbell, P., Cohen, J., Bratton, D., and Henson, P. (1992). Exposure of phosphatidylserine on the surface of apoptotic lymphocytes triggers specific recognition and removal by macrophages. *The Journal of Immunology* 148, 2207-2216.

Fagnoni, F.F., Vescovini, R., Passeri, G., Bologna, G., Pedrazzoni, M., Lavagetto, G., Casti, A., Franceschi, C., Passeri, M., and Sansoni, P. (2000). Shortage of circulating naive CD8(+) T cells provides new insights on immunodeficiency in aging. *Blood* 95, 2860-2868.

- Falk, I., Nerz, G., Haidl, I., Krotkova, A., and Eichmann, K. (2001). Immature thymocytes that fail to express TCRbeta and/or TCRgamma delta proteins die by apoptotic cell death in the CD44(-)CD25(-) (DN4) subset. *European journal of immunology* *31*, 3308-3317.
- Fearon, D.T., Manders, P., and Wagner, S.D. (2001). Arrested differentiation, the self-renewing memory lymphocyte, and vaccination. *Science* *293*, 248-250.
- Felli, M.P., Maroder, M., Mitsiadis, T.A., Campese, A.F., Bellavia, D., Vacca, A., Mann, R.S., Frati, L., Lendahl, U., Gulino, A., *et al.* (1999). Expression pattern of notch1, 2 and 3 and Jagged1 and 2 in lymphoid and stromal thymus components: distinct ligand-receptor interactions in intrathymic T cell development. *International immunology* *11*, 1017-1025.
- Fields, S., and Jang, S.K. (1990). Presence of a potent transcription activating sequence in the p53 protein. *Science* *249*, 1046-1049.
- Finco, T.S., Kadlecsek, T., Zhang, W., Samelson, L.E., and Weiss, A. (1998). LAT is required for TCR-mediated activation of PLCgamma1 and the Ras pathway. *Immunity* *9*, 617-626.
- Flurkey, K., Curren, J., Harrison, D., Fox, J., Davisson, M., Quimby, F., Barthold, S., Newcomer, C., and Smith, A. (2007). The mouse in biomedical research. *The Mouse in Aging Research*, 2nd ed Fox JG, Quimby FW, Barthold SW, Newcomer CE and Smith AL Elsevier, Burlington, MA, 637-672.
- Fowlkes, B.J., Edison, L., Mathieson, B.J., and Chused, T.M. (1985). Early T lymphocytes. Differentiation in vivo of adult intrathymic precursor cells. *The Journal of experimental medicine* *162*, 802-822.
- Gartel, A.L., and Radhakrishnan, S.K. (2005). Lost in transcription: p21 repression, mechanisms, and consequences. *Cancer research* *65*, 3980-3985.
- Gatei, M., Scott, S.P., Filippovitch, I., Soronika, N., Lavin, M.F., Weber, B., and Khanna, K.K. (2000). Role for ATM in DNA damage-induced phosphorylation of BRCA1. *Cancer research* *60*, 3299-3304.
- Gaud, G., Lesourne, R., and Love, P.E. (2018). Regulatory mechanisms in T cell receptor signalling. *Nature Reviews Immunology* *18*, 485-497.
- Gebhardt, A., Frye, M., Herold, S., Benitah, S.A., Braun, K., Samans, B., Watt, F.M., Elsässer, H.P., and Eilers, M. (2006). Myc regulates keratinocyte adhesion and differentiation via complex formation with Miz1. *The Journal of cell biology* *172*, 139-149.
- Gebhardt, A., Kosan, C., Herkert, B., Möröy, T., Lutz, W., Eilers, M., and Elsässer, H.-P. (2007). Miz1 is required for hair follicle structure and hair morphogenesis. *Journal of cell science* *120*, 2586-2593.
- Gebhardt, T., Wakim, L.M., Eidsmo, L., Reading, P.C., Heath, W.R., and Carbone, F.R. (2009). Memory T cells in nonlymphoid tissue that provide enhanced local immunity during infection with herpes simplex virus. *Nature immunology* *10*, 524-530.
- Gems, D., and Partridge, L. (2013). Genetics of longevity in model organisms: debates and paradigm shifts. *Annual review of physiology* *75*, 621-644.

Geoffroy, J.S., and Rosen, S.D. (1989). Demonstration that a lectin-like receptor (gp90MEL) directly mediates adhesion of lymphocytes to high endothelial venules of lymph nodes. *The Journal of cell biology* *109*, 2463-2469.

Germain, R.N. (2002). T-cell development and the CD4–CD8 lineage decision. *Nature reviews immunology* *2*, 309-322.

Godfrey, D.I., Kennedy, J., Mombaerts, P., Tonegawa, S., and Zlotnik, A. (1994). Onset of TCR-beta gene rearrangement and role of TCR-beta expression during CD3-CD4-CD8-thymocyte differentiation. *The Journal of Immunology* *152*, 4783-4792.

Godfrey, D.I., Kennedy, J., Suda, T., and Zlotnik, A. (1993). A developmental pathway involving four phenotypically and functionally distinct subsets of CD3-CD4-CD8- triple-negative adult mouse thymocytes defined by CD44 and CD25 expression. *Journal of immunology (Baltimore, Md : 1950)* *150*, 4244-4252.

Godfrey, D.I., Zlotnik, A., and Suda, T. (1992). Phenotypic and functional characterization of c-kit expression during intrathymic T cell development. *Journal of immunology (Baltimore, Md : 1950)* *149*, 2281-2285.

Goldrath, A.W., and Bevan, M.J. (1999). Low-affinity ligands for the TCR drive proliferation of mature CD8+ T cells in lymphopenic hosts. *Immunity* *11*, 183-190.

Goldrath, A.W., Bogatzki, L.Y., and Bevan, M.J. (2000). Naive T cells transiently acquire a memory-like phenotype during homeostasis-driven proliferation. *The Journal of experimental medicine* *192*, 557-564.

González-García, S., García-Peydró, M., Martín-Gayo, E., Ballestar, E., Esteller, M., Bornstein, R., de la Pompa, J.L., Ferrando, A.A., and Toribio, M.L. (2009). CSL–MAML-dependent Notch1 signaling controls T lineage-specific IL-7R α gene expression in early human thymopoiesis and leukemia. *Journal of Experimental Medicine* *206*, 779-791.

Gordon, S. (2002). Pattern recognition receptors: doubling up for the innate immune response. *Cell* *111*, 927-930.

Goronzy, J.J., Hu, B., Kim, C., Jadhav, R.R., and Weyand, C.M. (2018). Epigenetics of T cell aging. *Journal of leukocyte biology* *104*, 691-699.

Graef, P., Buchholz, V.R., Stemberger, C., Flossdorf, M., Henkel, L., Schiemann, M., Drexler, I., Höfer, T., Riddell, S.R., and Busch, D.H. (2014). Serial transfer of single-cell-derived immunocompetence reveals stemness of CD8+ central memory T cells. *Immunity* *41*, 116-126.

Groux, H., O'Garra, A., Bigler, M., Rouleau, M., Antonenko, S., de Vries, J.E., and Roncarolo, M.G. (1997). A CD4+ T-cell subset inhibits antigen-specific T-cell responses and prevents colitis. *Nature* *389*, 737-742.

Gu, Y., Jin, S., Gao, Y., Weaver, D.T., and Alt, F.W. (1997). Ku70-deficient embryonic stem cells have increased ionizing radiosensitivity, defective DNA end-binding activity, and inability to support V(D)J recombination. *Proceedings of the National Academy of Sciences of the United States of America* *94*, 8076-8081.

Han, J., Das, B., Wei, W., Van Aelst, L., Mosteller, R.D., Khosravi-Far, R., Westwick, J.K., Der, C.J., and Broek, D. (1997). Lck regulates Vav activation of members of the Rho family of GTPases. *Molecular and cellular biology* *17*, 1346-1353.

Harrington, L.E., Hatton, R.D., Mangan, P.R., Turner, H., Murphy, T.L., Murphy, K.M., and Weaver, C.T. (2005). Interleukin 17-producing CD4⁺ effector T cells develop via a lineage distinct from the T helper type 1 and 2 lineages. *Nature immunology* 6, 1123-1132.

Harty, J.T., and Badovinac, V.P. (2008). Shaping and reshaping CD8⁺ T-cell memory. *Nature reviews Immunology* 8, 107-119.

Haupt, Y., Maya, R., Kazaz, A., and Oren, M. (1997). Mdm2 promotes the rapid degradation of p53. *Nature* 387, 296-299.

Herkert, B., Dwertmann, A., Herold, S., Abed, M., Naud, J.F., Finkernagel, F., Harms, G.S., Orian, A., Wanzel, M., and Eilers, M. (2010). The Arf tumor suppressor protein inhibits Miz1 to suppress cell adhesion and induce apoptosis. *The Journal of cell biology* 188, 905-918.

Herold, S., Hock, A., Herkert, B., Berns, K., Mullenders, J., Beijersbergen, R., Bernards, R., and Eilers, M. (2008). Miz1 and HectH9 regulate the stability of the checkpoint protein, TopBP1. *The EMBO journal* 27, 2851-2861.

Herold, S., Wanzel, M., Beuger, V., Frohme, C., Beul, D., Hillukkala, T., Syvaioja, J., Saluz, H.P., Haenel, F., and Eilers, M. (2002). Negative regulation of the mammalian UV response by Myc through association with Miz-1. *Molecular cell* 10, 509-521.

Hönnemann, J., Sanz-Moreno, A., Wolf, E., Eilers, M., and Elsässer, H.P. (2012). Miz1 is a critical repressor of cdkn1a during skin tumorigenesis. *PloS one* 7, e34885.

Horvath, S., and Raj, K. (2018). DNA methylation-based biomarkers and the epigenetic clock theory of ageing. *Nature Reviews Genetics* 19, 371-384.

Hostert, A., Tolaini, M., Festenstein, R., McNeill, L., Malissen, B., Williams, O., Zamoyska, R., and Kioussis, D. (1997). A CD8 genomic fragment that directs subset-specific expression of CD8 in transgenic mice. *Journal of immunology (Baltimore, Md : 1950)* 158, 4270-4281.

Igarashi, H., Gregory, S.C., Yokota, T., Sakaguchi, N., and Kincade, P.W. (2002). Transcription from the RAG1 locus marks the earliest lymphocyte progenitors in bone marrow. *Immunity* 17, 117-130.

Iwashima, M., Irving, B.A., van Oers, N.S., Chan, A.C., and Weiss, A. (1994). Sequential interactions of the TCR with two distinct cytoplasmic tyrosine kinases. *Science* 263, 1136-1139.

Jäättelä, M., and Tschopp, J. (2003). Caspase-independent cell death in T lymphocytes. *Nature immunology* 4, 416-423.

Jain, J., McCaffrey, P.G., Valge-Archer, V.E., and Rao, A. (1992). Nuclear factor of activated T cells contains Fos and Jun. *Nature* 356, 801-804.

Jenkins, M.K., and Schwartz, R.H. (1987). Antigen presentation by chemically modified splenocytes induces antigen-specific T cell unresponsiveness in vitro and in vivo. *The Journal of experimental medicine* 165, 302-319.

Jenkins, M.K., Taylor, P.S., Norton, S.D., and Urdahl, K.B. (1991). CD28 delivers a costimulatory signal involved in antigen-specific IL-2 production by human T cells. *Journal of immunology (Baltimore, Md : 1950)* 147, 2461-2466.

- Jenne, D.E., and Tschopp, J. (1988). Granzymes, a family of serine proteases released from granules of cytolytic T lymphocytes upon T cell receptor stimulation. *Immunological reviews* 103, 53-71.
- Jiang, Q., Li, W.Q., Aiello, F.B., Mazzucchelli, R., Asefa, B., Khaled, A.R., and Durum, S.K. (2005). Cell biology of IL-7, a key lymphotrophin. *Cytokine & growth factor reviews* 16, 513-533.
- Ju, S.T., Panka, D.J., Cui, H., Ettinger, R., el-Khatib, M., Sherr, D.H., Stanger, B.Z., and Marshak-Rothstein, A. (1995). Fas(CD95)/FasL interactions required for programmed cell death after T-cell activation. *Nature* 373, 444-448.
- Kaech, S.M., Wherry, E.J., and Ahmed, R. (2002). Effector and memory T-cell differentiation: implications for vaccine development. *Nature Reviews Immunology* 2, 251-262.
- Kamijo, T., Weber, J.D., Zambetti, G., Zindy, F., Roussel, M.F., and Sherr, C.J. (1998). Functional and physical interactions of the ARF tumor suppressor with p53 and Mdm2. *Proceedings of the National Academy of Sciences of the United States of America* 95, 8292-8297.
- Karimian, A., Ahmadi, Y., and Yousefi, B. (2016). Multiple functions of p21 in cell cycle, apoptosis and transcriptional regulation after DNA damage. *DNA repair* 42, 63-71.
- Katzav, S., Martin-Zanca, D., and Barbacid, M. (1989). vav, a novel human oncogene derived from a locus ubiquitously expressed in hematopoietic cells. *The EMBO journal* 8, 2283-2290.
- Kawasaki, T., and Kawai, T. (2014). Toll-like receptor signaling pathways. *Frontiers in immunology* 5, 461.
- Kerr, J.F., Wyllie, A.H., and Currie, A.R. (1972). Apoptosis: a basic biological phenomenon with wide-ranging implications in tissue kinetics. *British journal of cancer* 26, 239-257.
- Kischkel, F.C., Hellbardt, S., Behrmann, I., Germer, M., Pawlita, M., Krammer, P.H., and Peter, M.E. (1995). Cytotoxicity-dependent APO-1 (Fas/CD95)-associated proteins form a death-inducing signaling complex (DISC) with the receptor. *The EMBO journal* 14, 5579-5588.
- Kisielow, P., Teh, H.S., Blüthmann, H., and von Boehmer, H. (1988). Positive selection of antigen-specific T cells in thymus by restricting MHC molecules. *Nature* 335, 730-733.
- Klein, L., Hinterberger, M., Wirnsberger, G., and Kyewski, B. (2009). Antigen presentation in the thymus for positive selection and central tolerance induction. *Nature reviews Immunology* 9, 833-844.
- Klein, S.L., and Flanagan, K.L. (2016). Sex differences in immune responses. *Nature Reviews Immunology* 16, 626-638.
- Ko, L.J., and Prives, C. (1996). p53: puzzle and paradigm. *Genes & development* 10, 1054-1072.
- Koch, U., and Radtke, F. (2011). Mechanisms of T cell development and transformation. *Annual review of cell and developmental biology* 27, 539-562.

Korać, P., Dotlić, S., Matulić, M., Zajc Petranović, M., and Dominis, M. (2017). Role of MYC in B Cell Lymphomagenesis. *Genes* 8.

Kosan, C., Rashkovan, M., Ross, J., Schaffer, A.M., Saba, I., Lemsaddek, W., Trudel, M., and Möröy, T. (2014). The transcription factor Miz-1 is required for embryonic and stress-induced erythropoiesis but dispensable for adult erythropoiesis. *American journal of blood research* 4, 7-19.

Kosan, C., Saba, I., Godmann, M., Herold, S., Herkert, B., Eilers, M., and Möröy, T. (2010). Transcription factor miz-1 is required to regulate interleukin-7 receptor signaling at early commitment stages of B cell differentiation. *Immunity* 33, 917-928.

Krammer, P.H., Arnold, R., and Lavrik, I.N. (2007). Life and death in peripheral T cells. *Nature reviews Immunology* 7, 532-542.

Kreis, N.N., Louwen, F., and Yuan, J. (2019). The Multifaceted p21 (Cip1/Waf1/CDKN1A) in Cell Differentiation, Migration and Cancer Therapy. *Cancers* 11.

Kruiswijk, F., Labuschagne, C.F., and Vousden, K.H. (2015). p53 in survival, death and metabolic health: a lifeguard with a licence to kill. *Nature reviews Molecular cell biology* 16, 393-405.

Kubbutat, M.H., Jones, S.N., and Vousden, K.H. (1997). Regulation of p53 stability by Mdm2. *Nature* 387, 299-303.

Kuida, K., Haydar, T.F., Kuan, C.Y., Gu, Y., Taya, C., Karasuyama, H., Su, M.S., Rakic, P., and Flavell, R.A. (1998). Reduced apoptosis and cytochrome c-mediated caspase activation in mice lacking caspase 9. *Cell* 94, 325-337.

Kurd, N., and Robey, E.A. (2016). T - cell selection in the thymus: A spatial and temporal perspective. *Immunological reviews* 271, 114-126.

Lai, J.H., and Tan, T.H. (1994). CD28 signaling causes a sustained down-regulation of I kappa B alpha which can be prevented by the immunosuppressant rapamycin. *The Journal of biological chemistry* 269, 30077-30080.

Lam, M., Dubyak, G., Chen, L., Nuñez, G., Miesfeld, R.L., and Distelhorst, C.W. (1994). Evidence that BCL-2 represses apoptosis by regulating endoplasmic reticulum-associated Ca²⁺ fluxes. *Proceedings of the National Academy of Sciences of the United States of America* 91, 6569-6573.

Lane, D., and Crawford, L. (1979). T antigen is bound to a host protein in SY40-transformed cells. *Nature* 278, 261-263.

Langenau, D.M., Traver, D., Ferrando, A.A., Kutok, J.L., Aster, J.C., Kanki, J.P., Lin, S., Prochownik, E., Trede, N.S., Zon, L.I., *et al.* (2003). Myc-induced T cell leukemia in transgenic zebrafish. *Science* 299, 887-890.

Lawen, A. (2003). Apoptosis-an introduction. *BioEssays : news and reviews in molecular, cellular and developmental biology* 25, 888-896.

Lee, J.H., and Paull, T.T. (2005). ATM activation by DNA double-strand breaks through the Mre11-Rad50-Nbs1 complex. *Science* 308, 551-554.

- Lee, P.P., Fitzpatrick, D.R., Beard, C., Jessup, H.K., Lehar, S., Makar, K.W., Pérez-Melgosa, M., Sweetser, M.T., Schlissel, M.S., Nguyen, S., *et al.* (2001). A critical role for Dnmt1 and DNA methylation in T cell development, function, and survival. *Immunity* *15*, 763-774.
- Lenardo, M.J. (1991). Interleukin-2 programs mouse alpha beta T lymphocytes for apoptosis. *Nature* *353*, 858-861.
- Lerner, A., Yamada, T., and Miller, R.A. (1989). Pgp-1hi T lymphocytes accumulate with age in mice and respond poorly to concanavalin A. *European journal of immunology* *19*, 977-982.
- Li, H., Zhu, H., Xu, C.J., and Yuan, J. (1998). Cleavage of BID by caspase 8 mediates the mitochondrial damage in the Fas pathway of apoptosis. *Cell* *94*, 491-501.
- Li, P., Nijhawan, D., Budihardjo, I., Srinivasula, S.M., Ahmad, M., Alnemri, E.S., and Wang, X. (1997). Cytochrome c and dATP-dependent formation of Apaf-1/caspase-9 complex initiates an apoptotic protease cascade. *Cell* *91*, 479-489.
- Lieber, M.R., Hesse, J.E., Mizuuchi, K., and Gellert, M. (1988). Lymphoid V(D)J recombination: nucleotide insertion at signal joints as well as coding joints. *Proceedings of the National Academy of Sciences of the United States of America* *85*, 8588-8592.
- Liu, H., Schneider, H., Recino, A., Richardson, C., Goldberg, M.W., and Rudd, C.E. (2015). The Immune Adaptor SLP-76 Binds to SUMO-RANGAP1 at Nuclear Pore Complex Filaments to Regulate Nuclear Import of Transcription Factors in T Cells. *Molecular cell* *59*, 840-849.
- Liu, J., Yan, J., Jiang, S., Wen, J., Chen, L., Zhao, Y., and Lin, A. (2012). Site-specific ubiquitination is required for relieving the transcription factor Miz1-mediated suppression on TNF- α -induced JNK activation and inflammation. *Proceedings of the National Academy of Sciences of the United States of America* *109*, 191-196.
- Liu, J., Zhao, Y., Eilers, M., and Lin, A. (2009). Miz1 is a signal- and pathway-specific modulator or regulator (SMOR) that suppresses TNF-alpha-induced JNK1 activation. *Proceedings of the National Academy of Sciences of the United States of America* *106*, 18279-18284.
- Liu, K., Paik, J.C., Wang, B., Lin, F.T., and Lin, W.C. (2006). Regulation of TopBP1 oligomerization by Akt/PKB for cell survival. *The EMBO journal* *25*, 4795-4807.
- López-Otín, C., Blasco, M.A., Partridge, L., Serrano, M., and Kroemer, G. (2013). The hallmarks of aging. *Cell* *153*, 1194-1217.
- Luckheeram, R.V., Zhou, R., Verma, A.D., and Xia, B. (2012). CD4+ T cells: differentiation and functions. *Clinical and developmental immunology* *2012*.
- Ma, Y., Pannicke, U., Schwarz, K., and Lieber, M.R. (2002). Hairpin opening and overhang processing by an Artemis/DNA-dependent protein kinase complex in nonhomologous end joining and V(D)J recombination. *Cell* *108*, 781-794.
- MacDonald, H.R., Lees, R.K., Schneider, R., Zinkernagel, R.M., and Hengartner, H. (1988). Positive selection of CD4+ thymocytes controlled by MHC class II gene products. *Nature* *336*, 471-473.

Mackay, C.R., Terpe, H.J., Stauder, R., Marston, W.L., Stark, H., and Günthert, U. (1994). Expression and modulation of CD44 variant isoforms in humans. *The Journal of cell biology* 124, 71-82.

Mägdefrau, A.-S., Ludwig, K., Weigel, C., Köse, N., Guerra, G.M., Dakhovnik, A., and Kosan, C. (2019). DNA-damage-induced hormetic responses. In *The Science of Hormesis in Health and Longevity* (Elsevier), pp. 149-159.

Malissen, M., Trucy, J., Jouvin-Marche, E., Cazenave, P.A., Scollay, R., and Malissen, B. (1992). Regulation of TCR alpha and beta gene allelic exclusion during T-cell development. *Immunology today* 13, 315-322.

Maraskovsky, E., O'Reilly, L.A., Teepe, M., Corcoran, L.M., Peschon, J.J., and Strasser, A. (1997). Bcl-2 can rescue T lymphocyte development in interleukin-7 receptor-deficient mice but not in mutant rag-1^{-/-} mice. *Cell* 89, 1011-1019.

Masuda, K., Kakugawa, K., Nakayama, T., Minato, N., Katsura, Y., and Kawamoto, H. (2007). T cell lineage determination precedes the initiation of TCR beta gene rearrangement. *Journal of immunology* (Baltimore, Md : 1950) 179, 3699-3706.

Matloubian, M., Lo, C.G., Cinamon, G., Lesneski, M.J., Xu, Y., Brinkmann, V., Allende, M.L., Proia, R.L., and Cyster, J.G. (2004). Lymphocyte egress from thymus and peripheral lymphoid organs is dependent on S1P receptor 1. *Nature* 427, 355-360.

McBlane, J.F., van Gent, D.C., Ramsden, D.A., Romeo, C., Cuomo, C.A., Gellert, M., and Oettinger, M.A. (1995). Cleavage at a V(D)J recombination signal requires only RAG1 and RAG2 proteins and occurs in two steps. *Cell* 83, 387-395.

McKinstry, K.K., Strutt, T.M., and Swain, S.L. (2010). Regulation of CD4⁺ T-cell contraction during pathogen challenge. *Immunological reviews* 236, 110-124.

Medema, J.P., Scaffidi, C., Kischkel, F.C., Shevchenko, A., Mann, M., Krammer, P.H., and Peter, M.E. (1997). FLICE is activated by association with the CD95 death-inducing signaling complex (DISC). *The EMBO journal* 16, 2794-2804.

Miao, L., Song, Z., Jin, L., Zhu, Y.M., Wen, L.P., and Wu, M. (2010). ARF antagonizes the ability of Miz-1 to inhibit p53-mediated transactivation. *Oncogene* 29, 711-722.

Miyashita, T., and Reed, J.C. (1995). Tumor suppressor p53 is a direct transcriptional activator of the human bax gene. *Cell* 80, 293-299.

Mohammadzadeh, A., Mirza-Aghazadeh-Attari, M., Hallaj, S., Saei, A.A., Alivand, M.R., Valizadeh, A., Yousefi, B., and Majidinia, M. (2019). Crosstalk between P53 and DNA damage response in ageing. *DNA repair* 80, 8-15.

Moore, T.A., and Zlotnik, A. (1995). T-cell lineage commitment and cytokine responses of thymic progenitors. *Blood* 86, 1850-1860.

Möröy, T., Saba, I., and Kosan, C. (2011). The role of the transcription factor Miz-1 in lymphocyte development and lymphomagenesis-Binding Myc makes the difference. *Seminars in immunology* 23, 379-387.

Mosmann, T.R., and Coffman, R.L. (1989). Heterogeneity of cytokine secretion patterns and functions of helper T cells. *Advances in immunology* 46, 111-147.

Muñoz-Ruiz, M., Sumaria, N., Pennington, D.J., and Silva-Santos, B. (2017). Thymic Determinants of $\gamma \delta$ T Cell Differentiation. *Trends Immunol* 38, 336-344.

Murphy, K., and Weaver, C. (2018). *Janeway immunologie* (Springer-Verlag).

Nakano, K., and Vousden, K.H. (2001). PUMA, a novel proapoptotic gene, is induced by p53. *Molecular cell* 7, 683-694.

Nauta, A.J., Roos, A., and Daha, M.R. (2004). A regulatory role for complement in innate immunity and autoimmunity. *International archives of allergy and immunology* 134, 310-323.

Nemazee, D. (2000). Receptor selection in B and T lymphocytes. *Annual review of immunology* 18, 19-51.

Ngoenkam, J., Schamel, W.W., and Pongcharoen, S. (2018). Selected signalling proteins recruited to the T-cell receptor-CD3 complex. *Immunology* 153, 42-50.

Niazi, S., Purohit, M., and Niazi, J.H. (2018). Role of p53 circuitry in tumorigenesis: A brief review. *European journal of medicinal chemistry* 158, 7-24.

Nikolic - Zugic, J., and Moore, M.W. (1989). T cell receptor expression on immature thymocytes with in vivo and in vitro precursor potential. *European journal of immunology* 19, 1957-1960.

Nikolich-Zugich, J. (2005). T cell aging: naive but not young. *The Journal of experimental medicine* 201, 837-840.

Nikolich-Žugich, J. (2014). Aging of the T cell compartment in mice and humans: from no naive expectations to foggy memories. *Journal of immunology (Baltimore, Md : 1950)* 193, 2622-2629.

Nikolich-Žugich, J. (2018). The twilight of immunity: emerging concepts in aging of the immune system. *Nature immunology* 19, 10-19.

Nussenzweig, A., Chen, C., da Costa Soares, V., Sanchez, M., Sokol, K., Nussenzweig, M.C., and Li, G.C. (1996). Requirement for Ku80 in growth and immunoglobulin V(D)J recombination. *Nature* 382, 551-555.

Oda, E., Ohki, R., Murasawa, H., Nemoto, J., Shibue, T., Yamashita, T., Tokino, T., Taniguchi, T., and Tanaka, N. (2000). Noxa, a BH3-only member of the Bcl-2 family and candidate mediator of p53-induced apoptosis. *Science* 288, 1053-1058.

Oehen, S., and Brduscha-Riem, K. (1999). Naïve cytotoxic T lymphocytes spontaneously acquire effector function in lymphocytopenic recipients: A pitfall for T cell memory studies? *European journal of immunology* 29, 608-614.

Offner, F., and Plum, J. (1998). The role of interleukin-7 in early T-cell development. *Leukemia & lymphoma* 30, 87-99.

Olive, P.L., and Banáth, J.P. (2006). The comet assay: a method to measure DNA damage in individual cells. *Nature protocols* 1, 23-29.

Opferman, J.T., and Korsmeyer, S.J. (2003). Apoptosis in the development and maintenance of the immune system. *Nature immunology* 4, 410-415.

Owen-Schaub, L.B., Zhang, W., Cusack, J.C., Angelo, L.S., Santee, S.M., Fujiwara, T., Roth, J.A., Deisseroth, A.B., Zhang, W.-W., and Kruzel, E. (1995). Wild-type human p53 and a temperature-sensitive mutant induce Fas/APO-1 expression. *Molecular and cellular biology* 15, 3032-3040.

Pargmann, D., Yücel, R., Kosan, C., Saba, I., Klein-Hitpass, L., Schimmer, S., Heyd, F., Dittmer, U., and Möröy, T. (2007). Differential impact of the transcriptional repressor Gfi1 on mature CD4+ and CD8+ T lymphocyte function. *European journal of immunology* 37, 3551-3563.

Park, H., Li, Z., Yang, X.O., Chang, S.H., Nurieva, R., Wang, Y.H., Wang, Y., Hood, L., Zhu, Z., Tian, Q., *et al.* (2005). A distinct lineage of CD4 T cells regulates tissue inflammation by producing interleukin 17. *Nature immunology* 6, 1133-1141.

Patel, J.H., and McMahon, S.B. (2007). BCL2 is a downstream effector of MIZ-1 essential for blocking c-MYC-induced apoptosis. *The Journal of biological chemistry* 282, 5-13.

Paull, T.T., Rogakou, E.P., Yamazaki, V., Kirchgessner, C.U., Gellert, M., and Bonner, W.M. (2000). A critical role for histone H2AX in recruitment of repair factors to nuclear foci after DNA damage. *Current biology : CB* 10, 886-895.

Pear, W.S., Aster, J.C., Scott, M.L., Hasserjian, R.P., Soffer, B., Sklar, J., and Baltimore, D. (1996). Exclusive development of T cell neoplasms in mice transplanted with bone marrow expressing activated Notch alleles. *The Journal of experimental medicine* 183, 2283-2291.

Pepper, M., and Jenkins, M.K. (2011). Origins of CD4(+) effector and central memory T cells. *Nature immunology* 12, 467-471.

Pepper, M., Linehan, J.L., Pagán, A.J., Zell, T., Dileepan, T., Cleary, P.P., and Jenkins, M.K. (2010). Different routes of bacterial infection induce long-lived TH1 memory cells and short-lived TH17 cells. *Nature immunology* 11, 83-89.

Perišić Nanut, M., Sabotič, J., Jewett, A., and Kos, J. (2014). Cysteine cathepsins as regulators of the cytotoxicity of NK and T cells. *Frontiers in immunology* 5, 616.

Petrie, H.T., Livak, F., Schatz, D.G., Strasser, A., Crispe, I.N., and Shortman, K. (1993). Multiple rearrangements in T cell receptor alpha chain genes maximize the production of useful thymocytes. *The Journal of experimental medicine* 178, 615-622.

Petrie, H.T., Scollay, R., and Shortman, K. (1992). Commitment to the T cell receptor-alpha beta or -gamma delta lineages can occur just prior to the onset of CD4 and CD8 expression among immature thymocytes. *European journal of immunology* 22, 2185-2188.

Peukert, K., Staller, P., Schneider, A., Carmichael, G., Hänel, F., and Eilers, M. (1997). An alternative pathway for gene regulation by Myc. *The EMBO journal* 16, 5672-5686.

Phan, R.T., Saito, M., Basso, K., Niu, H., and Dalla-Favera, R. (2005). BCL6 interacts with the transcription factor Miz-1 to suppress the cyclin-dependent kinase inhibitor p21 and cell cycle arrest in germinal center B cells. *Nature immunology* 6, 1054-1060.

Piskor, E.-M., Ross, J., Möröy, T., and Kosan, C. (2022). Myc-Interacting Zinc Finger Protein 1 (Miz-1) Is Essential to Maintain Homeostasis and Immunocompetence of the B Cell Lineage. *Biology* 11, 504.

Porritt, H.E., Gordon, K., and Petrie, H.T. (2003). Kinetics of steady-state differentiation and mapping of intrathymic-signaling environments by stem cell transplantation in nonirradiated mice. *The Journal of experimental medicine* 198, 957-962.

Porritt, H.E., Rumpf, L.L., Tabrizifard, S., Schmitt, T.M., Zúñiga-Pflücker, J.C., and Petrie, H.T. (2004). Heterogeneity among DN1 prothymocytes reveals multiple progenitors with different capacities to generate T cell and non-T cell lineages. *Immunity* 20, 735-745.

Preston, G.C., Sinclair, L.V., Kaskar, A., Hukelmann, J.L., Navarro, M.N., Ferrero, I., MacDonald, H.R., Cowling, V.H., and Cantrell, D.A. (2015). Single cell tuning of Myc expression by antigen receptor signal strength and interleukin-2 in T lymphocytes. *The EMBO journal* 34, 2008-2024.

Qi, Q., Zhang, D.W., Weyand, C.M., and Goronzy, J.J. (2014). Mechanisms shaping the naïve T cell repertoire in the elderly - thymic involution or peripheral homeostatic proliferation? *Experimental gerontology* 54, 71-74.

Quinn, K.M., Palchadhuri, R., Palmer, C.S., and La Gruta, N.L. (2019). The clock is ticking: the impact of ageing on T cell metabolism. *Clinical & translational immunology* 8, e01091.

Radtke, F., Wilson, A., Stark, G., Bauer, M., van Meerwijk, J., MacDonald, H.R., and Aguet, M. (1999). Deficient T cell fate specification in mice with an induced inactivation of Notch1. *Immunity* 10, 547-558.

Rashkovan, M., Vadnais, C., Ross, J., Gigoux, M., Suh, W.K., Gu, W., Kosan, C., and Möröy, T. (2014). Miz-1 regulates translation of Trp53 via ribosomal protein L22 in cells undergoing V(D)J recombination. *Proceedings of the National Academy of Sciences of the United States of America* 111, E5411-5419.

Reed, J.C. (1997). Double identity for proteins of the Bcl-2 family. *Nature* 387, 773-776.

Reed, J.C. (2000). Mechanisms of apoptosis. *The American journal of pathology* 157, 1415-1430.

Rogakou, E.P., Nieves-Neira, W., Boon, C., Pommier, Y., and Bonner, W.M. (2000). Initiation of DNA fragmentation during apoptosis induces phosphorylation of H2AX histone at serine 139. *The Journal of biological chemistry* 275, 9390-9395.

Rogakou, E.P., Pilch, D.R., Orr, A.H., Ivanova, V.S., and Bonner, W.M. (1998). DNA double-stranded breaks induce histone H2AX phosphorylation on serine 139. *The Journal of biological chemistry* 273, 5858-5868.

Ron-Harel, N., Notarangelo, G., Ghergurovich, J.M., Paulo, J.A., Sage, P.T., Santos, D., Satterstrom, F.K., Gygi, S.P., Rabinowitz, J.D., Sharpe, A.H., *et al.* (2018). Defective respiration and one-carbon metabolism contribute to impaired naïve T cell activation in aged mice. *Proceedings of the National Academy of Sciences of the United States of America* 115, 13347-13352.

Ross, J., Rashkovan, M., Fraszczak, J., Joly-Beauparlant, C., Vadnais, C., Winkler, R., Droit, A., Kosan, C., and Möröy, T. (2019). Deletion of the Miz-1 POZ Domain Increases Efficacy of Cytarabine Treatment in T- and B-ALL/Lymphoma Mouse Models. *Cancer research* 79, 4184-4195.

Roth, D.B., Menetski, J.P., Nakajima, P.B., Bosma, M.J., and Gellert, M. (1992). V(D)J recombination: broken DNA molecules with covalently sealed (hairpin) coding ends in scid mouse thymocytes. *Cell* 70, 983-991.

Rudd, C.E. (2021). How the Discovery of the CD4/CD8-p56(lck) Complexes Changed Immunology and Immunotherapy. *Frontiers in cell and developmental biology* 9, 626095.

Rutishauser, R.L., and Kaech, S.M. (2010). Generating diversity: transcriptional regulation of effector and memory CD8+ T - cell differentiation. *Immunological reviews* 235, 219-233.

Saba, I., Kosan, C., Vassen, L., Klein-Hitpass, L., and Möröy, T. (2011a). Miz-1 is required to coordinate the expression of TCRbeta and p53 effector genes at the pre-TCR "beta-selection" checkpoint. *Journal of immunology (Baltimore, Md : 1950)* 187, 2982-2992.

Saba, I., Kosan, C., Vassen, L., and Möröy, T. (2011b). IL-7R-dependent survival and differentiation of early T-lineage progenitors is regulated by the BTB/POZ domain transcription factor Miz-1. *Blood* 117, 3370-3381.

Sakaguchi, S., Sakaguchi, N., Asano, M., Itoh, M., and Toda, M. (1995). Immunologic self-tolerance maintained by activated T cells expressing IL-2 receptor alpha-chains (CD25). Breakdown of a single mechanism of self-tolerance causes various autoimmune diseases. *Journal of immunology (Baltimore, Md : 1950)* 155, 1151-1164.

Sallusto, F., Geginat, J., and Lanzavecchia, A. (2004). Central memory and effector memory T cell subsets: function, generation, and maintenance. *Annual review of immunology* 22, 745-763.

Sallusto, F., Lenig, D., Förster, R., Lipp, M., and Lanzavecchia, A. (1999). Two subsets of memory T lymphocytes with distinct homing potentials and effector functions. *Nature* 401, 708-712.

Sawada, S., Scarborough, J.D., Killeen, N., and Littman, D.R. (1994). A lineage-specific transcriptional silencer regulates CD4 gene expression during T lymphocyte development. *Cell* 77, 917-929.

Schaerli, P., Willimann, K., Lang, A.B., Lipp, M., Loetscher, P., and Moser, B. (2000). CXC chemokine receptor 5 expression defines follicular homing T cells with B cell helper function. *The Journal of experimental medicine* 192, 1553-1562.

Schatz, D.G., and Swanson, P.C. (2011). V (D) J recombination: mechanisms of initiation. *Annual review of genetics* 45, 167-202.

Schluns, K.S., Kieper, W.C., Jameson, S.C., and Lefrançois, L. (2000). Interleukin-7 mediates the homeostasis of naïve and memory CD8 T cells in vivo. *Nature immunology* 1, 426-432.

Schuebel, K.E., Movilla, N., Rosa, J.L., and Bustelo, X.R. (1998). Phosphorylation-dependent and constitutive activation of Rho proteins by wild-type and oncogenic Vav-2. *The EMBO journal* 17, 6608-6621.

Schulz, T.C., Hopwood, B., Rathjen, P.D., and Wells, J.R. (1995). An unusual arrangement of 13 zinc fingers in the vertebrate gene Z13. *The Biochemical journal* 311 (Pt 1), 219-224.

- Sebzda, E., Zou, Z., Lee, J.S., Wang, T., and Kahn, M.L. (2008). Transcription factor KLF2 regulates the migration of naive T cells by restricting chemokine receptor expression patterns. *Nature immunology* *9*, 292-300.
- Seoane, J., Le, H.V., and Massagué, J. (2002). Myc suppression of the p21(Cip1) Cdk inhibitor influences the outcome of the p53 response to DNA damage. *Nature* *419*, 729-734.
- Sharma, A., and Rudra, D. (2018). Emerging functions of regulatory T cells in tissue homeostasis. *Frontiers in immunology* *9*, 883.
- Shaw, J.P., Utz, P.J., Durand, D.B., Toole, J.J., Emmel, E.A., and Crabtree, G.R. (1988). Identification of a putative regulator of early T cell activation genes. *Science* *241*, 202-205.
- Shieh, S.Y., Ikeda, M., Taya, Y., and Prives, C. (1997). DNA damage-induced phosphorylation of p53 alleviates inhibition by MDM2. *Cell* *91*, 325-334.
- Shortman, K., and Wu, L. (1996). Early T lymphocyte progenitors. *Annual review of immunology* *14*, 29-47.
- Sieh, M., Batzer, A., Schlessinger, J., and Weiss, A. (1994). GRB2 and phospholipase C-gamma 1 associate with a 36- to 38-kilodalton phosphotyrosine protein after T-cell receptor stimulation. *Molecular and cellular biology* *14*, 4435-4442.
- Smith, J., Tho, L.M., Xu, N., and Gillespie, D.A. (2010). The ATM-Chk2 and ATR-Chk1 pathways in DNA damage signaling and cancer. *Advances in cancer research* *108*, 73-112.
- Staller, P., Peukert, K., Kiermaier, A., Seoane, J., Lukas, J., Karsunky, H., Möröy, T., Bartek, J., Massagué, J., Hänel, F., *et al.* (2001). Repression of p15INK4b expression by Myc through association with Miz-1. *Nature cell biology* *3*, 392-399.
- Stead, M.A., Trinh, C.H., Garnett, J.A., Carr, S.B., Baron, A.J., Edwards, T.A., and Wright, S.C. (2007). A beta-sheet interaction interface directs the tetramerisation of the Miz-1 POZ domain. *Journal of molecular biology* *373*, 820-826.
- Steinbach, K., Vincenti, I., and Merkler, D. (2018). Resident-memory T cells in tissue-restricted immune responses: for better or worse? *Frontiers in immunology*, 2827.
- Stritesky, G.L., Xing, Y., Erickson, J.R., Kalekar, L.A., Wang, X., Mueller, D.L., Jameson, S.C., and Hogquist, K.A. (2013). Murine thymic selection quantified using a unique method to capture deleted T cells. *Proceedings of the National Academy of Sciences of the United States of America* *110*, 4679-4684.
- Stürzbecher, H., Donzelmann, B., Henning, W., Knippschild, U., and Buchhop, S. (1996). p53 is linked directly to homologous recombination processes via RAD51/RecA protein interaction. *The EMBO journal* *15*, 1992-2002.
- Sullivan, K.D., Galbraith, M.D., Andrysiak, Z., and Espinosa, J.M. (2018). Mechanisms of transcriptional regulation by p53. *Cell death and differentiation* *25*, 133-143.
- Suzuki, K., Kodama, S., and Watanabe, M. (1999). Recruitment of ATM protein to double strand DNA irradiated with ionizing radiation. *The Journal of biological chemistry* *274*, 25571-25575.

- Taccioli, G.E., Rathbun, G., Oltz, E., Stamato, T., Jeggo, P.A., and Alt, F.W. (1993). Impairment of V(D)J recombination in double-strand break repair mutants. *Science* 260, 207-210.
- Taghon, T., Yui, M.A., Pant, R., Diamond, R.A., and Rothenberg, E.V. (2006). Developmental and molecular characterization of emerging beta- and gammadelta-selected pre-T cells in the adult mouse thymus. *Immunity* 24, 53-64.
- Tan, P., Anasetti, C., Hansen, J.A., Melrose, J., Brunvand, M., Bradshaw, J., Ledbetter, J.A., and Linsley, P.S. (1993). Induction of alloantigen-specific hyporesponsiveness in human T lymphocytes by blocking interaction of CD28 with its natural ligand B7/BB1. *The Journal of experimental medicine* 177, 165-173.
- Tibbetts, R.S., Brumbaugh, K.M., Williams, J.M., Sarkaria, J.N., Cliby, W.A., Shieh, S.Y., Taya, Y., Prives, C., and Abraham, R.T. (1999). A role for ATR in the DNA damage-induced phosphorylation of p53. *Genes & development* 13, 152-157.
- Trauth, B.C., Klas, C., Peters, A.M., Matzku, S., Möller, P., Falk, W., Debatin, K.M., and Krammer, P.H. (1989). Monoclonal antibody-mediated tumor regression by induction of apoptosis. *Science* 245, 301-305.
- Turvey, S.E., and Broide, D.H. (2010). Innate immunity. *The Journal of allergy and clinical immunology* 125, S24-32.
- Utsuyama, M., Hirokawa, K., Kurashima, C., Fukayama, M., Inamatsu, T., Suzuki, K., Hashimoto, W., and Sato, K. (1992). Differential age-change in the numbers of CD4+CD45RA+ and CD4+CD29+ T cell subsets in human peripheral blood. *Mechanisms of ageing and development* 63, 57-68.
- Vadnais, C., Chen, R., Fraszczak, J., Yu, Z., Boulais, J., Pinder, J., Frank, D., Khandanpour, C., Hébert, J., Delleire, G., *et al.* (2018). GF11 facilitates efficient DNA repair by regulating PRMT1 dependent methylation of MRE11 and 53BP1. *Nature communications* 9, 1418.
- van Riggelen, J., Müller, J., Otto, T., Beuger, V., Yetil, A., Choi, P.S., Kosan, C., Möröy, T., Felsher, D.W., and Eilers, M. (2010). The interaction between Myc and Miz1 is required to antagonize TGFbeta-dependent autocrine signaling during lymphoma formation and maintenance. *Genes & development* 24, 1281-1294.
- Varfolomeev, E.E., Schuchmann, M., Luria, V., Chiannikulchai, N., Beckmann, J.S., Mett, I.L., Rebrikov, D., Brodianski, V.M., Kemper, O.C., Kollet, O., *et al.* (1998). Targeted disruption of the mouse Caspase 8 gene ablates cell death induction by the TNF receptors, Fas/Apo1, and DR3 and is lethal prenatally. *Immunity* 9, 267-276.
- Varlakhanova, N., Cotterman, R., Bradnam, K., Korf, I., and Knoepfler, P.S. (2011). Myc and Miz-1 have coordinate genomic functions including targeting Hox genes in human embryonic stem cells. *Epigenetics & chromatin* 4, 20.
- Vermes, I., Haanen, C., Steffens-Nakken, H., and Reutellingsperger, C. (1995). A novel assay for apoptosis flow cytometric detection of phosphatidylserine expression on early apoptotic cells using fluorescein labelled annexin V. *Journal of immunological methods* 184, 39-51.

- Villalba, M., Bi, K., Rodriguez, F., Tanaka, Y., Schoenberger, S., and Altman, A. (2001). Vav1/Rac-dependent actin cytoskeleton reorganization is required for lipid raft clustering in T cells. *The Journal of cell biology* 155, 331-338.
- von Boehmer, H. (2005). Unique features of the pre-T-cell receptor alpha-chain: not just a surrogate. *Nature reviews Immunology* 5, 571-577.
- von Boehmer, H., Teh, H.S., and Kisielow, P. (1989). The thymus selects the useful, neglects the useless and destroys the harmful. *Immunology today* 10, 57-61.
- von Freeden-Jeffry, U., Solvason, N., Howard, M., and Murray, R. (1997). The earliest T lineage-committed cells depend on IL-7 for Bcl-2 expression and normal cell cycle progression. *Immunity* 7, 147-154.
- Vousden, K.H. (2002). Switching from life to death: the Miz-ing link between Myc and p53. *Cancer cell* 2, 351-352.
- Vousden, K.H., and Lu, X. (2002). Live or let die: the cell's response to p53. *Nature reviews Cancer* 2, 594-604.
- Walz, S., Lorenzin, F., Morton, J., Wiese, K.E., von Eyss, B., Herold, S., Rycak, L., Dumay-Odelot, H., Karim, S., Bartkuhn, M., *et al.* (2014). Activation and repression by oncogenic MYC shape tumour-specific gene expression profiles. *Nature* 511, 483-487.
- Wang, C., Collins, M., and Kuchroo, V.K. (2015). Effector T cell differentiation: are master regulators of effector T cells still the masters? *Current opinion in immunology* 37, 6-10.
- Wanzel, M., Kleine-Kohlbrecher, D., Herold, S., Hock, A., Berns, K., Park, J., Hemmings, B., and Eilers, M. (2005). Akt and 14-3-3eta regulate Miz1 to control cell-cycle arrest after DNA damage. *Nature cell biology* 7, 30-41.
- Wanzel, M., Russ, A.C., Kleine-Kohlbrecher, D., Colombo, E., Pelicci, P.G., and Eilers, M. (2008). A ribosomal protein L23-nucleophosmin circuit coordinates Miz1 function with cell growth. *Nature cell biology* 10, 1051-1061.
- Weiskopf, D., Weinberger, B., and Grubeck-Loebenstien, B. (2009). The aging of the immune system. *Transplant international : official journal of the European Society for Organ Transplantation* 22, 1041-1050.
- Wherry, E.J., Teichgräber, V., Becker, T.C., Masopust, D., Kaech, S.M., Antia, R., von Andrian, U.H., and Ahmed, R. (2003). Lineage relationship and protective immunity of memory CD8 T cell subsets. *Nature immunology* 4, 225-234.
- Wiese, K.E., Haikala, H.M., von Eyss, B., Wolf, E., Esnault, C., Rosenwald, A., Treisman, R., Klefström, J., and Eilers, M. (2015). Repression of SRF target genes is critical for Myc - dependent apoptosis of epithelial cells. *The EMBO journal* 34, 1554-1571.
- Wiese, K.E., Walz, S., von Eyss, B., Wolf, E., Athineos, D., Sansom, O., and Eilers, M. (2013). The role of MIZ-1 in MYC-dependent tumorigenesis. *Cold Spring Harbor perspectives in medicine* 3, a014290.
- Williams, A.B., and Schumacher, B. (2016). p53 in the DNA-Damage-Repair Process. *Cold Spring Harbor perspectives in medicine* 6.

- Wilson, A., MacDonald, H.R., and Radtke, F. (2001). Notch 1-deficient common lymphoid precursors adopt a B cell fate in the thymus. *The Journal of experimental medicine* 194, 1003-1012.
- Wilson, A., Petrie, H.T., Scollay, R., and Shortman, K. (1989). The acquisition of CD4 and CD8 during the differentiation of early thymocytes in short-term culture. *International immunology* 1, 605-612.
- Wolf, E., Gebhardt, A., Kawauchi, D., Walz, S., von Eyss, B., Wagner, N., Renninger, C., Krohne, G., Asan, E., Roussel, M.F., *et al.* (2013). Miz1 is required to maintain autophagic flux. *Nature communications* 4, 2535.
- Wolfer, A., Bakker, T., Wilson, A., Nicolas, M., Ioannidis, V., Littman, D.R., Lee, P.P., Wilson, C.B., Held, W., MacDonald, H.R., *et al.* (2001). Inactivation of Notch 1 in immature thymocytes does not perturb CD4 or CD8T cell development. *Nature immunology* 2, 235-241.
- Wu, G.S., Burns, T.F., McDonald III, E.R., Meng, R.D., Kao, G., Muschel, R., Yen, T., and El-Deiry, W.S. (1999). Induction of the TRAIL receptor KILLER/DR5 in p53-dependent apoptosis but not growth arrest. *Oncogene* 18, 6411-6418.
- Wu, L., Scollay, R., Egerton, M., Pearse, M., Spangrude, G.J., and Shortman, K. (1991). CD4 expressed on earliest T-lineage precursor cells in the adult murine thymus. *Nature* 349, 71-74.
- Wu, S., Cetinkaya, C., Munoz-Alonso, M.J., von der Lehr, N., Bahram, F., Beuger, V., Eilers, M., Leon, J., and Larsson, L.G. (2003). Myc represses differentiation-induced p21CIP1 expression via Miz-1-dependent interaction with the p21 core promoter. *Oncogene* 22, 351-360.
- Xu, S.Q., and El-Deiry, W.S. (2000). p21(WAF1/CIP1) inhibits initiator caspase cleavage by TRAIL death receptor DR4. *Biochemical and biophysical research communications* 269, 179-190.
- Yamane, K., Wu, X., and Chen, J. (2002). A DNA damage-regulated BRCT-containing protein, TopBP1, is required for cell survival. *Molecular and cellular biology* 22, 555-566.
- Yang, Y., Do, H., Tian, X., Zhang, C., Liu, X., Dada, L.A., Sznajder, J.I., and Liu, J. (2010). E3 ubiquitin ligase Mule ubiquitinates Miz1 and is required for TNFalpha-induced JNK activation. *Proceedings of the National Academy of Sciences of the United States of America* 107, 13444-13449.
- Yin, X.M., Wang, K., Gross, A., Zhao, Y., Zinkel, S., Klocke, B., Roth, K.A., and Korsmeyer, S.J. (1999). Bid-deficient mice are resistant to Fas-induced hepatocellular apoptosis. *Nature* 400, 886-891.
- Yokosuka, T., and Saito, T. (2009). Dynamic regulation of T-cell costimulation through TCR-CD28 microclusters. *Immunological reviews* 229, 27-40.
- Yonish-Rouach, E., Resnitzky, D., Lotem, J., Sachs, L., Kimchi, A., and Oren, M. (1991). Wild-type p53 induces apoptosis of myeloid leukaemic cells that is inhibited by interleukin-6. *Nature* 352, 345-347.

- Zhan, Y., Carrington, E.M., Zhang, Y., Heinzl, S., and Lew, A.M. (2017). Life and Death of Activated T Cells: How Are They Different from Naïve T Cells? *Frontiers in immunology* 8, 1809.
- Zhang, W., Sloan-Lancaster, J., Kitchen, J., Tribble, R.P., and Samelson, L.E. (1998). LAT: the ZAP-70 tyrosine kinase substrate that links T cell receptor to cellular activation. *Cell* 92, 83-92.
- Zhang, W., Tribble, R.P., Zhu, M., Liu, S.K., McGlade, C.J., and Samelson, L.E. (2000). Association of Grb2, Gads, and phospholipase C-gamma 1 with phosphorylated LAT tyrosine residues. Effect of LAT tyrosine mutations on T cell antigen receptor-mediated signaling. *The Journal of biological chemistry* 275, 23355-23361.
- Zindy, F., Eischen, C.M., Randle, D.H., Kamijo, T., Cleveland, J.L., Sherr, C.J., and Roussel, M.F. (1998). Myc signaling via the ARF tumor suppressor regulates p53-dependent apoptosis and immortalization. *Genes & development* 12, 2424-2433.
- Zipfel, P.F., and Skerka, C. (2009). Complement regulators and inhibitory proteins. *Nature reviews Immunology* 9, 729-740.
- Zou, H., Henzel, W.J., Liu, X., Lutschg, A., and Wang, X. (1997). Apaf-1, a human protein homologous to *C. elegans* CED-4, participates in cytochrome c-dependent activation of caspase-3. *Cell* 90, 405-413.
- Zou, H., Li, Y., Liu, X., and Wang, X. (1999). An APAF-1-cytochrome c multimeric complex is a functional apoptosome that activates procaspase-9. *The Journal of biological chemistry* 274, 11549-11556.
- Zou, L., and Elledge, S.J. (2003). Sensing DNA damage through ATRIP recognition of RPA-ssDNA complexes. *Science* 300, 1542-1548.

Declaration of independent assignment – Ehrenwörtliche Erklärung

Hiermit versichere ich, dass mir die geltende Promotionsordnung der Fakultät für Biowissenschaften der Friedrich-Schiller-Universität Jena bekannt ist.

Die vorliegende Dissertation habe ich selbst angefertigt, ohne dabei Textabschnitte Dritter oder eigener Prüfungsarbeiten ohne Kennzeichnung zu übernehmen. Dabei wurden stets alle von mir benutzten Quellen, Hilfsmittel und persönlichen Mitteilungen in dieser Arbeit angegeben.

Weiterhin wurden alle Personen namentlich benannt, welche mich bei der Auswahl und Auswertung des Materials, sowie bei der Herstellung des Manuskriptes unterstützt haben.

Hilfe einer kommerziellen Promotionsvermittlung habe ich nicht in Anspruch genommen und Dritte haben weder mittelbar noch unmittelbar geldwerte Leistungen für Arbeiten, welche in Zusammenhang mit dem Inhalt der vorliegenden Dissertation stehen, von mir erhalten.

Die vorliegende Dissertation wurde nie zuvor als Prüfungsarbeit für eine staatliche oder andere wissenschaftliche Prüfung von mir eingereicht. Weiterhin habe ich die gleiche, eine in wesentlichen Teilen ähnliche oder eine andere Abhandlung nie zuvor bei einer anderen Hochschule oder einer anderen Fakultät als Dissertation eingereicht.

Jena,

.....

Ann-Sophie Mägdefrau